



University of Kentucky
UKnowledge

Theses and Dissertations--Nutritional Sciences

Nutritional Sciences

2014

MOLECULAR MECHANISM OF HUMAN MISMATCH REPAIR INITIATION

Sanghee Lee

University of Kentucky, sh.lee@uky.edu

[Right click to open a feedback form in a new tab to let us know how this document benefits you.](#)

Recommended Citation

Lee, Sanghee, "MOLECULAR MECHANISM OF HUMAN MISMATCH REPAIR INITIATION" (2014). *Theses and Dissertations--Nutritional Sciences*. 15.
https://uknowledge.uky.edu/nutrisci_etds/15

This Doctoral Dissertation is brought to you for free and open access by the Nutritional Sciences at UKnowledge. It has been accepted for inclusion in Theses and Dissertations--Nutritional Sciences by an authorized administrator of UKnowledge. For more information, please contact UKnowledge@lsv.uky.edu.

STUDENT AGREEMENT:

I represent that my thesis or dissertation and abstract are my original work. Proper attribution has been given to all outside sources. I understand that I am solely responsible for obtaining any needed copyright permissions. I have obtained needed written permission statement(s) from the owner(s) of each third-party copyrighted matter to be included in my work, allowing electronic distribution (if such use is not permitted by the fair use doctrine) which will be submitted to UKnowledge as Additional File.

I hereby grant to The University of Kentucky and its agents the irrevocable, non-exclusive, and royalty-free license to archive and make accessible my work in whole or in part in all forms of media, now or hereafter known. I agree that the document mentioned above may be made available immediately for worldwide access unless an embargo applies.

I retain all other ownership rights to the copyright of my work. I also retain the right to use in future works (such as articles or books) all or part of my work. I understand that I am free to register the copyright to my work.

REVIEW, APPROVAL AND ACCEPTANCE

The document mentioned above has been reviewed and accepted by the student's advisor, on behalf of the advisory committee, and by the Director of Graduate Studies (DGS), on behalf of the program; we verify that this is the final, approved version of the student's thesis including all changes required by the advisory committee. The undersigned agree to abide by the statements above.

Sanghee Lee, Student

Dr. Guo-Min Li, Major Professor

Dr. Howard Glauert, Director of Graduate Studies

MOLECULAR MECHANISM OF HUMAN MISMATCH REPAIR INITIATION

ABSTRACT OF DISSERTATION

A dissertation submitted in partial fulfillment of the requirements for the degree of
Doctor of Philosophy in the College of Medicine at the University of Kentucky

By

Sanghee Lee

Lexington, Kentucky

Director: Dr. Guo-Min Li, Professor of Nutritional Sciences

Lexington, Kentucky

2014

Copyright © Sanghee Lee 2014

ABSTRACT OF DISSERTATION

MOLECULAR MECHANISM OF HUMAN MISMATCH REPAIR INITIATION

DNA mismatch repair (MMR) is a highly conserved pathway that maintains genomic stability primarily by correcting mismatches generated during DNA replication. MMR deficiency leads to microsatellite instability (MSI), which is a hallmark of HNPCC (Hereditary Nonpolyposis Colorectal Cancer). Human mismatch repair is initiated by MutS α , a heterodimer of MSH2 and MSH6 subunits. Mismatch binding by MutS α triggers a series of downstream MMR events including interacting and communicating with other MMR proteins. The ATPase domain of MutS α is situated in the C-termini of its both subunits, and ATP binding is required for dissociation of MutS α from a mismatch. In eukaryotic cells, a strand break, which resides either 3' or 5' to the mismatch up to several hundred base pair away, determines the strand specificity of MMR. However, in spite of extensive studies, the mechanism by which MutS α locates and senses a nick from the mismatch, and coordinates the subsequent steps of MMR remains poorly understood. Two controversial models have been proposed to explain how the mismatch and the strand break communicate each other. Sliding model proposes that MutS α slides along the DNA helix from the mismatch to the strand break in an ATP binding-dependent but not ATP hydrolysis-dependent manner. Stationary model postulates that MutS α remains bound at the mismatch, and a protein-mediated DNA loop forms, physically bringing the mismatch and the nick in contact. Here, we tested these models *in vitro*, using a circular plasmid DNA substrate with a single GT mismatch and two Lac repressor (Lac I) binding sites as conditional physical 'roadblocks', one on either side of the mismatch, which when present, prevent MutS α from sliding bi-directionally along the DNA. The results showed that DNA excision initiates under conditions that block MutS α sliding, suggesting that initiation of excision is independent of whether MutS α slides from the mismatch to the nick. This result implies that the communication between the mismatch and the nick is likely through interactions between the mismatch-bound MutS α and other MMR components at the strand break, supporting the stationary model. Therefore, these studies provide significant insight into the mechanisms of mismatch correction in human cells.

KEYWORDS: Mismatch repair, MutS α , ATPase, HNPCC, Walker A/B motif

"Lenny"

Students's Signature

06/11/14

Date

MOLECULAR MECHANISM OF HUMAN MISMATCH REPAIR INITIATION

By

Sanghee Lee

Guo-Min Li, Ph.D.

Director of Dissertation

Howard Glauert, Ph.D.

Director of Graduate Studies

06/17/14

Date

This dissertation is dedicated to my parent and husband,

Hyunwoo Lee, Hwajin Chang, and Dongsun Lee...

ACKNOWLEDGEMENTS

This dissertation would never have been able to finish without the support of my family, friends and colleagues, and the guidance of my advisor and committee members. I would like to express my deepest gratitude to my advisor, Dr. Guo-Min Li, for immeasurable amount of his guidance, caring and patience. He gave me a great opportunity to carry out my doctoral research in his lab and provided me with an excellent atmosphere to do my research. I was fortunate to have such an excellent mentor because his encouragement and support have inspired and enriched my doctoral work. His true joy and passion for science have motivated me a lot and served as driving force to keep up with my research even during difficult times in my Ph.D. I would like to thank to Dr. Liya Gu, who is my former advisor, for giving me an opportunity to join this lab, supporting and providing me with excellent guidance and advice. I am also heartily thankful to my Ph.D dissertation committee members: Dr. Ching Kuang Chow, Dr. Howard Perry Glauert, Dr. Rolf J Craven and an outside examiner, Dr. Alexander Sasha Rabchevsky, for their time, patience, interest, helpful comments and insightful questions.

It was always honor and pleasure to work with excellent scientists who have helped me not only physically but also spiritually and emotionally. Especially, I would like to thank Guogen Mao, who is willing to share his knowledge. He always spends his time to help and provide me with his best suggestions. His guidance and advice (for technical assistance with the basic skills and constructive comments on my results) have been invaluable to me, which significantly improve my research. I would also like to thank to all the lab members including previous members, Feng Li, Lei Tian, Fred Odago, Nelson Chan, Tianyi Zhang,

Dan Tong, Caixia Hou and Mark Ensor, and current members, Christine Kim, Janice Ortega, Kara Chan, and Nidhi Shukla, for their daily support in the lab.

I would also like to thank Dr. Geza Bruckner, a previous director of Graduate Studies, for helping me to enter Graduate Center for Nutritional Sciences program, and to Dr. Lisa A Cassis, a Chair of Department of Pharmacology and Nutritional Sciences, for giving me an opportunity to start my Ph.D program in Department of Nutritional Sciences. I would especially like to thank Dr. Howard Glauert for his support in the role of Director of Graduate Studies. I extend my appreciation to the faculty and staff in the department Nutritional Sciences.

I also want to thank to Dr. Mary Vore, Director of Toxicology, and Dr. David Orren, previous director of Graduate Studies for Toxicology, for their support. I am grateful to Dr. Jane Harrison, who made it possible for me to come to the University of Kentucky.

I would like to show my gratitude to Dr. Wei Yang in Macromolecular Crystallography at National Institute of Diabetes and Digestive and Kidney Diseases, whose collaborative work based on her crystal structure improves my work on developing mutant MutSa. This work would not have been possible without her suggestions. I have benefited from advice and comments offered by Dr. Miriam Sander who helped me in shaping up my manuscript and dissertation.

I want to extend my appreciation to my mentor in Korea, Youngseo Park, for giving me an opportunity to work in his genetic engineering lab, when I did my undergraduate at Kyungwon University. I would not have been able to start my Ph.D research without my lab experience in his lab. His support and encouragement helped me to become interested in science. I was luck to meet him there.

I appreciate my friends in Lexington who have made my Lexington life enjoyable, especially Yunyoung Go, Yoonie Choi, Jungmin Kim, Jiae Kim, Jieun Kim, Hyein Jang, Euijin Song, Jiyeon Park, and Hyunjung Kim who became a part of my life. In my time here at University of Kentucky, I am fortunate enough to meet them. I would also like to thank to all my friends, who are in Korea. They have mentally supported me by chatting on the phone when I had hard time.

I would express my sincere gratitude to my parents, Hyunwoo Lee and Hwajin Chang, for their spirit of sacrifice, unconditional love, strength, example and support. I am heartily thankful to my sister and brother, Sangsoo Lee and Sangyoon Lee, my maternal grandma /grandpa, all my relatives and my extended family, my mother-in-law, brother-in-law, and sister-in-law, for supporting and encouraging me with their best wishes. I would also like to thank to my paternal grandma who passed away this year for encouraging me with her wishes (may her soul rest in peace).

Very special thanks go to my husband, Dongsun Lee, who has been always with me. I would never have been able to finish my study without his love, care, trust, support and encouragement. I feel extremely blessed to have him in my life. Thank you so much for waiting for me for several years, living apart each other. Lastly, I want to express thanks and send blessings to everyone else who has supported me.

TABLE OF CONTENTS

ACKNOWLEDGEMENTS.....	iii
LIST OF TABLES.....	viii
LIST OF FIGURES.....	ix
CHAPTER ONE: INTRODUCTION AND RESEARCH OBJECTIVES.....	1
1-1. Genomic Instability and Carcinogenesis.....	1
1-2. DNA Mismatch Repair and Cancer.....	1
1-2-a. Colorectal Cancer (HNPCC and sporadic MSI-CRC).....	2
1-2-b. Acute Myeloid Leukemia (AML).....	2
1-3. DNA Mismatch Repair.....	3
1-3-a. Mismatch Repair in <i>Escherichia coli</i>	5
1-3-b. Mismatch Repair in Human Cells.....	8
1-4. Characteristics of MutS α protein.....	11
1-5. Involvement of MutS α in Initiation of Mismatch Repair.....	14
Research Objectives.....	17
CHAPTER TWO: MATERIALS AND METHODS.....	18
2-1. Chemicals and Reagents.....	18
2-2. Agarose Gel Electrophoresis.....	19
2-3. ATPase activity Analysis.....	19
2-4. Buffer Preparation.....	19
2-5. Cell Culture.....	19
2-6. Electrophoretic Mobility Shift Assay (Gel Shift Assay).....	20
2-7. Immunoprecipitation Assay.....	20
2-8. <i>In vitro</i> MMR Assay and Excision Assay.....	21
2-8-a. <i>In vitro</i> MMR Assay.....	21
2-8-b. Excision and Southern Blot Assay.....	21
2-9. Nuclear Extract Preparation.....	24
2-10. Nucleotide Binding Analysis.....	24
2-11. Preparation of DNA Substrate.....	25
2-11-a. Preparation of Bacteriophage Stock.....	25

2-11-b. Preparation of dsDNA and ssDNA.....	25
2-11-c. Preparation of circular heteroduplex substrates.....	27
2-12. Purification of Lac repressor and Nuclease activity Assay.....	30
2-13. Purification of MutS α , MutS β , and MutL α from High-Five insect cells.....	31
2-14. SDS-Polyacrylamide Gel Electrophoresis (SDS-PAGE).....	32
2-15. Site-directed Mutagenesis.....	33
2-16. Transfections into the Insect cells.....	33
2-17. Transformations of Competent Cells.....	33
2-18. Western Blot Analysis.....	34
CHAPTER THREE: SLIDING OF MUTS α TO COMMUNICATE WITH A STRAND BREAK IS NOT ESSENTIAL FOR THE INITIATION OF MISMATCH REPAIR.....	35
INTRODUCTION.....	35
RESULTS.....	38
Purification and functional tests of Lac repressor and MutS α proteins.....	38
Sliding of MutS α along the DNA is restricted by Lac repressor roadblock.....	41
Lac repressor roadblocks significantly inhibit <i>in vitro</i> MMR.....	43
Mismatch-provoked excision in the presence of Lac repressor roadblock.....	45
DISCUSSION.....	49
CHAPTER FOUR: MOLECULAR REGULATION OF MUTS α ATPASE AND ITS INVOLVEMENT IN MMR INITIATION.....	51
INTRODUCTION.....	51
RESULTS.....	53
Characterization of MutS α with mutations in Walker A and Walker B motifs of MSH2 and/or MSH6.....	53
Initiation of Mismatch-provoked excision <i>in vitro</i> is independent of MutS α sliding, but dependent of MutS α remained bound at the mismatch.....	60
MutS α -mediated signaling during initiation of MMR <i>in vitro</i>	63
DISCUSSION.....	68
APPENDIX.....	73
REFERENCES.....	76
VITA.....	84

LIST OF TABLES

Table 1.1 MMR components and functions.....	4
---	---

LIST OF FIGURES

Figure 1.1 Schematic representation of the <i>E. coli</i> MMR.....	7
Figure 1.2 Schematic representation of the human MMR.....	10
Figure 1.3 Structure of MutS α	11
Figure 1.4 Mismatch Binding Mode of MutS α	12
Figure 1.5 Proposed conformational change of MutS α in the presence of nucleotide.....	14
Figure 1.6 Schematic diagrams strand discrimination during MMR initiation in human cells.....	16
Figure 2.1 Principle of <i>in vitro</i> mismatch repair and excision assay.....	23
Figure 2.2 Preparation of 5' nicked G-T mismatch substrate.....	29
Figure 2.3 Schematic representations of 5' nicked G-T heteroduplexes substrates containing two Lac repressor-binding sites.....	30
Figure 2.4 Purification of Lac repressor.....	31
Figure 3.1 Purification of Lac repressor and MutS α proteins.....	38
Figure 3.2 Crystal structure of tetramer Lac repressor and its binding sequence.....	38
Figure 3.3 Binding of purified Lac repressor to Lac repressor-binding site and dissociation of Lac repressor from DNA by induction of IPTG.....	40
Figure 3.4 Interaction between MutS α and mismatch-contained heteroduplex DNA in the presence or absence of Lac repressor roadblocks.....	42
Figure 3.5 Lac repressor roadblock significantly inhibits <i>in vitro</i> MMR.....	44
Figure 3.6 Effect of Lac repressor roadblock on <i>in vitro</i> MMR in nuclear extracts from MMR-defective cells complemented with purified protein.....	44
Figure 3.7 Mismatch-provoked excision still proceeded from the 5' nick regardless of the presence of Lac repressor roadblock.....	47
Figure 3.8 Increasing concentration of Lac repressors improves the roadblock effect on excision termination at the first downstream roadblock.....	48
Figure 4.1 Purification and <i>in vitro</i> MMR assay of ATPase-defective MutS α mutants.....	55
Figure 4.2 ATP binding and ATPase activities of MutS α wild type and ATPase-deficient mutants.....	56

Figure 4.3 Effects of ATPase-defective MutS α mutants on mismatch binding and ATP binding-induced mismatch release.....	59
Figure 4.4 Requirement for stable binding of MutS α to the mismatch during initiation of MMR.....	62
Figure 4.5 Biochemical characteristics ATPase-deficient MutS α with G-A substitution mutations in the Walker A motif.....	65
Figure 4.6 Exo1-catalyzed excision occurs efficiently from the nick independently of whether MutS α slides from the mismatch to the nick.....	66
Figure 4.7 Requirement for mismatch-bound MutS α during initiation of MMR.....	67
Figure 4.8 Models for signaling between the mismatch and the strand discrimination signal of MMR event.....	71
Figure 4.9 Proposed model for initiation of MMR.....	72

CHAPTER ONE

INTRODUCTION

1-1. Genomic Instability and Carcinogenesis

Genomic instability which refers to a high frequency of mutations within the genome during the life cycle of cells is the hallmark of cancers. It is a major driving force in carcinogenesis and can be caused by genetic or epigenetic mechanisms (Waddington 1940, Holliday and Pugh 1975, Issa 2000, Nguyen and Massague 2007). In general, genomic instability occurs as a result of exposure to high levels of DNA damaging agents, or because of defective DNA repair pathways. Exogenous agents that damage DNA or DNA precursors include physical or chemical damage such as ultraviolet light (UV), ionizing radiation, or reactive chemicals. Defective DNA replication can also lead to high levels of misincorporated nucleotides, strand slippage-induced small deletions or insertions (Modrich 1989, Modrich 1997) while aberrant homologous recombination events also contribute to genome instability (Holliday 2007). Although mutations in DNA repair genes are infrequent specifically in sporadic (non-hereditary) cancers (Drake 1991, Drake 1999), they are common in hereditary cancers. However, genomic instability is reduced by effective, error-free and somewhat redundant high capacity DNA repair pathways, high-fidelity DNA replication in S-phase, precise chromosome segregation during mitosis, coordinated cell cycle progression, and cell death pathways that eliminate severely damaged cells and/or lower the rate at which mutant cells proliferate.

1-2. DNA Mismatch Repair and Cancer

DNA repair systems provide a crucial defense mechanism against DNA damage caused by exogenous or endogenous agents. MMR is a highly conserved DNA repair pathway that maintains genomic stability primarily by correcting base-base or small insertion/deletion mismatches. MMR enhances the fidelity of DNA replication 100–1000 fold (Kolodner 1996, Schofield and Hsieh 2003, Iyer, Pluciennik et al. 2006). Defects in MMR increase the spontaneous mutation rate in human cells (Eshleman and Markowitz 1995) and are tightly linked to hereditary non-polyposis colon cancer (HNPCC) and microsatellite instability (MSI). Majority of HNPCC patients exhibits MSI, which is a hallmark of HNPCC (Loukola, Eklin et al. 2001). Microsatellites are simple 1-6 bp tandem DNA sequence repeats typically present in 100s of copies distributed in coding and non-coding regions of the genome (Chen, Chen et al. 1997). Instability in microsatellite repeats is caused by the

failure to repair small slip-mispairing loops that form during meiotic DNA replication (Tautz and Schlotterer 1994), which is inheritently hypermutable. Instability in microsatellite repeats gives rise to generation of small insertion-deletion (ID) mispairs (or loops), which are typically repaired by MMR. Therefore, MSI is diagnostic for MMR dysfunction and for hereditary nonpolyposis colon cancer (HNPCC) and acute myeloid leukemia (AML) (Lynch and de la Chapelle 1999, Umar and Srivastava 2004).

1-2-a. Colorectal Cancer (HNPCC and sporadic MSI-CRC)

Approximately 10% of all colorectal cancer patients carry inherited mutations in MMR genes and are diagnosed with the autosomal dominant disorder HNPCC (also called Lynch syndrome). HNPCC is characterized by early onset adenomatous colorectal polyps (~44 years old) and increased risk of developing colorectal, endometrial, stomach, small intestine and ovarian cancers as well as leukemia (Kohlmann and Gruber 1993). HNPCC-linked germline mutations are primarily observed in *MSH2* and *MLH1*, but are also occasionally found in *MSH6*, *MSH3* and *PMS2* (Peltomaki and Vasen 1997, Lynch and de la Chapelle 1999). This thus strongly supports the association of MMR deficiency with HNPCC syndrome. Discovery of the strong link between MMR dysfunction and HNPCC stimulated investigation into mechanisms of MMR in human cells, which provides significant insights into finding treatment of HNPCC. Interestingly, approximately 15% of sporadic human colorectal cancers lack detectable mutations in known human MMR genes, suggesting either that mutations in other (not yet identified) MMR genes or mutations in non-MMR genes contribute to development of colorectal cancer, or that epigenetic changes in MMR gene expression play a role (Bellizzi and Frankel 2009). In fact, hypermethylation in the promoter region of *MLH1* has been observed in MSI- positive colorectal cancer cells, which leads to silencing of *MLH1* gene expression (Kane, Loda et al. 1997, Herman, Umar et al. 1998). This modification reduces and/or blocks expression of *MLH1*, causing a mutator phenotype, which indicates that epigenetic modifications can also be responsible for a mutator phenotype.

1-2-b. Acute Myeloid Leukemia (AML)

In addition to HNPCC, MMR defects increase the incidence of acute myeloid leukemia (AML), which is one of the most common adult onset acute leukemia (Mao, Pan et al. 2008, Mao, Yuan et al. 2008). The incidence of AML is higher in men than in women and increases with age, but is rare in individuals younger than 40 years old. It is characterized by rapid proliferation of abnormal white blood cells in the bone marrow, frequent infections

and increased risk of bleeding. Non-genetic risk factors for AML include exposure to cigarette smoke, radiation, chemotherapy, and other genetic disorders including Down syndrome (trisomy 21). Basically, somatic mutation is not the only mechanism in which cancers arise, but the accumulation of somatic mutation is the only process that can account for cancer progression in different ages (Frank and Nowak 2004). In addition, somatic mutations in some of the genes involved in MMR pathway have been identified in AML patients while either being at the time of diagnosis or after leukemia relapse, suggesting that MMR defects are involved in the formation and progression of AML (Mao, Pan et al. 2008, Mao, Yuan et al. 2008). Interestingly, leukemic cells from AML patients can display higher mutation rate and a more aggressive phenotype during relapse than at time of diagnosis, and mutations in MMR genes are found more frequently in leukemic cells from AML patients during relapse (Mao, Yuan et al. 2008). Therefore, the appropriate expression of MMR genes would modulate over the process of AML cancer progression, decreasing the mutation rate and eventually enhancing genomic stability.

1-3. DNA Mismatch Repair

The MMR deficiency contributes to exhibition of mutator phenotype, and mutation rates in tumor cells caused by MMR deficiency are up to 1000 fold higher than normal cells. The MMR plays an essential role in cancer avoidance, because it increases genomic stability, restoring DNA homeostasis in cells (Li 2008). MMR proteins (Table 1.1) and mechanisms are highly conserved in prokaryotes and eukaryotes. Mismatch repair generally involves three steps: 1) mismatch recognition, 2) excision (removal of a mismatch), and 3) DNA resynthesis. The MMR mechanism in prokaryotes and eukaryotes differs during initiation, and the strand discrimination signal, which differentiates the newly synthesized strand from the template strand, is also thought to differ (see below for further discussion) (Lahue, Au et al. 1989, Constantin, Dzantiev et al. 2005, Zhang, Yuan et al. 2005).

Table 1.1 MMR components and functions

<i>E.coli</i>	Human	Function	
(MutS) ₂	hMutS α (MSH2-MSH6)	Recognition of DNA mismatch or damage	Nucleotide Mismatch or 1-2 IDs
	hMutS β (MSH2-MSH3)		2-16 ID Loops
(MutL) ₂	hMutL α (MLH1-PMS2)	Molecular matchmaker, Endonuclease activity, and Termination of mismatch-provoked excision	
	hMutL β (MLH1-PMS1)	Unknown	
	hMutL γ (MLH1-MLH3)	Unknown	
MutH	Unknown	Strand discrimination	
UvrD	Unknown	DNA helicase	
Exo I, Exo VII, Exo X, Rec J	Exo I	DNA mismatch-provoked excision	
Pol III holoenzyme	Pol δ	DNA Resynthesis	3' nick-directed MMR
	PCNA		
SSB	RPA, HMGB1	ssDNA binding/protection, enhancement of MMR	
	RFC	ssDNA binding and PCNA loading for 3' nick-directed MMR	
DNA Ligase	DNA ligase I	Ligation of a nick	

*Modified from Li G.M.; Mechanism and functions of DNA mismatch repair, *Cell Research*, 18, 85-98, (2008) (Li 2008)

Given the major function of MMR in correcting biosynthetic errors, MMR also plays a crucial role in DNA damage-induced cell cycle arrest and apoptosis (programmed cell death) (Stojic, Brun et al. 2004, Li 2008). Thus, defects in MMR not only lead to carcinogenesis, but also render cancer cells highly resistant to cytotoxic agents. Treatment of cells with DNA damaging agents such as an alkylating agent, *N*-methyl-*N'*-nitro-*N*-nitrosoguanidine MMR (MNNG), generally stimulates cell death. However, MMR defective cells cannot trigger apoptosis because MMR proteins are involved in apoptosis pathway, resulting in drug resistance. Since most cytotoxic agents are used in chemotherapy, the cancer patients with defects in MMR proteins are hard to be treated by chemotherapeutic drugs. Therefore, understanding MMR mechanism is necessary for developing chemotherapeutic drugs to treat MMR deficiency-induced cancers.

1-3-a. Mismatch Repair in *Escherichia coli*

The MMR pathway in *E.coli* was elucidated in great molecular detail by Paul Modrich's laboratory in the late 1980's. Recombinant DNA technology was used to clone *E. coli* MMR genes and an *in vitro* assay was used to purify MutS, MutL and MutH. Then, MMR was reconstituted *in vitro* using purified proteins, and the components of the MMR pathway were found to include four exonucleases (ExoI, ExoVII, ExoX, and RecJ), DNA helicase II (MutU/UvrD), single-stranded DNA binding protein (SSB), DNA polymerase III holoenzyme, and DNA ligase, as well as MutS, MutL and MutH (Table 1.1). In *E.coli* (Su and Modrich 1986, Grilley, Welsh et al. 1989, Kunkel and Erie 2005), MMR is initiated by MutS, an enzyme that recognizes all base-base mismatches except C:C. In order of relative affinity, MutS binds G:T, A:C, G:A, T:C, A:A, G:G, T:T, G:A, C:T mispairs (Kramer, Kramer et al. 1984, Dohet, Wagner et al. 1985, Su, Lahue et al. 1988). MutS also binds insertion-deletion (ID) mispairs up to four bases in length (Dohet, Wagner et al. 1985, Parker and Marinus 1992). MutS forms a homodimer and possesses intrinsic ATPase, which is essential for its function in MMR. MutS is recruited to mismatches by β -clamp, a critical component of DNA polymerase III holoenzyme and a processivity factor in DNA replication and repair (Lopez de Saro and O'Donnell 2001). After mismatch recognition by MutS, MutS recruits MutL to the DNA (Grilley, Welsh et al. 1989), stimulating ATP-dependent translocation of the MutS–MutL complex (Allen, Makhov et al. 1997). The physical interaction of MutS with MutL enhances mismatch recognition, and the MutS / MutL complex recruits MutH and UvrD (DNA helicase II). Like MutS, MutL possesses an ATPase activity. As mentioned above, the major distinction of *E.coli* MMR from human MMR is how to discriminate between newly synthesized strand and template strand. In

E.coli, the strand specificity of MMR is determined by the asymmetry of hemimethylated dGATC sites (Schofield and Hsieh 2003, Kunkel and Erie 2005), which appears transiently during DNA replication. After DNA replication, the hemi-methylated dGATC sites are rapidly converted to their fully methylated form by DNA adenine methylase (Dam methylase) by addition of a methyl group to the N⁶ position of the adenine in nascent DNA (Junop, Obmolova et al. 2001). However, the newly synthesized strand remains transiently unmethylated during DNA replication, which is called hemimethylated DNA. MutH, whose endonuclease activity is stimulated by MutS / MutL complex, recognizes the asymmetry of hemimethylated DNA (Ban and Yang 1998) and makes a strand specific nick on the daughter (unmethylated) DNA strand (Au, Welsh et al. 1992, Modrich and Lahue 1996). This mechanism is capable of recognizing a hemimethylated dGATC site as a strand specificity signal up to 1 kb 3' or 5' away from the mismatch. The nick becomes the entry point for DNA excision, which is catalyzed by one of four exonucleases (Rec J, Exo I, Exo VII or ExoX) and UvrD helicase, which unwinds dsDNA. Single-strand binding protein (SSB) binds to and protects the template DNA strand from nuclease attack, while the nick-containing strand is degraded by the exonuclease. The DNA excision proceeds bidirectionally in *E.coli*, either 5' → 3' or 3' → 5'. After removal of up to or beyond the DNA mismatch, the single-stranded DNA gap is filled in by DNA polymerase holoenzyme III, and the nick is ligated by DNA ligase. (Figure 1.1)

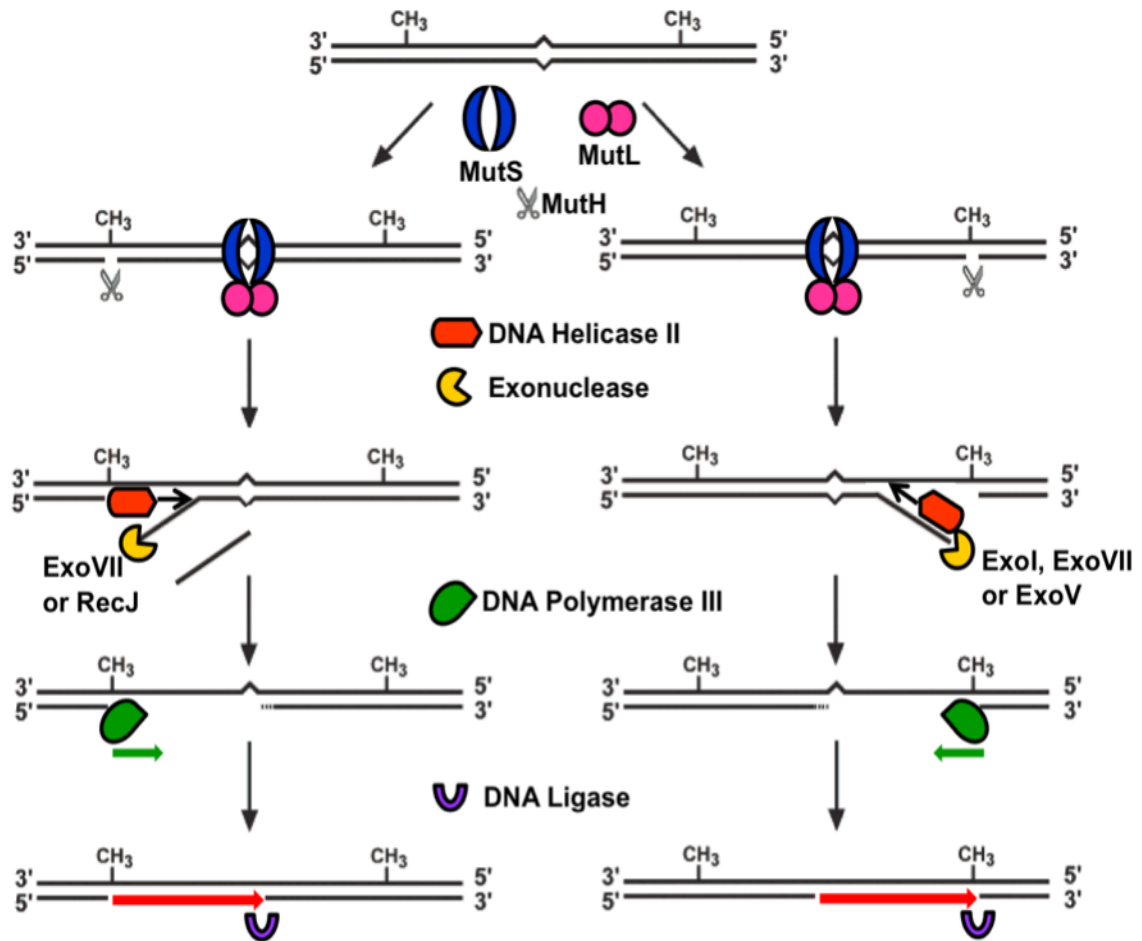


Figure 1.1 Schematic representation of the *E. coli* MMR.

E. coli mismatch repair is initiated by MutS, which recognizes the mismatch and recruits MutL to form the MutS-MutL complex. MutH, which has endonuclease activity, binds and then creates a strand break at the newly synthesized strand of hemimethylated dGATC sites. Excision is initiated at the nick by UvrD and 5'-3' or 3'-5' exonuclease, depending on the location of the nick relative to the mismatch. SSB binds the parental strand and prevents its degradation by nucleases. The single-stranded gap is filled in by DNA polymerase holoenzyme III, and the nick is sealed by DNA ligase.

1-3-b. Mismatch Repair in Human Cells

Human MMR share many features including nick-dependent specificity and bi-directionality with *E.coli* MMR, indicating that MMR is a highly conserved pathway. However, eukaryotic MMR is more complex and does not involve hemimethylated DNA as a strand specificity signal. The number of components is increased in human MMR (Table 1.1). Although a human homolog of MutH has not been identified (Kunkel and Erie 2005), the process still involves a strand specific nick as a strand discrimination signal. However, discontinuities between Okazaki fragments on the lagging strand or the 3' terminus on the leading strand might also play a role in strand discrimination in human MMR, in which hemimethylated dGATC site does not reside (Lopez de Saro and O'Donnell 2001). In human cells, 5 genes encode distinct MutS homologs (MSH2, MSH3, MSH6, MSH4, MSH5), and although bacterial MutS is active as homodimer, human MutS is active as a heterodimer. The most abundant MutS heterodimers are MutS α (MSH2-MSH6) and MutS β (MSH2-MSH3) (Drummond, Li et al. 1995, Genschel, Littman et al. 1998, Bocker, Barusevicius et al. 1999, Kneitz, Cohen et al. 2000). MutS α recognizes base-base mismatches and small insertion/deletions (IDs) (1 or 2 bases) whereas MutS β recognizes longer IDs than 2 bases (Kunkel and Erie 2005). Both MutS α and MutS β possess intrinsic ATPase activity and initiate MMR by recognizing and binding the mismatch. Human MutL homologs also form heterodimers including MutL α (MLH1-PMS2), MutL β (MLH1-PMS1) and MutL γ (MLH1-MLH3) (Li and Modrich 1995, Porter, Westmoreland et al. 1996, Wang and Kung 2002), but only MutL α is thought to be involved in MMR. The biological role of MutL β is not identified, while MutL γ is known to play a role in meiosis. MutL α has weak ATPase activity and binds nonspecifically to DNA, and is recruited by MutS α binding to the mismatch (Kunkel and Erie 2005). MutL α is required for termination of mismatch-provoked excision (Zhang, Yuan et al. 2005) and for initiation of 3' nick-directed MMR serving as an endonuclease (Kunkel and Erie 2005, Kadyrov, Dzantiev et al. 2006, Li 2008). Since human EXO1 exhibits only 5' to 3' exonuclease, MutL α is required for 3' nick-directed MMR to create a nick at 5' side of the mismatch where EXO1 is loaded onto (Kadyrov, Dzantiev et al. 2006). However, knockdown of EXO1 does not cause a mutator phenotype as strong as knockdown of MutS α or MutL α , suggesting that other nucleases may also be involved in MMR (Genschel and Modrich 2003, Wei, Clark et al. 2003). Other MMR components such as RFC (Replication Factor C) and PCNA (Proliferating Cell Nuclear Antigen) are required to activate MutL α endonuclease (Kadyrov, Holmes et al. 2007, Pluciennik, Dzantiev et al. 2010). RFC binds and then loads PCNA onto DNA, and PCNA, which is a processivity factor for DNA polymerase, interacts with several proteins through PIP (PCNA Interaction Proteins) boxes. The PIP box is an 8 amino acids motif: QXXhXXaa (Warbrick 1998, Xu, Zhang et al. 2001). It has been

reported that PCNA enhances the binding ability of MutS α to mismatches, which is induced by PIP-mediated protein-protein interactions (Flores-Rozas, Clark et al. 2000, Shell, Putnam et al. 2007). HMGB1 is a non-histone chromatin protein that facilitates protein-protein interactions and bends DNA molecules (Bustin 1999). It is also involved in mismatch recognition: it interacts physically with MSH2 and MLH1 and enhances mismatch-provoked excision (Yuan, Gu et al. 2004, Zhang, Yuan et al. 2005). Following removal of the mismatch, the gap generated by excision is filled in by DNA polymerase δ with the help of PCNA and RFC, and the nick is ligated by a DNA ligase (Modrich 1991, Hsieh 2001, Kunkel and Erie 2005).

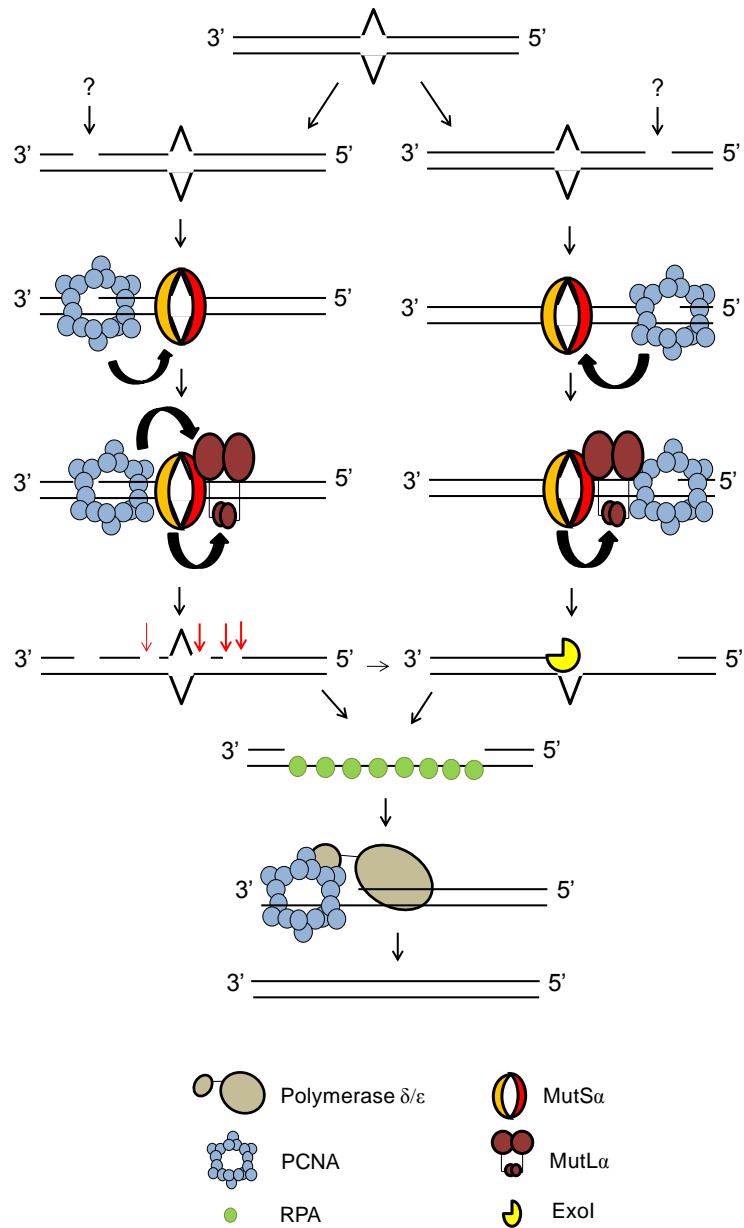


Figure 1.2 Schematic representation of the human MMR.

The mechanism of human MMR is similar to that of *E.coli* MMR, being strand specific, bi-directional and nick-directed. The human MMR is initiated by mismatch recognition of MutS α . Mismatch binding of MutS α triggers downstream signal of MMR including recruitments of MutL α to the DNA and EXO1 to the strand break. Following the removal of the mismatch by excision, the gap on the newly synthesized strand is filled-in by DNA polymerases, and the nick is sealed by a DNA ligase. (Figure adapted from Janice Ortega's dissertation, under preparation)

1-4. Characteristics of MutS α protein

MutS α exists as a heterodimer that consists of two subunits, MSH2 and MSH6, each of which has five functional domains (Figure 1.3): 1) Mismatch binding (1-124 in MSH2/ 362-518 in MSH6), 2) Connector (125-297 in MSH2/ 519-717 in MSH6), 3) Levers (300-456 and 554-619 in MSH2/ 718-934 and 1009-1075 in MSH6), 4) Clamp (457-553 in MSH2/ 935-1008 in MSH6), and 5) ATPase (620-885 in MSH2/ 1076-1355 in MSH6) (Warren, Pohlhaus et al. 2007).

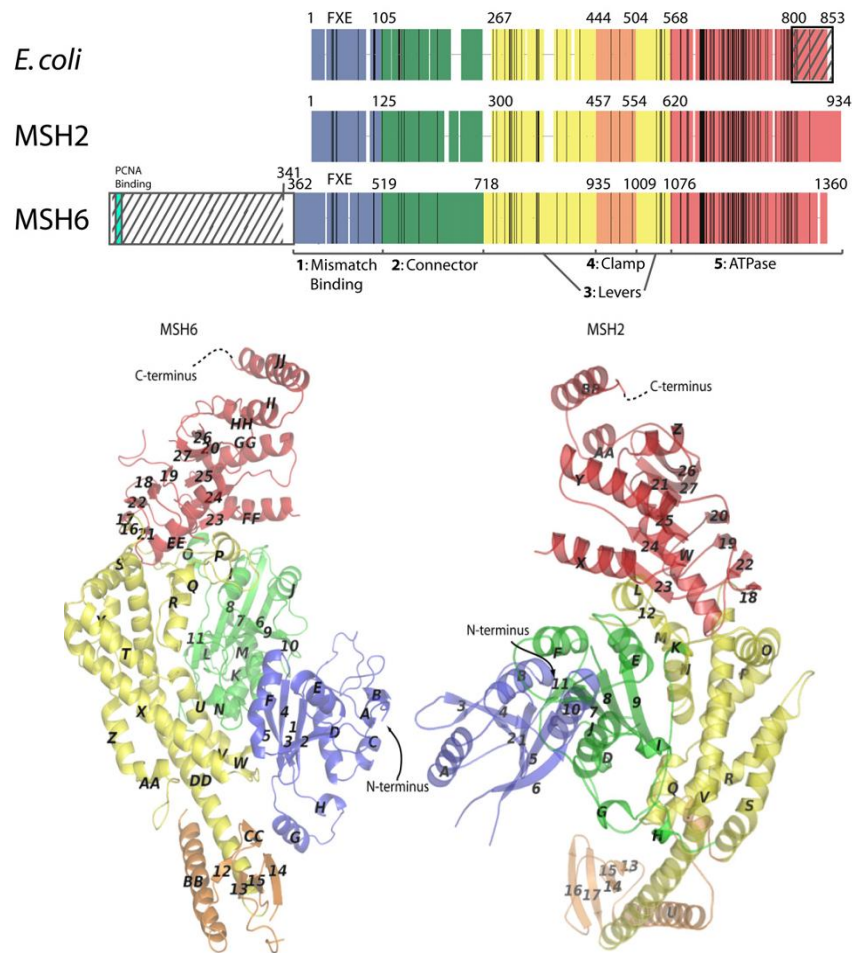


Figure 1.3 Structure of MutS α . (adapted from (Warren, Pohlhaus et al. 2007))

Each subunit of MutS α has 5 functional domains, color-coded as follows: blue, mismatch binding; green, connector; yellow, levers; orange, clamp; red, ATPase. A) Schematic showing color-coded domain structure for *E. coli* MutS, hMSH2 and hMSH6. B) Ribbon diagram representing X-ray structure of MutS α .

MMR is initiated by MutS α (MSH2/MSH6). Previous studies have shown that MSH6 is unstable in the absence of its heterodimer partner, MSH2. Interestingly, only MSH6, but not MSH2, has a conserved Phe-X-Glu motif that recognizes and directly binds to a mismatch (Lamers, Perrakis et al. 2000, Obmolova, Ban et al. 2000, Warren, Pohlhaus et al. 2007, Edelbrock, Kaliyaperumal et al. 2013). The phenylalanine (Phe) residue in Phe-X-Glu motif stacks with a mismatched base and the glutamate (Glu) residue forms a hydrogen bond with the N-3 of a mismatched thymine or the N-7 of mismatched purine (Lamers, Perrakis et al. 2000, Obmolova, Ban et al. 2000, Warren, Pohlhaus et al. 2007, Edelbrock, Kaliyaperumal et al. 2013) (Figure 1.4).

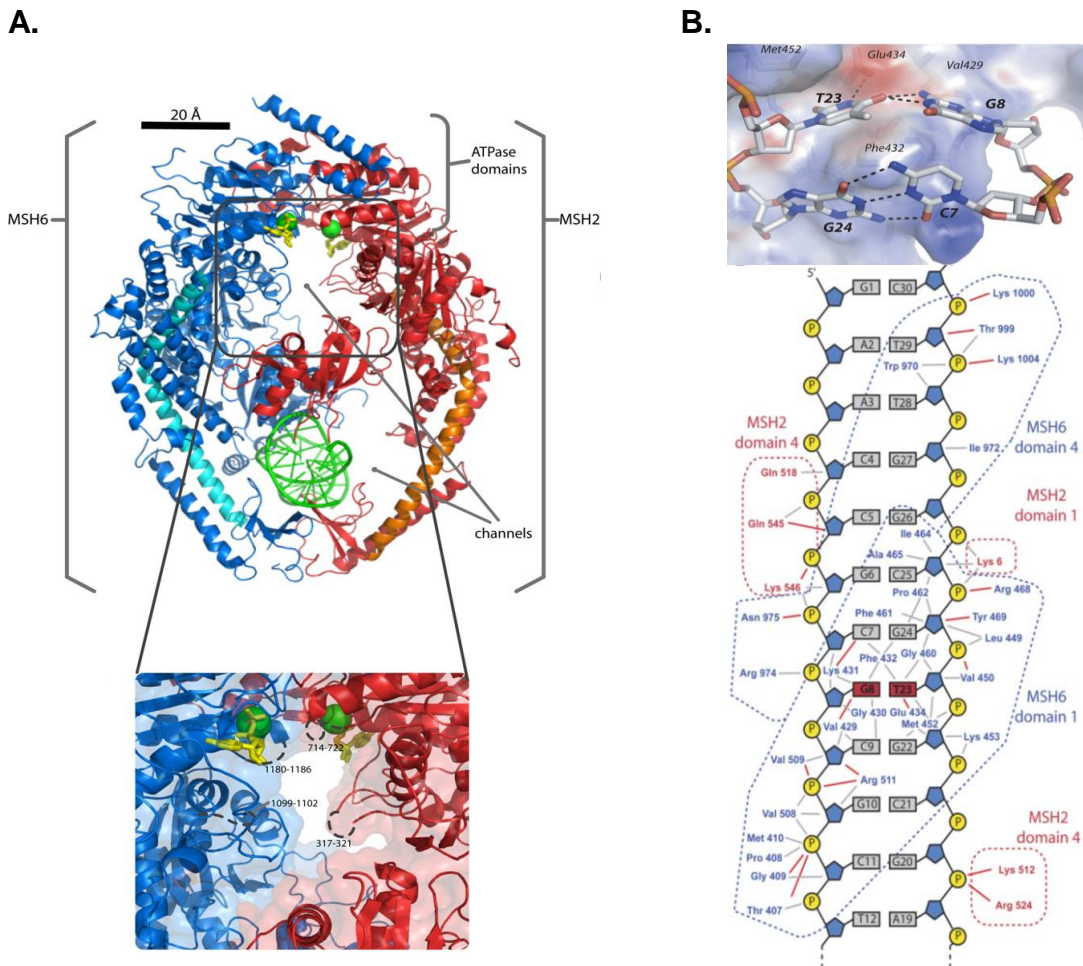


Figure 1.4 Mismatch Binding Mode of MutS α . (adapted from (Warren, Pohlhaus et al. 2007))

(A) Ribbon diagram structure of mismatch-bound MutS α complexed with ADP. MSH6 is shown in blue, MSH2 in red, mismatched DNA in green, ADP in yellow, and Mg²⁺ ions in green spheres. (B) Interactions between MSH6 domain 1 with a G-T mispair and an adjacent base pair. In upper diagram, base pairs are represented with stick diagrams, and electrostatic surface potential is represented by shaded background (shown as sticks under a semitransparent electrostatic surface).

MutS α possess intrinsic ATPase activity, which belongs to the ATP binding cassette (ABC) superfamily. Mutations in the ATPase domains of MSH2 and MSH6 impair MMR, indicating that the ATPase of MutS α is essential during MMR (Iaccarino, Marra et al. 1998, Dufner, Marra et al. 2000). Both MSH2 and MSH6 have ATPase domains that contain highly conserved Walker A and Walker B motifs (Hopfner and Tainer 2003): The Walker A motif- GXXXXGKS/T is the site for nucleotide binding, and the Walker B motif- DD/EXX where aspartic acid is required for ATP hydrolysis (Ramakrishnan, Dani et al. 2002). MSH6 has higher affinity for ATP than MSH2, and stable binding of ATP to MSH6 decreases the affinity of MSH2 for ADP, suggesting that MSH2 and MSH6 have different affinities for the nucleotides (Antony and Hingorani 2003, Martik, Baitinger et al. 2004) . The ATPase domain is the most highly conserved region of MSH2/6 (Warren, Pohlhaus et al. 2007) and is involved in MutS α dimerization (Figure 1.4). The positive charge of the clamp region interacts with the negative charge of the DNA backbone to induce a clamp-like binding pocket in the presence of DNA, and MutS α simultaneously binds ATP and ADP (Blackwell, Bjornson et al. 1998, Blackwell, Martik et al. 1998, Bjornson, Allen et al. 2000). Consequently, ATP binding of MutS α induces its conformational change and then modulates mismatch binding (Figure 1.5). Its ATP binding promotes tightening of the clamp around DNA and initiates sliding along the DNA. However, ATP inhibits mismatch binding by MutS α , subsequently being exchanged for ADP (Gradia, Acharya et al. 1997, Gradia, Subramanian et al. 1999, Wilson, Guerrette et al. 1999, Acharya, Foster et al. 2003, Mendillo, Mazur et al. 2005). Dissociation of MutS α from the mismatch is facilitated by its ATP binding, which results in signaling a series of downstream MMR events (Drummond, Li et al. 1995, Alani, Sokolsky et al. 1997, Gradia, Subramanian et al. 1999). In spite of the extensive studies regarding biochemical functions of MutS α , the role of MutS α ATPase, and the requirement for ATP hydrolysis during MMR remains unclear. Although ATPase activity of MutS α is obviously essential for its function in MMR, whether ATP hydrolysis is required for the initiation of MMR is still under debate.

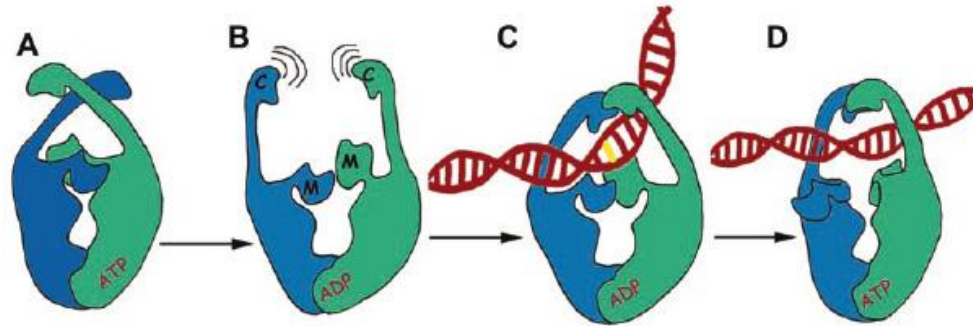


Figure 1.5 Proposed conformational change of MutS α in the presence of nucleotide.

(adapted from (Lamers, Georgijevic et al. 2004))

(A and B) MutS α binds and hydrolyzes ATP in the absence of a mismatch, releasing phosphate. (C and D) MutS α binds to a mismatch in the ADP bound state (short-lived form), and ADP is rapidly replaced with ATP. ATP binding triggers conformational change, resulting in a sliding (long-lived form). The MutS α sliding clamp complexed with ATP facilitates its dissociation from the mismatch and slides along the DNA.

1-5. Involvement of MutS α in Initiation of Mismatch Repair

A strand break is indispensable for discriminating the newly synthesized strand containing a mismatch from the parental strand to initiate MMR in human. In spite of improving effort and progress to identify MMR components over the years, how mismatch-bound MutS α interacts with the strand break to initiate MMR remains a matter of debate. Since the strand break is located several hundred base pairs away from the mismatch *in vivo*, how two physically distant sites communicate each other has been concerned.

Several models to explain initiation of MMR in human cells have been developed. These models are generally classified into “stationary (*trans*)” or “moving (*cis*)” models. The “stationary” model (Figure 1.6 right) postulates that MutS α remains bound to the mismatch, while interactions of MMR proteins are attributed to DNA bending or looping that brings two physical distant sites in proximity (Junop, Obmolova et al. 2001, Guarne, Ramon-Maiques et al. 2004). This model implies the ATPase activity of MutS α is required for mismatch recognition and MutS α interactions with other MMR proteins are required to trigger downstream MMR events.

On the other hand, another proposed model, which is called the “moving” or “*cis*”, propose movement of MMR proteins along the DNA, and are based on the observation that ATP binding induces a conformational change in MutS α , ATP to ADP exchange, and movement of MutS α along the DNA. There are two ‘moving’ models: one postulates translocation and the other postulates sliding. The translocation model (Figure 1.6 left)

proposes that MutS α binds to a mismatch in a nucleotide-free state. ATP binding of MutS α reduces its mismatch-binding affinity, and ATP hydrolysis drives unidirectional translocation of MutS along the DNA away from the mismatch. This model is supported by an electron microscopy study demonstrating that MutS mediates formation of DNA loops at mismatches in an ATP hydrolysis-dependent manner (Allen, Makhov et al. 1997, Blackwell, Bjornson et al. 1998, Blackwell, Martik et al. 1998). However, there is no evidence showing that this model is relevant to human MMR.

In the sliding model (Figure 1.6 middle), MutS α searches for a mismatch in the ADP-bound state, and mismatch binding induces conformational change, resulting in exchange of ADP for ATP. This model invokes that MutS α forms a “sliding clamp”, which travels along the DNA until it encounters a strand discrimination signal (Gradia, Acharya et al. 1997, Fishel 1998, Gradia, Subramanian et al. 1999, Jiang, Bai et al. 2005, Mendillo, Mazur et al. 2005). This model posits that ATP binding, but not ATP hydrolysis, signals downstream MMR events including recruitment of MutL α to a ternary complex and dissociation of MutS α from the mismatch. SPR data has supported this model, showing that MutS α diffuses away from the mismatch faster in the presence of ATP than in the presence of ADP or in the absence of nucleotide (Selmane, Schofield et al. 2003).

Because there is evidence for each model, none of them can be ruled out. Therefore, the studies described in Chapters 3 and 4 of this dissertation were carried out to clarify the molecular mechanism of MMR in human cells.

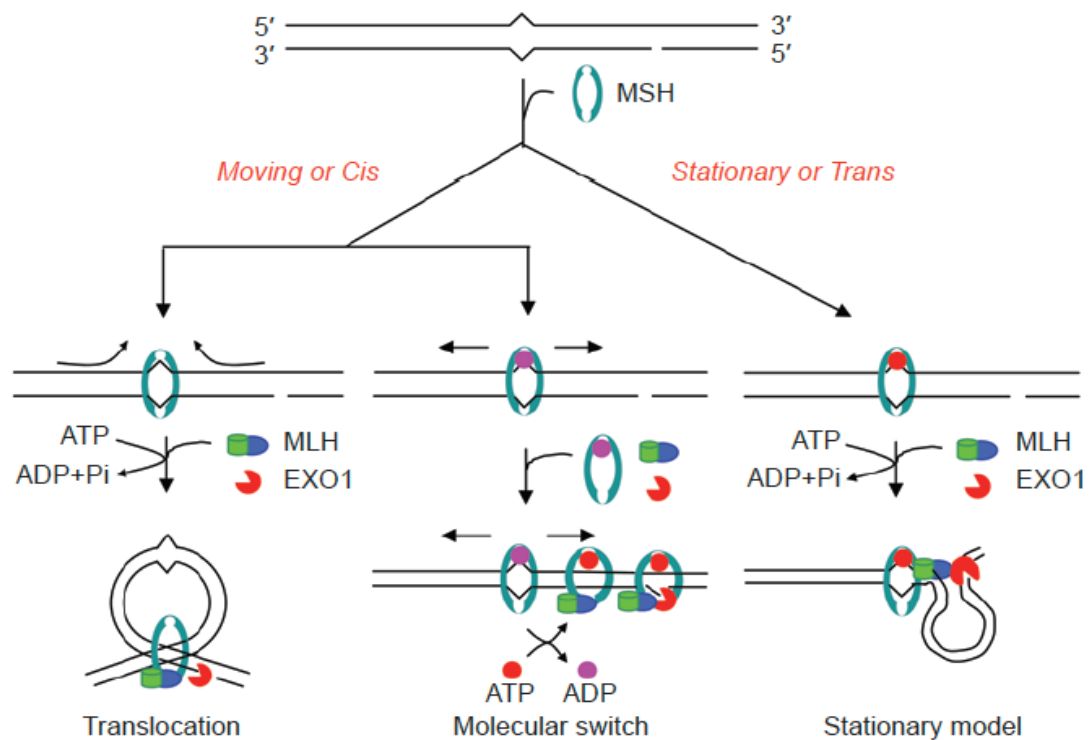


Figure 1.6 Schematic diagrams of strand discrimination during MMR initiation in human cells. (adapted from (Li 2008))

Human MMR targets the newly synthesized strand containing a strand break, because the strand discrimination signal in human MMR is thought to involve a strand break several hundred bp away from the mismatch. In the “stationary” or “trans” model (right), ATP-bound MutS α binds to the mismatch and remains bound at the mismatch, while the DNA bends or forms a loop, allowing the mismatch and the nick in proximity; the DNA looping process requires hydrolysis of ATP by MutS α . There are two “moving-” or “cis-” models for human MMR, the “molecular switch” or “sliding” model, and the “translocation” model. The “translocation” model (Left panel) suggests that MutS α binds to a mismatch in the absence of nucleotide, ATP binding then releases MutS α from the mismatch, and ATP hydrolysis drives translocation of MutS α away from the mismatch. The sliding model proposes that ADP-bound MutS α searches for a mismatch and mismatch binding induces conformational change, resulting in exchange of ADP for ATP. ATP-bound MutS α then dissociates and moves away from the mismatch in an ATP-hydrolysis independent manner.

Research Objectives

Defects in human MMR genes, mainly MSH2 and MLH1, reduce replication fidelity in human cells, increasing the spontaneous mutation rates and promoting carcinogenesis. MMR deficiency is tightly linked to HNPCC and increases risk of endometrial, ovarian, gastric, cervical, breast, skin, lung, prostate, and bladder cancer as well as glioma, leukemia, and lymphoma. Since MMR is also involved in apoptosis pathway, MMR defects cause a decrease in apoptosis and increased survival of cells with DNA damage. Therefore, tumors that carry defects in MMR are resistant to chemotherapeutic drugs such as temozolomide, procarbazine, or cisplatin, which induce apoptotic death in proliferating cells (Li 2008). Human MMR is initiated by MutS α and involves a strand break as a strand discrimination signal (Kolodner and Marsischky 1999). However, in spite of extensive studies, it remains unclear how MutS α transmits a signal from the mismatch to the strand discrimination signal and the precise roles played by MutS α ATPase activity and the nucleotide-induced conformational changes of MutS α . Two controversial models have been proposed to explain this process. Here, we tested these models *in vitro*, using a circular plasmid DNA substrate with a single GT mismatch and conditional physical 'roadblocks', which when present, prevent MutS α from sliding bidirectionally along the DNA. Therefore, improved understanding of the mechanism of MMR is critical to develop tools to selectively kill MMR-deficient (such as HNPCC) or MMR-proficient cancer cells.

CHAPTER TWO

MATERIALS AND METHODS

2-1. Chemicals and Reagents

- Amersham: ECL Detection Reagent
- Fisher Biotech: 1-Butanol, Iso-propanol, KH_2PO_4 (Potassium Phosphate Monobasic), K_2HPO_4 (Potassium Phosphate Dibasic), $\text{KAcNaH}_2\text{PO}_4$ (Sodium Phosphate Monobasic), KOH (Potassium Hydroxide -pellets), NaOH (Sodium Hydroxide), Na_2HPO_4 (Sodium Phosphate Dibasic), $\text{Na}_3\text{C}_6\text{H}_5\text{O}_7 \cdot 2\text{H}_2\text{O}$ (Sodium Citrate), P.E.G.-8000 (Polyethylene Glycol), SDS (Sodium Dodecyl Sulfate), Sodium Bisulfate, Tween-20.
- Gibco: FBS (Fetal Bovine Serum)
- New England Biolab: Restriction enzymes
- MP Biomedicals: bis-acrylamide (N,N'-Methylene-bis-acrylamide)
- Perkin Elmer: $[\gamma\text{-}^{32}\text{P}]\text{-ATP}$, $[\alpha\text{-}^{32}\text{P}]\text{-ATP}$
- Research Products International Corp: Agar, Boric Acid, CsCl (Cesium Chloride), Glycerol, Glycine, HEPES (Free Acid), LB Broth, 2x YT Broth, CH_3COOK (Potassium Acetate), Urea
- Roche: ATP (Adenosine Triphosphate), $\text{ATP}\gamma\text{S}$ (Adenosine-5'-O-(3-thio triphosphate)), dNTPs (deoxy Nucleotides triphosphate), DTT (Dithiothreitol), NP-40 (Nonidet P-40), Superdex G25 column, Protein G-agarose beads, Fugene HD transfection reagent
- Sigma: Acrylamide, Aphidicolin, D-(+)-Glucose, MgCl_2 (Magnesium Chloride), NaCl (Sodium Chloride), KCl (Potassium Chloride), PVP (Polyvinylpyrrolidone), Tris (Trizma-base)
- USB: Agarose, Ammonium Sulfate, Ammonium Persulfate, Exonuclease V (Exo V), EDTA, Ethidium Bromide, Glycine, Heparin, Imidazole, T4-PNK, Phenol, Sucrose.
- USBiological: TNM-FH medium
- Santa Cruz: MSH2, and Tubulin antibodies
- BD Pharmingen: MLH1 and PMS2 antibodies
- Bethyl: MSH6 antibody

2-2. Agarose Gel Electrophoresis

Agarose gel (1% agarose in 1x TAE) electrophoresis was performed in 1x TAE (40 mM Tris-Acetate, pH 8.5, 2 mM EDTA) (Johnson and Grossman 1977). DNA samples were prepared by adding 10x agarose gel loading buffer containing 40% (w/v) sucrose, 0.05% (w/v) bromophenol blue, 0.05% (w/v) xylene cyanol, 20 mM EDTA, and 0.2% SDS. Gels were stained for 30 min in 0.5 µg/mL ethidium bromide (EtBr) and destained for 20 min in ddH₂O. DNA fragments were visualized on an ultraviolet (UV) transilluminator and gel images were captured using a Kodak Image Gel Logic 112 system.

2-3. ATPase activity Analysis

3000 Ci/mmol [γ -³²P]-ATP was purchased from PerkinElmer. ATPase activity of MutS α was analyzed in 20 µL reactions containing 30 Ci/mmol [γ -³²P]-ATP, 1.0 µg protein and 100 ng of mismatch-contained DNA substrates in 25 mM Hepes-KOH (pH 7.6), 4 mM MgCl₂. After incubation at 37°C for 10 min, the reactions were terminated by adding 2x SSCP(Single-Strand Conformation Polymorphism) loading buffer containing 95% (v/v) formamide, 0.05% (v/v) bromophenol blue, 0.05% (v/v) xylene cyanol, and 20 mM EDTA. 5 µL samples were loaded and fractionated through a 20% denaturing polyacrylamide gel (Acrylamide:bis-acrylamide 19:1) in 1x TBE buffer (8.9 mM Tris-HCl, 8.9 mM boric acid, and 0.2 mM EDTA). Dried gels were visualized and quantified using a Typhoon PhosphorImager.

2-4. Buffer Preparation

All solutions and cell culture media were prepared in double-distilled water (ddH₂O). Solutions were sterilized either by autoclaving at 121°C for 30 min or by passage through a 0.22 µm filter.

2-5. Cell Culture

High-Five insect cells were purchased from Invitrogen. The cells were grown in monolayer culture at 25°C in TNM-FH medium (pH 6.2) with 10% heat-inactivated FBS (incubated at 56°C for 30 min and then on ice for 30 min). Sloughing or tapping the flask using moderate force dislodged cells. Since High-Five insect cells doubled in less than 24 hours and provide higher expression level than Sf9 insect cells, High-Five insect cells were used for expressing mismatch repair proteins.

2-6. Electrophoretic Mobility Shift Assay (Gel Shift Assay)

DNA oligonucleotides were synthesized by Integrated DNA Technologies (IDT). Linearized heteroduplex (100 bp) was generated by annealing two complementary 100-mer synthetic oligonucleotides, which form a single G·T mismatch at position 52.

A:5'-GTGGTGGTTACGCGCAGCGTGACCGCTACACTTGCCAGCGCCCTAGCGCC
CGCTCCTTTCGCTTCTTCCCTTCCCTTCTCGCCACGTTCCGCGAATTG-3'

B:5'-CAATTTCGGCGAACGTGGCGAGAAAGGAAGGGAAGAAAGCGAAAGGAGT
GGGCGCTAGGGCGCTGGCAAGTGTAGCGGTCACGTGCGCGTAACCACCAC-3'

The "A" oligomer was radiolabeled with [γ - 32 P]-ATP (3000 Ci/mmol, PerkinElmer) using T4 Polynucleotide kinase in buffer containing 70 mM Tris-HCl (pH 7.6), 10 mM MgCl₂, and 5 mM DTT at 37°C for 1 hr. The reaction was stopped by heating at 75°C for 10 min. After purification through a Sephadex G25 column (Roche), radiolabeled oligonucleotide was annealed to the complementary "B" strand in buffer containing 30 mM HEPES-KOH (pH 7.4), 100 mM KOAc, and 2 mM Mg(OAc)₂·4H₂O. The reactions were terminated by heating at 75°C for 10 min and slowly cooled down to room temperature.

Samples were incubated on ice for 20 min in the presence of 20 mM HEPES (pH 7.5), 40 μ g/mL BSA, 2 mM MgCl₂, 1 mM DTT, 100 mM KCl, and 8% (w/v) sucrose. Reactions were terminated by adding 5 μ L 50% (w/v) sucrose and analyzed by 6% non-denaturing polyacrylamide gel in buffer containing 6.7 mM Tris-acetate (pH 7.5) and 1 mM EDTA as described previously (Gu and Li 2006). 32 P-containing species were detected by Typhoon PhosphorImager.

2-7. Immunoprecipitation Assay

Protein samples were mixed and incubated on ice for 30 min, and diluted antibody was added. The mixture was then incubated at 4°C overnight with rotation. 15-30 μ L of protein G- agarose beads (Roche) were prewashed with 50 mM Tris-HCl (pH 7.6), 500 mM NaCl, and 0.1% NP-40 (washing buffer), added to the protein mixtures and incubated for 1 hr at 4°C with rotation. Immunoprecipitates were recovered by centrifugation at 100 x g at 4°C for 2 min. The supernatant was removed, and the pellet was washed with washing buffer three times. Precipitated protein was resuspended in 6x protein loading buffer containing 125 mM Tris-HCl (pH 6.8), 2% SDS, 20% glycerol, 0.2% bromophenol blue and heated at 90°C for 5 min and loaded onto the gel. SDS-PAGE was performed at 150 V in running buffer containing 2.5 mM Tris, 0.2 M glycine, and 0.1% SDS.

2-8. *In vitro* MMR Assay and Excision Assay

2-8-a. *In vitro* MMR Assay

The *in vitro* MMR assay was performed as described previously (Holmes, Clark et al. 1990) in a 20 μ L reaction containing 30 fmol heteroduplex DNA substrate, 110 mM KCl, 75 μ g nuclear extract (HeLa, N6, or H6) or purified proteins (if required), 10 mM Tris-HCl (pH 7.6), 5 mM MgCl₂, 1.5 mM ATP, 1 mM Glutathione, 50 μ g/mL BSA, and 0.1 mM dNTPs. The heteroduplex DNA substrate contains a mismatch and a strand break which is located at 5' side of the mismatch. Reactions were incubated at 37°C for 20 min, followed by addition of 30 μ L of a proteinase K (PK) solution containing 2.5 mM Tris-HCl (pH 7.5), 5 mM CaCl₂, 12.5% (v/v) glycerol, 6.7% SDS, 25 mM EDTA, and 5 mg/mL proteinase K. PK digestion was performed at 37°C for 20 min, and DNA samples were recovered by phenol extraction twice. DNA was precipitated by addition of 1/10 volume 3 M sodium acetate (NaOAc, pH 5.5) and 2.5 volume of 100% ethanol and incubated at 80°C for 15 min. DNA was pelleted by centrifugation at 14,000 x g at 4°C for 15 min, and washed with 500 mL 70% ethanol, followed by centrifugation at 14,000 x g at room temperature for 5 min. The precipitated DNA pellet was dried by speed vacuum centrifugation and then suspended in 10 μ L ddH₂O. The DNA samples were then incubated with NsiI and BseRI, and cleavage products were separated by 1% agarose gel electrophoresis and visualized by ethidium bromide staining with UV. Typical MMR reaction products include linear dsDNA heteroduplex (7.6 kb) (resistant to restriction enzyme cleavage) and linear homoduplex fragments 4.2 kb and 3.4 kb in length, corresponding to restriction enzyme-cleavage products of correctly repaired DNA.

2-8-b. Excision and Southern Blot Assay

The excision assay was described previously (Holmes, Clark et al. 1990) and was identical to the MMR assay, except that 0.1 mM of dNTPs were omitted to inhibit DNA synthesis. The assay was carried out in 20 μ L containing 30 fmol DNA heteroduplex, 110 mM KCl, 75 μ g nuclear extract (HeLa, N6, or H6) or purified proteins (if required), 10 mM Tris-HCl (pH 7.6), 5 mM MgCl₂, 1.5 mM ATP, 1 mM Glutathione, and 50 μ g/mL BSA. Reactions were incubated at 37°C for 10 min, followed by addition of 30 μ L PK solution. The mixtures were incubated at 37°C for 20 min and DNA was recovered by phenol extraction followed by ethanol precipitation (described above). DNA was resuspended in 10 μ L ddH₂O, incubated with PstI and BglI to score excision products (Figure 2.1.B).

DNA excision intermediates were analyzed using by Southern blot, essentially as described previously (McCulloch, Gu et al. 2003). After digestion with PstI and BglII, the reactions were terminated by addition of 2x SSCP (95% formamide, 0.05% bromophenol blue, 0.05% xylene cyanol, and 20 mM EDTA) and heated at 90°C for 10 min. The excision products were analyzed on a 6% Urea-polyacrylamide denaturing gel (10 g of urea, 3 mL of 40% Acr:Bis (19:1), 3 mL of 10x TBE, 155 µL of 10% APS, 14 µL of TEMED, and 8 mL of distilled water). The gel was pre-run in 1x TBE buffer containing 89 mM Tris-HCl, 89 mM boric acid, and 2 mM EDTA at 16 W for 30 min prior to sample loading (Johnson and Grossman 1977) and run at 8 W for 2 h after sample loading. The gel was transferred to nylon membrane (GE healthcare) in 1x TBE buffer using a Hoefer electrotransfer apparatus at 1 A (38 V) for 1 hr at 4°C. After the electrotransfer, the membrane was air-dried for 10 min and DNA was UV-crosslinked to the membrane for 7 min. The membrane was prehybridized in 50 mM Tris-HCl (pH 7.5), 1 M NaCl, 2% SDS, 1 mM EDTA, 0.5% polyvinylpyrrolidone, and 0.2% heparin and then hybridized at 37°C overnight in 10 mL of the same buffer containing a ³²P-labeled oligonucleotide that hybridizes adjacent to the PstI site in the DNA substrate. The membrane was washed twice with 2x SSC buffer (2x SSC + 0.1% SDS, 20x SSC: 3 M NaCl + 0.3 M Sodium Citrate, pH 7.0) and twice with 1x SSC buffer (1x SSC + 0.1% SDS). Reaction products were visualized by autoradiography.

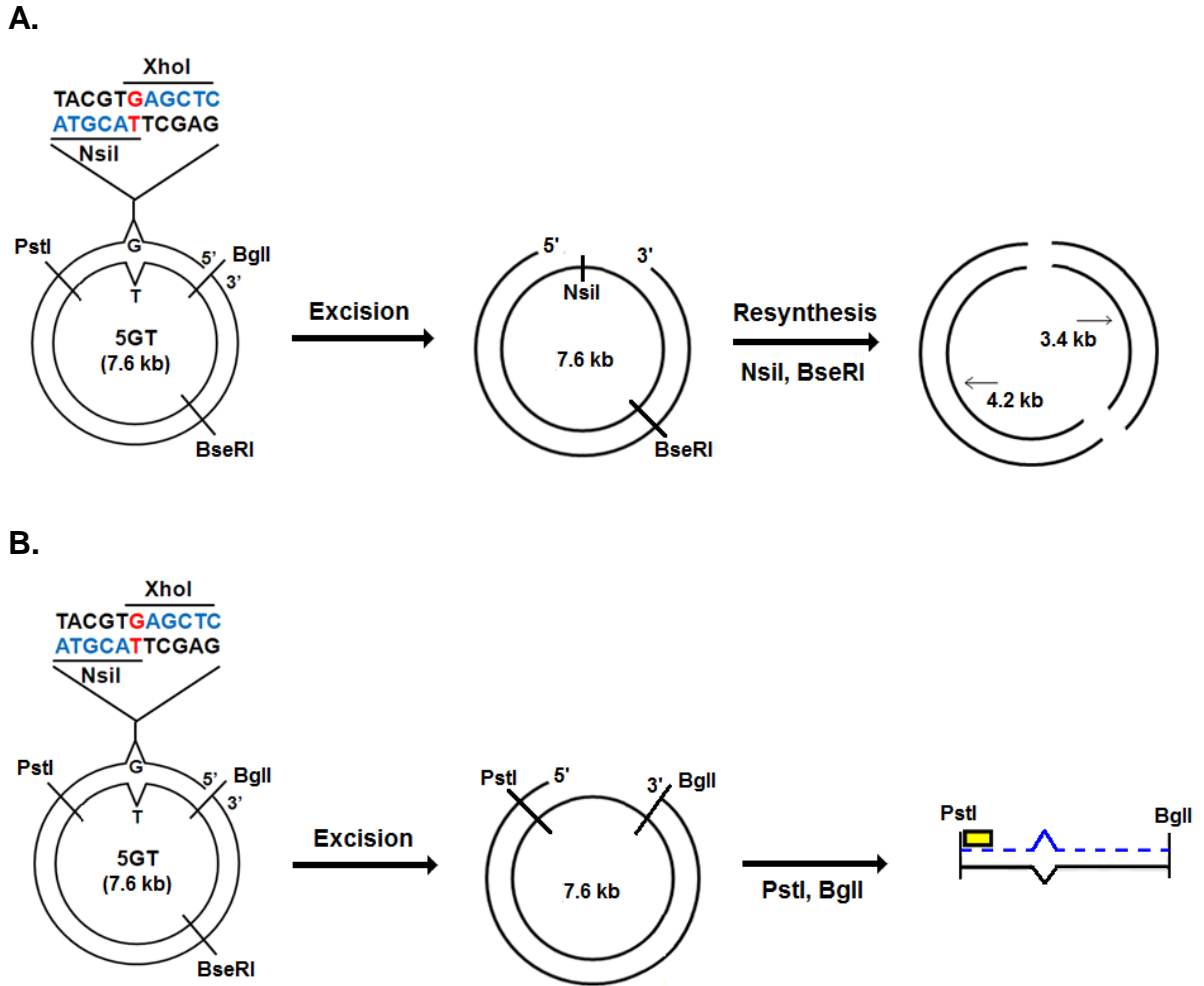


Figure 2.1 Principle of *in vitro* mismatch repair and excision assay.

(A) *In vitro* MMR assay. Heteroduplex DNA substrates contain a G-T mismatch within the overlapping recognition sites for NsiI and XhoI and a strand break 5' to the mismatch. The heteroduplex DNA substrate is incubated with HeLa nuclear extract or purified MMR proteins. Products of nick-directed specific DNA repair are susceptible to cleavage by NsiI, but the non-repaired DNA substrate is not. Thus, 3.4 kb and 4.2 kb Nsi/BseRI cleavage fragments reflect correct repair, while a 7.6 kb DNA fragment reflects lack of repair.

(B) *In vitro* excision assay. Excision assay was performed essentially same as repair assay except omitting exogenous dNTPs to inhibit DNA resynthesis. The reaction products were subjected to cleavage with PstI and BglI and then analyzed by Southern blot using a probe complementary to the PstI site sequence (yellow bar).

2-9. Nuclear Extract Preparation

HeLa-S3 cells and N6 cells were cultured in RPMI-1640 containing 10% Fetal Bovine Serum (FBS) and DMEM containing 10% FBS, respectively. Nuclear extracts were prepared on ice or at 4°C, as described previously (Holmes, Clark et al. 1990). Protease inhibitor cocktail (0.1% PMSF, 1 µg/mL leupeptin, 1 µg/mL pepstatin A) was added to all solutions. Cultured cells were harvested by centrifugation at 3,000 x g for 10 min in an H-6000A rotor. The supernatant was discarded, and the cell pellet was resuspended in wash buffer containing 20 mM Hepes-KOH (pH 7.5), 5 mM KCl, 0.5 mM MgCl₂, 0.2 M Sucrose, 0.5 mM DTT, followed by centrifugation at 3,300 x g for 5 min. Cells were resuspended in hypotonic buffer (2.78 ml/g of cells) including 20 mM Hepes-KOH (pH 7.5), 5 mM KCl, 0.5 mM MgCl₂, 0.5 mM DTT and incubated on ice for 10 min. Swollen cells were disrupted by using a dounce homogenizer on ice to obtain intact nuclei (about 10 to 15 strokes with the B pestle). Cell nuclei were then collected by centrifugation at 2,000 x g, using the Beckman Coulter JA-20 rotor. The cell nuclei pellet was resuspended in extraction buffer (1.39 ml/g cells) containing 20 mM Hepes-KOH (pH 7.5), 5 mM KCl, 0.5 mM MgCl₂, 10% (w/v) sucrose, 0.5 mM DTT, followed by addition of 0.031 volumes of 5 M NaCl. Nuclear proteins were extracted by incubation of the resuspended nuclei on a rotating rack for 60 min at 4°C. After centrifugation at 14,500 x g for 20 min, the nuclear debris was discarded, and the supernatant was collected. 0.42 g/ml of ammonium sulfate was added to the supernatant to precipitate nuclear proteins, and the mixture was slowly stirred on ice for 20 min. Precipitated proteins were pelleted by centrifugation at 15,800 x g for 20 min. The supernatant was completely removed and the protein pellet was resuspended in dialysis buffer (~90 µl) including 20 mM Hepes-KOH (pH 7.6), 50 mM KCl, 2 mM DTT, 0.1 mM EDTA. The slurry was transferred to a dialysis bag, and the mixture was dialyzed until conductivity of the sample reached 50 µS/cm (10 µl sample/4 ml ddH₂O). Dialyzed extract was clarified by centrifugation at 16,000 x g for 15 min at 4°C. Aliquots of 30 to 50 µl were frozen by adding them to liquid nitrogen and stored at -80°C until use. Protein concentrations were measured by the Bradford method (Ausubel and Gitler 1987).

2-10. Nucleotide Binding Analysis

Nucleotide binding was analyzed as described previously (Mazur, Mendillo et al. 2006) with minor modifications. 3000 Ci/mmol [γ -³²P]-ATP and 3000 Ci/mmol [α -³²P]-ATP were purchased from PerkinElmer. Reactions were performed in 20 µL containing 50 mM Tris-HCl (pH 7.8), 110 mM NaCl, 2 mM DTT, 100 mg/mL BSA, 0.5 mM EDTA, 5% glycerol, with or without 5 mM MgCl₂. Non-radiolabeled 1 µM DNA containing a mismatch was added 10 min prior to addition of nucleotide. 1 µg purified MutS α was mixed with [γ or

α -³²P]-ATP and incubated on ice for 20 min. Samples were then subjected to 7 min of crosslinking (UVP Crosslinkers) and immediately heated at 90°C for 5 min after adding 6x protein loading buffer containing 125 mM Tris-HCl (pH 6.8), 2% SDS, 20% glycerol, 0.2% bromophenol blue, which was fractionated by 10% SDS-PAGE gel. Gels were dried by vacuum (BioRad gel dryer) at 80°C for 1 hr and quantified using a Typhoon PhosphorImager.

2-11. Preparation of DNA Substrate

2-11-a. Preparation of Bacteriophage Stock

The M13mp18-GC and M13mp18-AT phage were derived from M13mp18 parental DNA (New England Biolab) as described previously (They were called M13mp18-UKY1 and M13mp18-UKY2) (Su, Lahue et al. 1988). Phage DNA (10-100 ng) was added to 50 μ L XL-1 Blue competent cells (Stratagene) and then placed on ice for 30 min. The mixtures were heated at 42°C for 45 sec, followed by incubation on ice for 2 min. 0.5 mL SOC media (0.5% Yeast Extract, 2% Tryptone, 10 mM NaCl, 2.5 mM MgCl₂, 10 mM MgSO₄, 20 mM Glucose) was added to the transformed cells and then grown at 37°C for 1 hr with shaking at 180 rpm. 30 μ L of transformed cells was mixed well with 3 mL pre-warmed 2x YT soft agar (0.6% agar) containing 200 μ L of fresh overnight-cultured XL-1 Blue cells. The mixture was spread on LB plates, and the plates were incubated at 37°C for overnight. Individual plaques were picked and inoculated into 3 mL 2x YT containing 3 μ L tetracycline (Tet) and 30 μ L overnight-cultured XL-1 Blue cells and cultured at 37°C for 6 hr with shaking at 250 rpm. Cells were harvested by centrifugation at 12,000 x g for 10 min at 4°C to isolate DNA, and the supernatant was collected and stored at 4°C for phage stock. For large scale preparation of phage stock, 50 mL 2x YT containing 50 μ L Tet and 1 mL overnight-cultured XL-1 Blue cells was incubated at 37°C for 90-120 min with shaking at 250 rpm until OD₅₉₀ reached 0.3, and then 500 μ L phage stock was added. The culture was incubated with shaking at 37°C for 6 to 8 hr, and cells were centrifuged at 10,000 x g for 10 min. The cell pellet was removed and the supernatant was saved as phage stock.

2-11-b. Preparation of dsDNA and ssDNA

20 mL of an overnight-cultured of XL-1 Blue cells was inoculated into 3 L 2x YT and the cell culture was grown at 37°C in a shaking incubator for approximately 2.5 hr until OD₅₉₀ reached 0.3. Phage stock (0.8 mL) was then added to the 3 L culture and it was incubated with continuous shaking at 250 rpm at 37°C for 8 h. The culture was allowed to

cool down for 20 min and then cells were harvested by centrifugation at 4,500 x g for 10 min at 4°C. The supernatant was kept for ssDNA preparation. The cell pellet was resuspended in 120 mL ice-cold solution I containing 25 mM Tris-HCl (pH 8.0), 10 mM EDTA, 0.9% (w/v) sucrose and 5 mg/mL lysozyme and incubated at room temperature for 10 min. 240 mL freshly prepared solution II (0.2 N NaOH and 1% SDS) was added, gently mixed, and incubated on ice for 10 min. 180 mL ice-cold solution III including 3 M potassium acetate and 2 M acetic acid was mixed with the lysed cell solution and placed on ice for 10 min. The supernatant was separated from protein debris by centrifugation at 12,000 x g at 4°C for 60 min and filtered through 4 layers of cheesecloth. After measuring the volume of the supernatant, 0.6 volume isopropanol was added, and the mixture was mixed vigorously. The mixture was incubated at -20°C for 15 min and followed by centrifugation at 16,000 x g at 4°C for 30 min to precipitate DNA. The supernatant was discarded, and the pellet was washed with 100 mL 70% ice-cold ethanol. The pellet was air-dried and dissolved in 20 mL 1x TE (pH 8.0) containing 10 mM Tris-HCl pH 8.0, 1 mM EDTA. The solution was weighed and mixed with CsCl (1.1 g/g solution) and 10 mg/mL EtBr (50 µl/g solution) according to the solution weight. All procedures were performed in the dark. The CsCl and EtBr-mixed DNA was transferred to an ultracentrifuge tube, and tubes were placed in a Beckman NVT65 rotor. Samples were spun at 45,000 rpm for 16-18 hr at 25°C. The band of supercoiled DNA was located near to the middle of the tube (nicked DNA is located above the supercoiled DNA) and was removed from the tube using a syringe with a needle. Ethidium bromide was removed from the DNA by extraction with 1 vol water-saturated n-butanol. The aqueous solution containing supercoiled DNA was then dialyzed in TE buffer (pH 8.0). DNA concentration was measured by UV absorption at 260 and 280 nm.

Phage particles were precipitated from the culture supernatant by adding 36 g NaCl/L and 50 g PEG-8000/L of the supernatant. The solution was stirred at room temperature for 1 hr, followed by centrifugation at 5,500 x g at 4°C for 30 min. The pellet was suspended in 22 mL TE buffer, incubated for 1 hr at 37°C with shaking at 150 rpm, and then centrifuged for 10 min at 14,500 x g at 4°C. The pellet was discarded, and the supernatant volume was measured. Phage particles were concentrated by CsCl (0.4342g CsCl/g phage solution) equilibrium centrifugation using the same conditions for dsDNA isolation. The band of phage particles was collected from the centrifuge tube by using a syringe with a needle, and dialyzed against 500 mL TE buffer (10 mM Tris, pH 7.6 and 1 mM EDTA). The buffer was changed at least three times every 6-8 hrs. Single-stranded DNA (ssDNA) was isolated from phage particles by extraction with TE-balanced phenol (3 times) and ethylether (2 times). The extractions were followed by centrifugation at 12,000 x g for 5 min at 25°C. After the last ether extraction, the trace of ether remaining in the solutions was evaporated by

incubation at 37°C for 10 to 30 min. The solution was then dialyzed as described for dsDNA isolation. The DNA concentration was measured by UV absorption at 260 nm.

2-11-c. Preparation of circular heteroduplex substrates

To construct a plasmid DNA substrate containing Lac repressor binding sites, Lac repressor binding sequence was inserted into HindIII restriction enzyme site of M13mp18 dsDNA (Figure 2.3). A mismatch and a ssDNA break (nick) 5' to the mismatch was introduced by denaturing linear dsDNA (GC) and annealing it with circular ssDNA (T) containing one base difference within the complementary sequences (Figure 2.2.C) (Su, Lahue et al. 1988). For this purpose, dsDNA digested with BglI and the ssDNA were mixed with a 5-fold excess of circular ssDNA relative to dsDNA in 30 ml reaction containing 50 mM Tris-HCl (pH 7.6), 100 mM NaCl, 1 mM EDTA, which was adjusted to 0.3 N NaOH (900 μ L of 10 N NaOH). The mixture was incubated at room temperature for 5 min and then added to 3 mL of 2.9 N acetic acid, 1.35 mL of 3 M KCl, and 3.7 mL of 1 M Na-Pi (pH7.4). The reaction was incubated at 65°C for 30 min, slowly cooled down to 37°C for 5 hr, and then incubated for 30 min at 37°C. The solution was placed on ice. The efficiency of annealing was determined by analysis of pre- and post-annealing mixtures (100 ng) using 0.8% agarose gel electrophoresis. (Nicked hetetroduplex migrates more slowly than linear dsDNA and ssDNA.)

Annealing reaction products were applied to Hydroxyapatite (HAP) resin (8 g HAP resin, 1-1.2 g/mg of total DNA) pre-washed and pre-equilibrated at a flow rate of 1-1.3 volume/hr with 30 mM Na-Pi (pH 6.9). The HAP column was washed sequentially with 30 mM Na-Pi (pH 6.9), 160 mM Na-Pi (pH 6.9) (160 drops, 5 ml/tube), and 420 mM Na-Pi (pH 6.9) (40 drops, 1.25 ml/tube) to elute ssDNA and dsDNA respectively (Figure 2.2.D). Aliquots (3 μ L) of fractions eluted by 420 mM Na-Pi (pH6.9) were mixed with 7 μ L EtBr (1 μ g/mL), placed on plastic wrap, and illuminated with shortwave UV (Fisher Sicientific) to estimate DNA content. Fractions with higher DNA concentration were pooled, concentrated 3- to 4-fold by n-butanol extraction, and dialyzed against 500 mL TE buffer (pH 7.6) at 4 °C with 3 buffer changes over approximately 24 h. The DNA concentration was measured by UV absorbance at 260 nm.

Nick-contained circular heteroduplex DNA was separated from linearized homoduplex by digestion with E. coli Exonuclease V (ExoV) (USB) (Figure 2.2.E) in buffer containing 66.7 mM glycine (pH 9.4), 5 mM MgCl₂, 8.3 mM β -mercaptoethanol (β -ME), 0.5 mM adenosine triphosphate (ATP) and 0.2 U/ μ L Exo V (10 U/ μ l) at 37°C for 3 h. During the ExoV digestion (after about 1 hr digestion), pre- and post- ExoV digested DNA samples were taken out to analyze by a 1.0% agarose gel electrophoresis. In the ExoV-digested

product, the linear dsDNA, which migrates faster than the circular heteroduplex would be disappeared. In case of that traces of the linear dsDNA could be observed, ExoV digestion should be continuously incubated at 37°C until the linear dsDNA was undetectable. The reaction was extracted once with phenol, concentrated to 1.0 mL by n-butanol extraction, and exchanged into TE buffer by dialysis.

Oligomers and nucleotides were removed by Sephacryl S500 column chromatography (Pharmacia) equilibrated with TE with 0.3 M NaCl (pH 7.6) at a flow rate of 10-15 mL/hr (40 drops, 1ml/tube). Aliquots (3 μ L) of fractions were mixed with 7 μ L EtBr (1 μ g/mL), placed on plastic wrap, and illuminated with shortwave UV (Fisher Scientific) to estimate DNA content. The purity of the substrate was checked by 1% agarose gel electrophoresis, and fractions with higher DNA concentration were pooled. The DNA substrate was concentrated by n-butanol extraction and exchanged into TE (pH 7.6) buffer by dialysis. The concentration of the DNA was measured by UV absorbance at 260 nm.

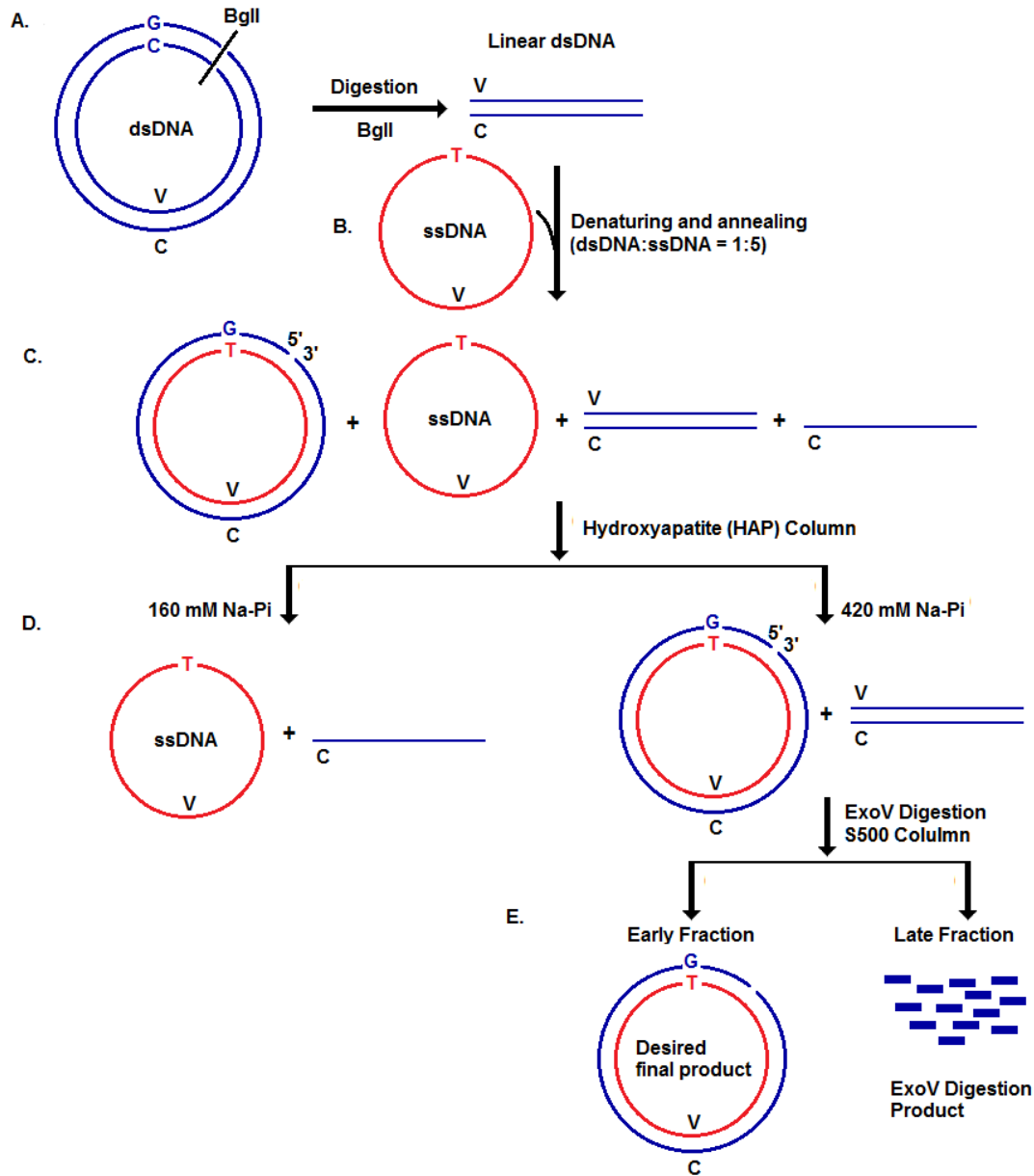


Figure 2.2 Preparation of 5' nicked G-T mismatch substrate.

(A) Circular homoduplex M13mp18-GC dsDNA (blue) was linearized with BglII (V= viral strand; C= complementary strand). (B) Linear dsDNA was denatured and annealed in the presence of excess circular M13mp18-AT ssDNA (red). (C) Reaction products include nicked circular heteroduplex, circular ssDNA, linear dsDNA and linear ssDNA. (D) Hydroxyapatite column was used to separate dsDNA from ssDNA. (E) Linear homoduplex dsDNA was digested with *E. coli* Exo V into 1-5 nucleotide fragments, which were separated from circular heteroduplex dsDNA by Sephacryl S500 size exclusion chromatography.

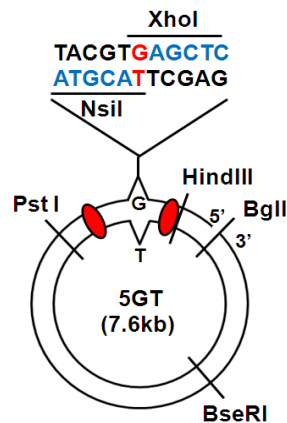


Figure 2.3 Schematic representations of 5' nicked G-T heteroduplex substrates containing two Lac repressor-binding sites.

5' nicked G-T heteroduplex substrate used for *in vitro* MMR assay was derived from M13mp18 phage. It was constructed to contain a mismatch, a strand break (a strand discrimination signal) and two Lac repressor-binding sites. A mismatch is located within the overlapping recognition sites for two restriction enzyme sites, NsiI and XhoI.

2-12. Purification of Lac repressor and Nuclease activity Assay

The gene encoding Lac repressor was cloned into the EcoR I site of pBR322 (Chen and Matthews 1992, Falcon, Swint-Kruse et al. 1997, Glascock and Weickert 1998, Swint-Kruse, Zhan et al. 2003) and the resulting plasmid was transformed into *E.coli* BLIM cells. After transformation, cells were cultured in LB overnight at 37°C with shaking and then harvested by centrifugation. The pellets were dissolved in lysis buffer (0.2 M Tris-HCl (pH 7.6), 0.2 M KCl, 0.01 M MgAC₂, 0.3 mM DTT, 5% glucose, 50 µg/L PMSF) plus 0.5 mg/mL lysozyme. Cell debris was removed by centrifugation, the supernatant was recovered, and proteins were precipitated by addition of 40% Ammonium Sulfate (Figure 2.4.A). Samples were incubated at 4°C for 1 hr, protein pellets recovered by centrifugation, pellets resuspended in dialysis buffer containing 0.05 M Potassium phosphate (pH 7.5), 0.3 mM DTT, 5% glucose and dialyzed overnight at 4°C. The dialyzed protein was passed through a 5 mL heparin column (GE Healthcare) pre-equilibrated with 20% buffer D (1 M NaCl, 25 mM Hepes (pH 7.8), 1 mM EDTA, 2 mM DTT, 1x protease inhibitor cocktail). The column was washed with 6 column volume of 20% buffer D and eluted with a gradient of 20-75% buffer D. Fractions containing Lac repressor were identified by SDS-PAGE (Figure 2.4.B), and pooled fractions were concentrated to 1 mL using a centrifugal filter spin column (Amicon Ultra Centrifugal Filters). The concentrated protein was further

purified by Superdex™ 200 Gel filtration column (GE healthcare) in 15% of buffer D. Fractions containing Lac repressor were identified by SDS-PAGE and pooled (Figure 2.4.C), and protein concentration was measured by Bradford assay. To store the purified protein, 1 mg/mL bovine serum albumin (BSA) and 10% sucrose were added to stabilize the protein in freezing and thawing process. The proteins were dispensed into aliquots, frozen in liquid nitrogen and stored at -80°C until use.



Figure 2.4 Purification of Lac repressor.

Red rectangle indicates Lac repressor. (A) Cell lysate precipitated by 40% Ammonium Sulfate. (B) Lac repressor purified via heparin column, which is used for purification of DNA binding protein. (C) Lac repressor purified through S200 Gel Filtration column. All steps after the purification were analyzed by 10-12% SDS-PAGE.

To test contaminating nuclease activity of the purified protein, protein samples were incubated with 30 bp of 5'-³²P-labeled dsDNA in buffer containing 125 mM Tris-HCl (pH 7.6), 25 mM MgCl₂, 0.5 mg/mL BSA, 50% glycerol, and 10 μM DTT. Reaction products were separated by denaturing 20% PAGE (12.5 g of Urea, 12.5 ml of 40% Acr/Bis (19:1), 2.5 ml of 10x TBE, 190 μl of 10% APS, and 13 μl of TEMED).

2-13. Purification of MutS α , MutS β , and MutL α from High-Five insect cells

Baculovirus stocks for overexpression of human MSH2 and MSH6 were generous gifts of Dr. Josef Jiricny (University of Zurich). These reagents are based on the Bac-to-Bac expression system (Invitrogen), which was used to express and purify MutS α protein subunits according to the manufacturer's instructions. The pFastbac1 plasmids encoding MSH2, and MSH6_{his} were transformed into DH10-Bac *E. coli* cells and positive colonies were identified by PCR. High Five insect cells were purchased from Invitrogen and cultured

in TNM-FH medium (US biological) including 10% FBS (Gibco). Bacmids bearing encoding MSH2 or MSH6_{his} were transfected into High-Five insect cells using Fugene HD transfection reagent in 6 well plates. The virus-inoculated insect cells were cultured for 48-72 hr and collected by centrifugation at 1,200 x g for 5 min, followed by washing in PBS. The baculovirus stock was amplified and used to inoculate 60-80% confluent insect cells in 10 dishes of 150 cm². Infected cells were incubated for 48 hr, collected by centrifugation at 1,200 x g for 5 min, washed once with PBS and centrifuged at 1,200 x g for 5 min. Pellets were resuspended in buffer A (5 mL/g) containing 20 mM Imidazole, 25 mM Hepes-KOH (pH 7.8), 2 mM DTT, 300 mM NaCl, 10% (v/v) glycerol, and 1x protease inhibitor cocktail and then disrupted using a Dounce homogenizer (10 to 12 strokes). The homogenized cells were then sonicated 10X for 15 seconds at 15 sec intervals, using a Fisher Scientific sonicator at 30-40% strength. Cell debris was removed by centrifugation at 20,000 x g for 1 hr at 4°C using the Beckman Coulter JA-20 rotor. The supernatant was collected and loaded onto a 5 mL His-tag Nickel column (GE Healthcare) pre-equilibrated with buffer A. The column was washed with 8 column volume of 100% buffer A and then eluted with a gradient of 0-80% buffer B (500 mM Imidazole, 25 mM Hepes-KOH (pH 7.8), 2 mM DTT, 300 mM NaCl, 10% (v/v) glycerol, and 1x protease inhibitor cocktail). Peak fractions were identified by SDS-PAGE, pooled and diluted with buffer C (25 mM Hepes (pH 7.8), 1 mM EDTA, 2 mM DTT, and 1x protease inhibitor cocktail) to a conductivity equivalent 150 mM KCl. The pooled protein was loaded onto a 1 mL Mono Q column (GE healthcare) pre-equilibrated with 15% buffer D containing 1 M NaCl, 25 mM Hepes (pH 7.8), 1 mM EDTA, 2 mM DTT, and 1x protease inhibitor cocktail. The column-bound protein was washed with 10 column volume of 15% buffer D and eluted with 15-70% buffer D. Peak fractions were pooled, concentrated to 1 mL, using a centrifugal filter spin column (Amicon Ultra Centrifugal Filters) at 5,000 rpm. The concentrated protein was then loaded onto 25mL SuperdexTM 200 Gel Filtration (GE healthcare) and eluted with 15% buffer D. Peak protein fractions were detected by SDS-PAGE, protein concentration was measured by Bradford assay, adjusted to 1 mg/mL bovine serum albumin (BSA) and 10% sucrose, and divided into aliquots, which were frozen in liquid nitrogen and stored at -80°C until use.

2-14. SDS-Polyacrylamide Gel Electrophoresis (SDS-PAGE)

SDS-PAGE gels were prepared using a 30% acrylamide stock solution (acrylamide:bis-acrylamide=30%:0.8%) (Okajima, Tanabe et al. 1993). Protein samples were mixed with 6x protein loading buffer containing 125 mM Tris-HCl (pH 6.8), 2% SDS, 20% glycerol, 0.2% bromophenol blue, followed by heating at 90°C for 5 min. SDS-PAGE

was performed at 150 V in the buffer containing 2.5 mM Tris, 0.2 M glycine, and 0.1% SDS.

2-15. Site-directed Mutagenesis

Site-directed mutagenesis, which was used to make point mutations, switch amino acids, and delete or insert single or multiple amino acids, was performed as described previously (Kirsch 1987, Kirsch and Joly 1998). Briefly, primers for PCR were constructed by using QuikChange primer design program through Agilent Technologies website. Parental DNA was amplified by PCR using the designed primers and high fidelity DNA polymerase. The amplified products were treated with *Dpn I* to cleave methylated G^mATC sites in parental DNA, sparing newly synthesized DNA containing site-directed mutations. *Dpn I*-digested product was transformed into XL-1 Blue or DH5 α cells by heat-shock. Positive colonies were selected and cultured in LB containing 100 μ g/mL of ampicillin. DNA was isolated from individual colonies and screened by PCR and sequencing.

2-16. Transfections into the Insect cells

Transfections into insect cells were performed using the Fugene HD transfection reagent. DNA was diluted in 100 μ l of serum-free medium with appropriate diluents (around 1-2 μ g). Fugene HD reagent was directly added into the diluted DNA with 3:1 ratio (3 μ l Fugene HD reagent: 1-2 μ g DNA) and mixed vigorously by either tapping or vortexing. The mixture was incubated at room temperature for 30 min to allow complex formation and then added into the 60 to 80% confluence cell cultures in 6-well plates. Transfection was performed based on Fugene HD protocol.

2-17. Transformations of Competent Cells

Frozen aliquots of 50 μ L competent cells (*E.coli* XL-1 Blue or DH5 α , or DH10 Bac) were thawed on ice. DNA (100 to 500 ng) was added to the competent cells and incubated on ice for 30 min. The DNA-cell mixture was heated at 42°C for 45 sec, followed by incubation on ice for 2 min (Mandel and Higa 1970). Then, 0.5 mL of SOC (or LB or 2x YT) was added and cells were incubated for 1 hr at 37°C with shaking at 200 rpm. Transformed cells were spread on LB plates containing selective antibiotic and the plates were incubated overnight at 37°C.

2-18. Western Blot Analysis

50 µg whole lysates or nuclear extract or 1 µg purified-protein was fractionated by 8~15% SDS-PAGE. Proteins were transferred onto nitrocellulose membrane using a BioRad electrotransfer device for 1 hr at 400 mA in transfer buffer (3.03 g Tris, 14.4 g glycine/L, and 200 ml/L methanol) (Renart, Reiser et al. 1979, Towbin, Staehelin et al. 1979, Okajima, Tanabe et al. 1993). The nitrocellulose membrane was blocked in 5% nonfat dry milk and TBS-T (10 mM Tris-HCl (pH 7.5), 0.8% NaCl, 0.1% (v/v) Tween 20) for 1 h at room temperature. The membrane was incubated overnight with the same solution containing primary antibody (1:1000 dilution in 5% nonfat dry milk). The blot was washed 3X for 5 min in TBS-T, incubated at room temperature for 1-3 hr with secondary antibody conjugated with horseradish peroxidase (Sigma) diluted in the same buffer. The membrane was washed 3X for 5 min with TBS-T at room temperature, and proteins were detected using ECL detection reagents (Roche) and autoradiography.

CHAPTER THREE

SLIDING OF MUTS α TO COMMUNICATE WITH A STRAND BREAK IS NOT ESSENTIAL FOR THE INITIATION OF MISMATCH REPAIR.

INTRODUCTION

Mismatch repair (MMR) is mainly responsible for improving replication fidelity by reducing the spontaneous mutation rates and carcinogenesis, which induces to maintain the integrity of the whole genome. Defects in human MMR eventually lead to development of hereditary non-polyposis colorectal cancer (HNPCC) and are also linked to other human cancers. The mechanism of MMR is highly conserved through evolution, but there are notable differences in how prokaryotic and eukaryotic MMR discriminate between the parental and the newly synthesized DNA strands. It has been proposed that eukaryotic MMR utilizes a strand-specific nick, and is therefore nick-directed, while prokaryotic MMR utilizes hemi-methylated dGATC sites for this purpose. MutS α , which consists of the MSH2 and the MSH6 subunits and recognizes a mismatch, initiates human mismatch repair. Mismatch binding by MutS α triggers a series of downstream mismatch repair (MMR) reactions including interacting and communicating with other MMR proteins (Gradia, Acharya et al. 1997, Blackwell, Bjornson et al. 1998). Since eukaryotic EXO1 exhibits only 5' \rightarrow 3' excision, mismatch binding by MutS α activates EXO1-catalyzed excision directly only when a strand break is located at 5' side of the mismatch. For the 3'-directed MMR, more MMR proteins such as MutL α , PCNA, and RFC play a role in formation of a strand break as an initial point of MMR (Zhang, Yuan et al. 2005). However, in spite of improving effort and progress to identify MMR components over the years, it remains unknown how MutS α facilitates communication between the mismatch and the strand discrimination signal (the nick) to initiate MMR, and how the MutS ATPase and/or ATP-dependent conformational changes of MutS α contributes to the mechanism of MMR in human cells. The experiments described in this chapter were designed to provide new molecular information about the process of strand discrimination during MMR in human cells.

Several putative models to explain initiation of MMR have been developed and proposed. Since the entry point, a single-strand break, is positioned several hundred base pairs away from the mismatch *in vivo*, identifying how two physically distant sites communicate each other is essential to understand MMR mechanism. MMR initiation models are generally classified into “stationary (*trans*)” or “moving (*cis*)” models. The “stationary” model (Figure 1.6 right) proposed that MutS α remains bound at the mismatch, while interactions of MMR proteins are attributed to DNA bending or looping that brings

two physical distant sites in proximity (Junop, Obmolova et al. 2001, Guarne, Ramon-Maiques et al. 2004). This model postulated that ATPase activity of MutS α is required for proofreading mismatch recognition and inducing MutS α interactions with other MMR proteins that trigger downstream signaling of MMR (Wang and Hays 2003, Wang and Hays 2004). Another proposed model, which is called the “moving” or “cis”, is based on the movement of MutS α along the DNA, but varies in terms of energy requirement for the movement of MMR proteins along the DNA. There are two ‘moving’ models: One is translocation model, and the other is sliding model. In translocation model (Figure 1.6 left), it is proposed that MutS α binds to a mismatch in a nucleotide-free state, and ATP binding of MutS α reduces its mismatch-binding affinity. ATP hydrolysis consequently drives unidirectional translocation of MutS along the DNA away from the mismatch (Allen, Makhov et al. 1997, Blackwell, Bjornson et al. 1998, Blackwell, Martik et al. 1998). However, there is no evidence showing that this model is relevant to human MMR. In the sliding model (Figure 1.6 middle) ADP-bound MutS α searches for a mismatch, and mismatch binding by MutS α induces its conformational change and exchange of ADP for ATP. ATP-bound MutS α then forms a “sliding clamp”, which travels along the DNA until it encounters a strand discrimination signal (Gradia, Acharya et al. 1997, Fishel 1998, Gradia, Subramanian et al. 1999, Jiang, Bai et al. 2005, Mendillo, Mazur et al. 2005). This model posits that ATP binding, but not ATP hydrolysis, signals downstream MMR events including recruitment of MutL α to a ternary complex and dissociation of MutS α from the mismatch (Selmane, Schofield et al. 2003).

As described in Chapter 1, there is evidence to support the stationary and the sliding models for human MMR, but it is not possible at present to rule one of the models in or out. To provide definitive evidence for or against one model, we developed a specialized DNA substrate with physical “roadblocks” and used them in an *in vitro* DNA excision or MMR assay system. Lac repressor/Lac operator was used as a physical “roadblock” to restrict sliding window of ATP-bound MutS α to the DNA region intervening between two roadblocks.

The Lac repressor/operator system is well studied, and its role in regulating genetic expression in bacteria is well understood. In brief, the Lac repressor (Lac I), a high affinity 37 kDa DNA binding protein that exists as a homotetramer (Swint-Kruse, Elam et al. 2001), is released from the DNA by IPTG (Isopropyl β -D-1-thiogalactopyranoside). In the experimental system used here, the roadblocks can be turned on by omitting IPTG and turned off by adding IPTG, a feature used here as a switch to turn MutS α sliding off or on, respectively. Our results demonstrated that restriction of MutS α sliding by presence of dual physical roadblocks significantly inhibits *in vitro* MMR, but they do not inhibit

mismatch-provoked excision. Therefore, the results presented here provide evidence that MutS α sliding is not required during the strand discrimination step of human MMR.

RESULTS

Purification and functional tests of Lac repressor and MutS α proteins.

The first steps for these experiments was to prepare Lac repressor protein and human MutS α , as described in Chapter 2, to characterize the quality of the protein samples and to test the assumptions inherent in the experimental system. Figure 3.1.A & C show protein gel analysis of the purified proteins to verify their level of purity and assay of Lac repressor for contaminating nuclease activity (Figure 3.1.B)

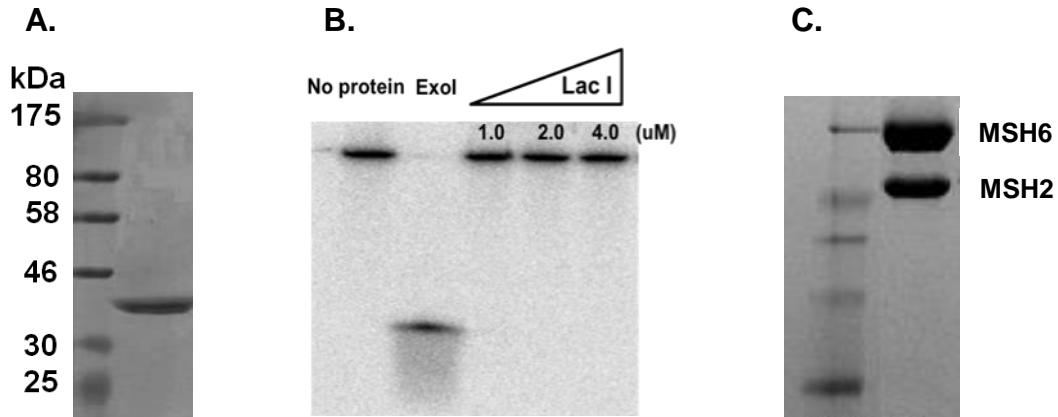


Figure 3.1 Purification of Lac repressor and MutS α proteins.

(A) Purified Lac repressor analyzed by 12% SDS-PAGE. (35 kDa) (B) Nuclease activity of purified Lac repressor on ³²P-labeled linear dsDNA was analyzed by 20% sequencing gel. (C) Purified MutS α analyzed by 10% SDS-PAGE (MSH2: 104.7 kDa, MSH6: 163 kDa).

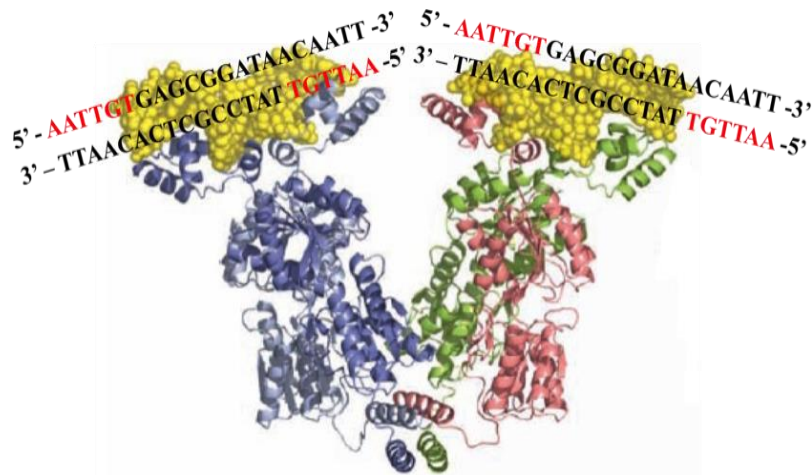
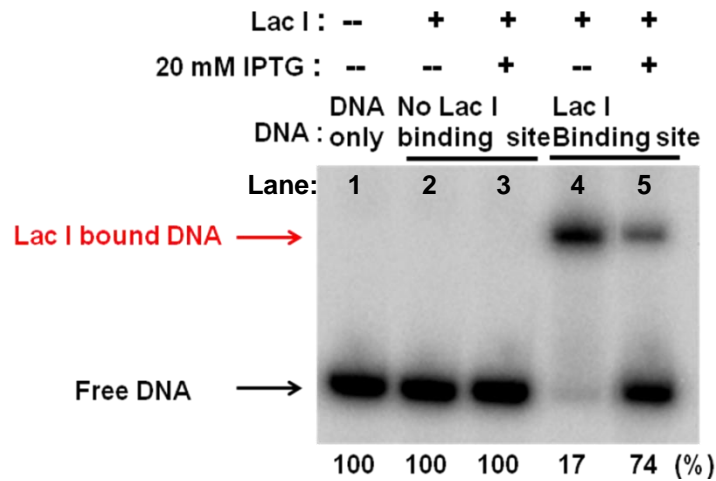


Figure 3.2 Crystal structure of tetramer Lac repressor and its binding sequence.

Lac repressor is a homotetramer DNA binding protein that recognizes 5'-AATTGT-3' in the context of the 20 nucleotides Lac operator 5'-AATTGTGAGCGGATAACAATT-3'.

To examine the interaction between purified Lac repressor and Lac repressor-binding site, 198 bp of ³²P-labeled DNA containing either random sequence or Lac repressor-binding sequence (Figure 3.2) was used to perform EMSA. As shown in Figure 3.3.A, Lac repressor binds to DNA containing Lac repressor-binding sequence (lane 4), but not to a nonspecific DNA oligonucleotide substrate. Another experiment was performed to confirm that IPTG releases Lac repressor from its binding site (Figure 3.3.A, lane 5). The result showed that addition of IPTG causes dissociation of most Lac repressor complexes, but some Lac repressor-DNA complexes persist in the presence of 20 mM IPTG. However, higher concentration than 20 mM IPTG did not stimulate more complete dissociation of Lac repressor from its binding site (Figure 3.3.B).

A.



B.

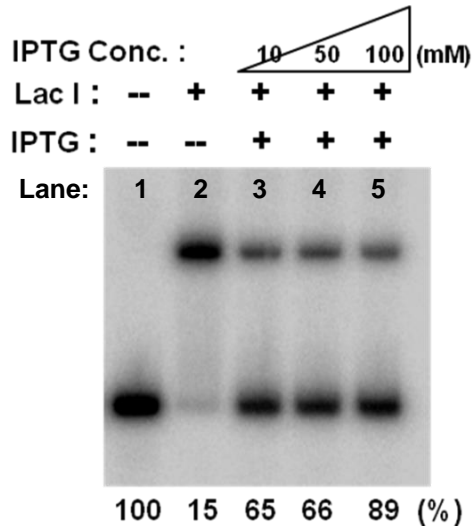


Figure 3.3 Binding of purified Lac repressor to Lac repressor-binding site and dissociation of Lac repressor from DNA by induction of IPTG.

(A) Specific interaction of Lac repressor with its binding sequence. Lac repressor ($0.7 \mu\text{M}$) was incubated with $0.32 \mu\text{M}$ ^{32}P -labeled DNA substrate and 10x fold excess of nonspecific competitor DNA (198 bp of ^{32}P -nonlabeled DNA composed of random sequence) and reactions were analyzed by EMSA. (B) EMSA was performed in the presence of increasing concentration of IPTG. Bands were quantified using Kodak Image Software.

Sliding of MutS α along the DNA is restricted by Lac repressor roadblock.

EMSA assays were performed to identify if MutS α sliding was prevented by Lac repressor roadblock. Linear ^{32}P -labeled dsDNA substrate (300bp) containing a G-T mismatch as well as 5' and 3' flanking Lac repressor-binding sites were pre-incubated with Lac repressors and then incubated with MutS α in the presence or absence of ATP. As expected, both Lac repressor and MutS α bind to the DNA substrate (Figure 3.4-lane 2 and 6) and the MutS α -bound DNA band was supershifted in the presence of Lac repressor (Figure 3.4-lane 4), indicating that both Lac repressor and MutS α can bind to a single DNA molecule. Furthermore, binding of Lac repressor was ATP-independent (Figure 3.4-lane 3), while binding of MutS α was ATP-dependent (Figure 3.4, lane 7). Because MutS α can dissociate from the mismatch and slide along the DNA in the presence of ATP but not in its absence, or in the presence of ADP, the complex between MutS α and the DNA is reduced in amount or absent in the presence of ATP (Figure 3.4-lane 7). This is consistent with the idea that ATP-bound MutS α diffuses away from a mismatch (Gradia, Acharya et al. 1997, Gradia, Subramanian et al. 1999, Wilson, Guerrette et al. 1999, Acharya, Foster et al. 2003, Mendillo, Mazur et al. 2005) and falls off the end of a linear DNA substrate. As predicted, the supershifted DNA-protein complex containing MutS α and Lac repressor remained supershifted and did not dissociate from the DNA in the presence of ATP (Figure 3.4-lane 5). This indicates that the Lac repressor roadblock lying between the mismatch and each end of the linear dsDNA restricted movement of MutS α . Therefore, these data confirmed that MutS α moves by sliding along DNA but not bypassing the Lac repressor roadblock, which validates the experimental system and its ability to test the prevailing models of human MMR.

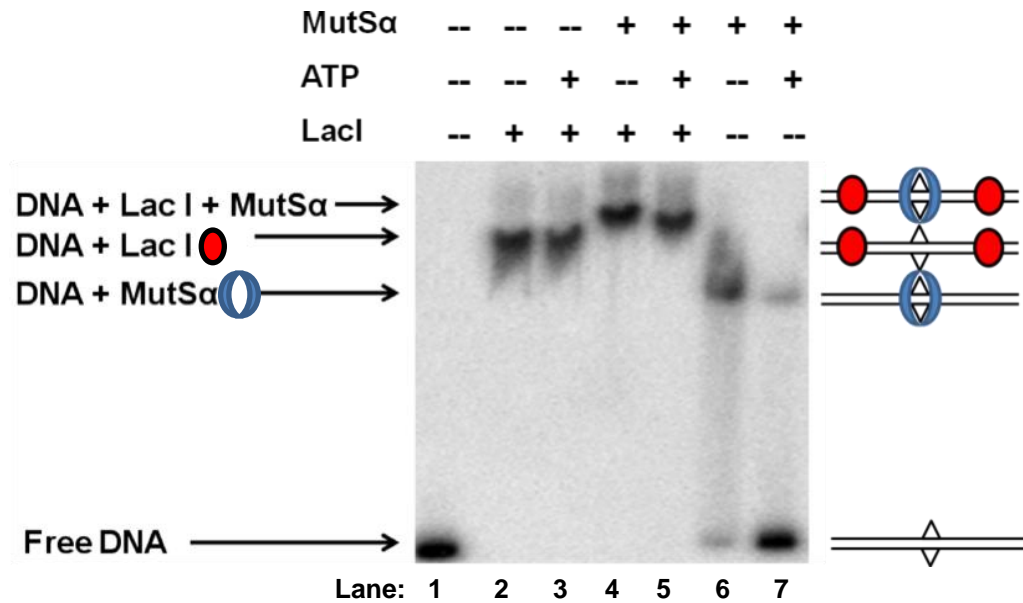


Figure 3.4 Interaction between MutS α and mismatch-contained heteroduplex DNA in the presence or absence of Lac repressor roadblocks.

EMSA was performed, incubating 300 bp ^{32}P -labeled linear homoduplex substrate containing a centrally located G-T mismatch as well as Lac repressor binding sites 5' and 3' to the mismatch with MutS α (two blue-colored moon shapes facing each other) in the presence or absence of Lac repressor (red oval) and ATP. Reaction products were analyzed on a non-denaturing gel (see methods). Movement of MutS α is restricted to the region intervening between two Lac repressor-binding sites

Lac repressor roadblocks significantly inhibit *in vitro* MMR.

EMSA data demonstrate that sliding of ATP-bound MutS α on the 300 bp DNA substrate is limited to the region in between the two Lac repressor roadblocks. Therefore, the assay system provides a way to test the hypothesis that MutS α slides from the mismatch to the strand break, and that such sliding is an essential step in the MMR pathway (Gradia, Acharya et al. 1997, Fishel 1998, Gradia, Subramanian et al. 1999, Jiang, Bai et al. 2005, Mendillo, Mazur et al. 2005).

In order to evaluate the effect of Lac repressor roadblocks on MMR *in vitro*, a heteroduplex DNA substrate containing a single G-T mismatch centrally-located and Lac repressor-binding sites 5' and 3' to the mismatch was constructed (see section 2.11). The DNA substrate also includes a DNA strand break 5' to the mismatch for strand discrimination (Ghodgaonkar, Lazzaro et al. 2013) (Figure 2.3). The G-T mismatch lies within overlapping recognition sites for restriction enzyme site, NsiI and XhoI. The DNA substrate is insensitive to cleavage by NsiI, and the reaction product after correct repair of the G-T mismatch to G-C is susceptible to NsiI digestion (Figure 2.1.A).

As shown in Figure 3.5, Lac repressor significantly inhibits *in vitro* MMR in the presence of HeLa nuclear extract, which is consistent with the hypothesis. Moreover, addition of IPTG, which dissociates Lac repressor from its binding site and removes the roadblock, reduced but did not completely eliminate the Lac repressor-induced inhibition of MMR (Figure 3.5-lane 3). Similar results were observed when the HeLa cell extract was substituted with MSH-2 deficient NALM-6 (N6) nuclear extract (Matheson and Hall 2003), or MLH1-deficient HCT116 (H6) nuclear extract, complemented with purified MutS α (Figure 3.6.A-lane 1 and 2) or MutL α (Figure 3.6.B-lane 1 and 2), respectively (Figure 3.6.A/B-lane 4). Interestingly, MMR was not completely abolished by the Lac repressor roadblocks (Figure 3.5-lane 2, Figure 3.6.A-lane 4, and Figure 3.6.B-lane 4), which suggests that the system is slightly 'leaky', allowing some communication between the mismatch and the nick. Although not shown here, increasing concentration of IPTG did not fully alleviate Lac repressor-induced inhibition of MMR. Therefore, we conclude that sliding of MutS α from the mismatch to a distal ssDNA break plays a role in MMR, but may not be essential for MMR initiation, implying that MutS α may communicate with the strand break in a manner that is independent of 2-dimensional sliding on the DNA.

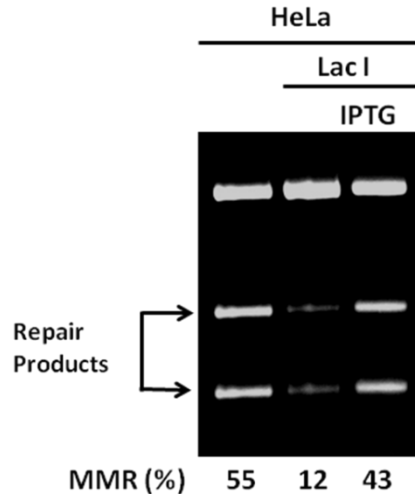


Figure 3.5 Lac repressor roadblock significantly inhibits *in vitro* MMR.

In vitro MMR assay was performed by incubating 30 fmol of 5' G-T mismatch heteroduplex substrate with 75 μ g of HeLa nuclear extract in the presence or absence of Lac repressor (as described previously in chapter 2.8.a). Products were visualized by using 1% agarose gel with ethidium bromide staining. Addition of 4 fmol of Lac repressor (Lac I) significantly inhibits MMR and displacement of Lac repressor by IPTG recovered the inhibition of MMR, and displacement of Lac repressor by IPTG reduced the inhibition of MMR. MMR (%) was quantified using Kodak Image Software.

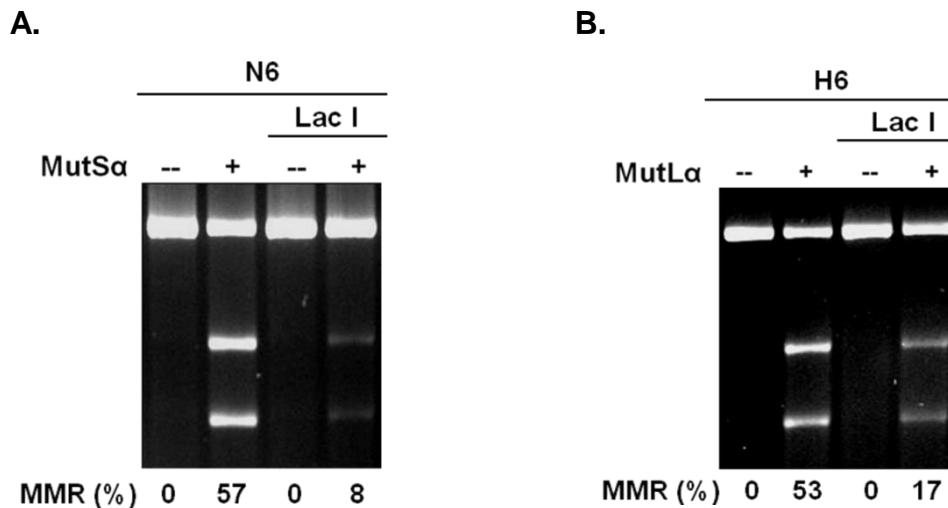


Figure 3.6 Effect of Lac repressor roadblock on *in vitro* MMR in nuclear extracts from MMR-defective cells complemented with purified protein.

(A) *In vitro* MMR assay in the presence of MSH2-defective N6 nuclear extract complemented with purified MutSa protein in the presence or absence of Lac repressor. (B) *In vitro* MMR assay in the presence of MLH1-deficient H6 nuclear extract complemented with purified MutLa. MMR (%) was quantified using Kodak Image Software.

Mismatch-provoked excision in the presence of Lac repressor roadblock.

The data presented above prompted us to hypothesize that MutS α sliding may not be essential for initiation of DNA excision at the strand break. To investigate the molecular details of the involvement of MutS α sliding in MMR initiation, *in vitro* DNA excision assay was performed, followed by Southern blot analysis, postulating that the presence of excision intermediates would provide evidence to support our hypothesis. *In vitro* excision assay was carried out in the same manner as the MMR assay, except that dNTPs are omitted, such that DNA resynthesis cannot occur. 5' nick-directed heteroduplex DNA containing a G-T mismatch and two Lac repressor-binding sites was incubated with HeLa or MutS α -complemented N6 nuclear extract. 5' nicked homoduplex DNA, otherwise identical to the heteroduplex DNA substrate, was used as a negative control.

No excision intermediates were detected in reactions with homoduplex DNA, indicating that DNA excision only initiates on heteroduplex DNA (i.e., only when a mismatch is detected by MutS α). In the absence of Lac repressor, *in vitro* DNA excision proceeded efficiently from the 5' strand break in mismatch-dependent manner in HeLa nuclear extracts (Figure 3.7-lane 4). Similar results were observed in MutS α -complemented N6 nuclear extract (Fig. 3.7-lane 7), but not when the extract was 'complemented' with heat-inactivated WT MutS α (Fig. 3.7-lane 10).

As we confirmed in our EMSA (Figure 3.4-lane 5), placement of Lac repressor roadblock leads to restriction of the sliding window of ATP-bound MutS α to the DNA region intervening between two Lac repressor roadblocks. In addition, our previous *in vitro* MMR assay demonstrated that Lac repressor roadblock significantly inhibits repair activity (Figure 3.5-lane 2). Therefore, we assumed that mismatch-provoked excision would be impeded in the presence of Lac repressor positioned between a mismatch and a strand break, because prevention of MutS α sliding would suppress communication between two distal sites, which appears consistent with "sliding" model. Surprisingly, however, mismatch-provoked excision proceeded efficiently from the strand break even in the presence of Lac repressor roadblock (Figure 3.7-lane 5 and 8), suggesting that DNA excision is independent of whether MutS α can or can not slide from the mismatch to the 5'-nick. However, DNA excision is also susceptible to inhibition by Lac repressor roadblock, because the majority of DNA excision products ended at or close to the edge of the Lac repressor roadblock. Addition of IPTG, which allows displacement of Lac repressor, reversed this inhibition (Figure 3.7-lane 6 and 9). These data show that mismatch-provoked DNA excision begins at the strand break and terminates at the Lac repressor-binding site, when the roadblock is present. These results imply that mismatch-bound MutS α can communicate with (or interact with) the strand break even if it can not slide from the mismatch to the strand break.

In the Figure 3.7-lane 5 and 8, some excision intermediates terminate in between the two Lac repressor roadblocks. These excision-termination products suggest that DNA excision initiates from more than one entry point, or that the amount of Lac repressor was not sufficient to maintain full occupancy on all DNA substrate molecules in the reaction. In case of the former, endogenous MutL α might have introduced additional nicks into the DNA substrate. However, MutL α is not essential for 5' nick-directed MMR on the present DNA substrate, such that the majority of DNA excision must have started at the original 5' strand break, not at MutL α -generated strand breaks. Thus, most of the excision products were terminated at the first downstream roadblock as we found.

To test whether the amount of Lac repressor was insufficient, *in vitro* DNA excision assay was carried out with increasing concentrations of Lac repressor, followed by southern blotting analysis (Figure 3.8). In fact, the fraction of DNA excision intermediates terminating at the first downstream roadblock increased with elevating amount of Lac repressor (lane 6-8). However, Lac repressor could not be efficiently released by IPTG at high concentration, so that high concentration of Lac repressor was not utilized in the *in vitro* DNA excision assay. Moreover, 1.5 μ M concentration of Lac repressor was used to rule out the possibility that high concentration of Lac repressor would form unnecessary DNA looping (Rutkauskas, Zhan et al. 2009). Taken as a whole, these results suggest that MutS α sliding is not essential to initiate MutS α -dependent signaling between the mismatch and a strand break and that some other mechanisms may be involved in such communication between two distal sites. Therefore, we conclude that MutS α can interact with the strand break by sliding or by another as yet poorly defined mechanism, which appears not reliable only on “sliding” model.

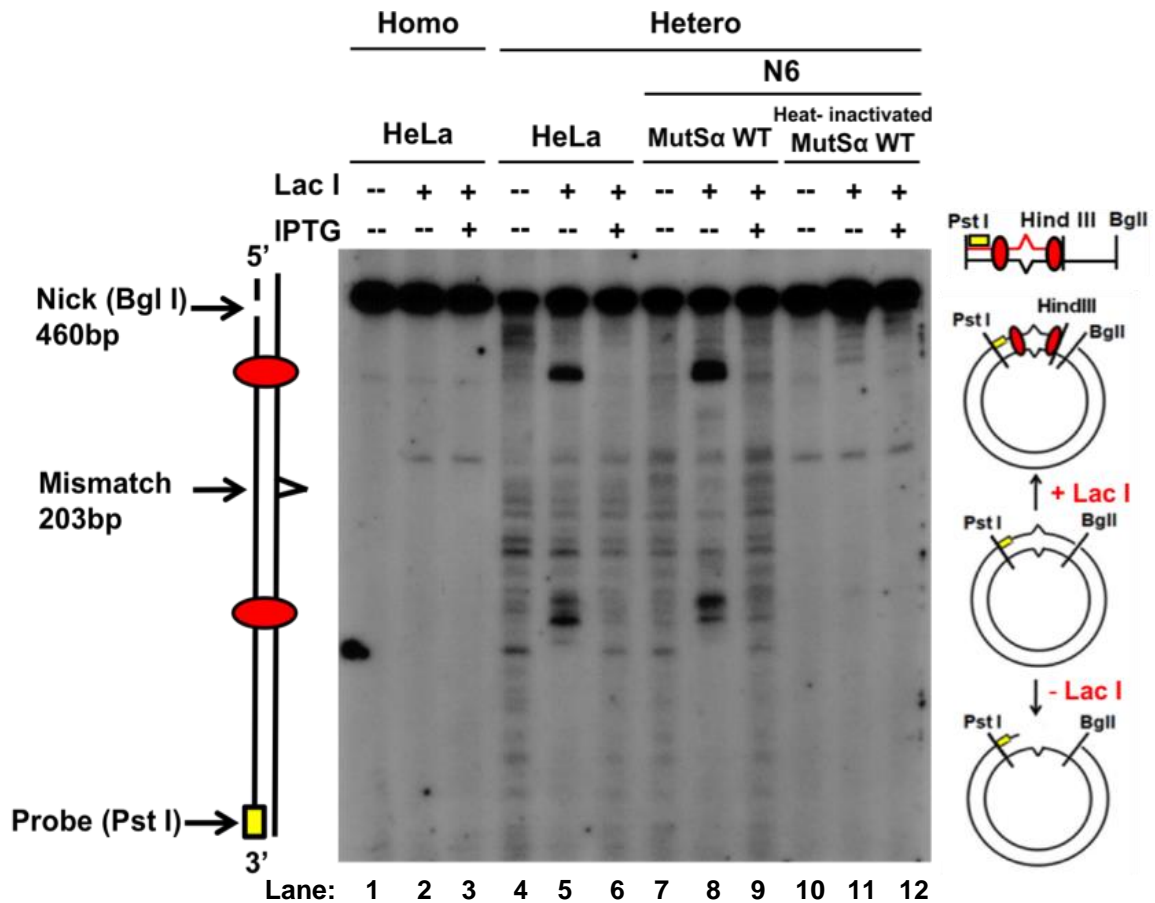


Figure 3.7 Mismatch-provoked excision still proceeded from the 5' nick regardless of the presence of Lac repressor roadblock.

In vitro excision assay was performed basically in the same manner as *in vitro* mismatch repair assay, except dNTPs were omitted to prevent DNA resynthesis (as described in chapter 2.8). Either homoduplex or heteroduplex DNA was incubated with HeLa or MutS α -complemented NALM-6 (N6) nuclear extract in the presence or absence of 1.5 μ M Lac repressor. The excision products were digested with PstI and BglII, followed by southern blotting analysis. The arrows indicate the position of the 5'- nick, the mismatch, and the probe-binding site. Red circle and yellow bar show where Lac repressor (Lac I) binds and where 32 P-labeled probe anneals, respectively.

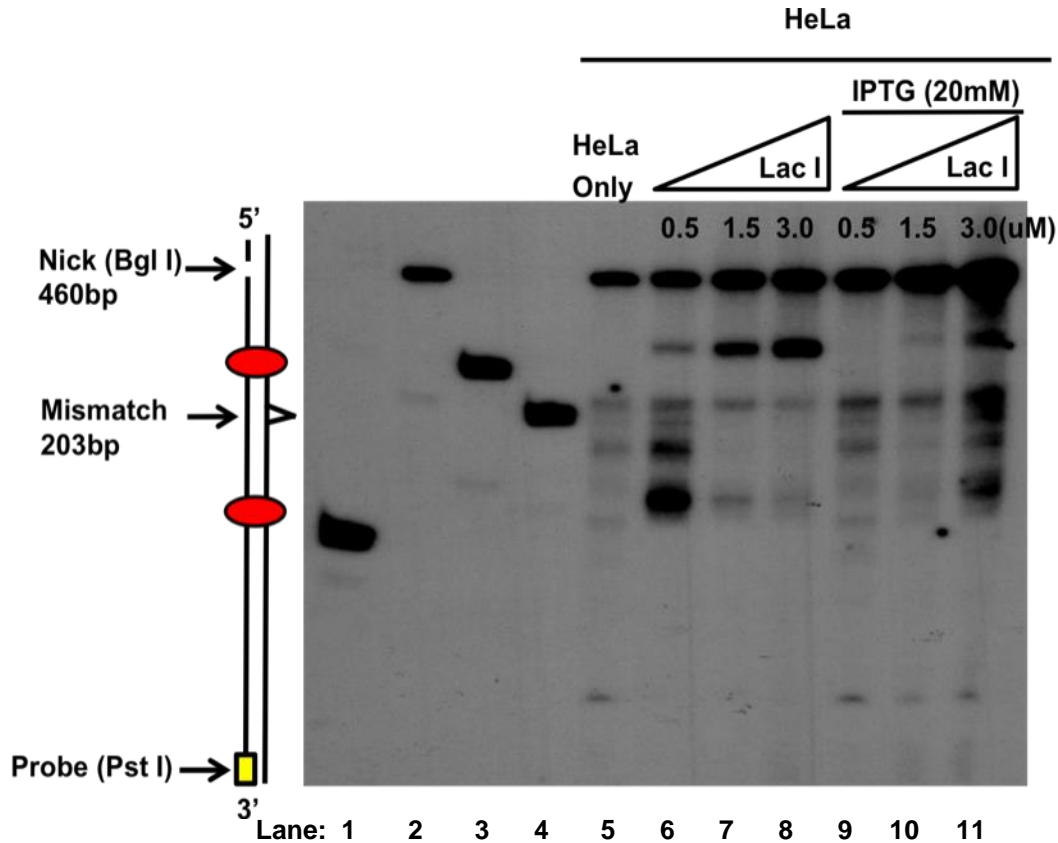


Figure 3.8 Increasing concentration of Lac repressors improves the roadblock effect on excision termination at the first downstream roadblock.

In vitro excision assay was performed basically in the same manner as *in vitro* mismatch repair assay, except dNTPs were omitted to prevent DNA resynthesis (as described in chapter 2.8). Heteroduplex DNA was incubated with HeLa nuclear extract in the presence or absence of Lac repressors and IPTG. Different concentrations (0.5, 1.5, and 3.0 μM) of Lac repressors were used to see the effect of Lac repressor concentration on termination of excision at the first downstream roadblock site. The excision products were scored by PstI and BglI and then followed by southern blotting analysis. The arrows indicate the position of the 5'- nick, the mismatch, and the probe-binding site. Red circle and yellow bar show where Lac repressor (Lac I) binds and where ^{32}P -labeled probe anneals, respectively. (Lane 1: first downstream Lac I binding site close to a nick, lane 2: full size of the non-excised fragment, lane 3: another Lac I binding site, lane 4: mismatch)

DISCUSSION

Our study investigated the molecular mechanism by which mismatch-bound MutS α transmits a signal from the mismatch to a distal strand break during MMR. Several models explaining the mechanism of MMR initiation have been developed and proposed (Figure 1.6), including “stationary” model (Junop, Obmolova et al. 2001, Guarne, Ramon-Maiques et al. 2004), “translocation” model (Allen, Makhov et al. 1997, Blackwell, Bjornson et al. 1998, Blackwell, Martik et al. 1998), and “sliding” model (Gradia, Acharya et al. 1997, Fishel 1998, Gradia, Subramanian et al. 1999, Jiang, Bai et al. 2005, Mendillo, Mazur et al. 2005). In this study, we demonstrated that mismatch-provoked excision is independent of whether sliding of MutS α is restricted by Lac repressor roadblock, which appears to dispute the validity of MMR models that invoke “sliding” by MutS α as a critical step.

A strand break is indispensable for discriminating the newly 'nascent' daughter DNA strand from the parental strand in human MMR. However, the strand break can be several hundred bp away from the mismatch, raising the question of how two physically distant sites communicate each other during MMR. To explore the mechanism that mediates the communication, Lac repressor/Lac operator system was used as a physical “roadblock” intervening between the mismatch and the nick and applied to *in vitro* excision or MMR system to prevent MutS α sliding.

EMSA results shown in Figure 3.4 confirm that MutS α diffuses away from a mismatch in ATP-dependent manner. This result is consistent with previous studies showing that the exchange of ADP for ATP triggers conformational change in MutS α (Blackwell, Bjornson et al. 1998, Blackwell, Martik et al. 1998, Bjornson, Allen et al. 2000) and reduces the affinity of MutS α for the mismatch. ATP-binding also promotes opening of the DNA clamp, allowing DNA sliding to initiate (Gradia, Acharya et al. 1997, Gradia, Subramanian et al. 1999, Wilson, Guerrette et al. 1999, Acharya, Foster et al. 2003, Mendillo, Mazur et al. 2005). The observation that MutS α sliding was restricted to the DNA region between two Lac repressor roadblocks (Figure 3.4) indicates that the movement of MutS α induced by the presence of ATP is indeed mediated by “sliding”, not by “hopping”. If ATP-bound MutS α utilizes “hopping” to move along the DNA, it would bypass the roadblock and most likely fall off the DNA. However, in the presence of Lac repressor roadblock, MutS α remained bound to the DNA substrate even in the presence of ATP, indicating that the physical roadblock limits MutS α sliding to an internal segment of the linear DNA substrate.

Restriction of MutS α sliding significantly inhibits *in vitro* MMR (Figure 3.5 and 3.6), and IPTG reduces the inhibition, suggesting that MutS α sliding plays a role in signaling MMR initiation. However, IPTG did not fully reverse Lac repressor-induced inhibition of MMR, suggesting that IPTG fails to completely remove Lac repressors roadblocks. Furthermore, MMR was not fully abolished in the presence of Lac repressor, implying that

sliding of MutS α is not absolutely required to initiate MMR. This could mean that MutS α can communicate with a distal ssDNA break by a mechanism that does not involve sliding.

More importantly, *in vitro* excision assays surprisingly revealed that mismatch-provoked DNA excision initiates from the strand break even in the presence of Lac repressor roadblock (Figure 3.7), which prevents MutS α from sliding from the mismatch to the nick. The observation that DNA excision was terminated at the first downstream roadblock site suggests that MutS α may translocate and then transmit MMR-start signal to the strand break during the early steps of MMR. However, previous theoretical studies suggest that ATP-induced sliding of MutS α away from the mismatch is essential during overall MMR process, because it promotes accessibility for Exo1-catalyzed excision (Jeong, Cho et al. 2011, Cho, Jeong et al. 2012, Qiu, DeRocco et al. 2012). Taken together, these results question the validity of MMR models that invoke “sliding” of MutS α between the mismatch and the nick, lending support to models that invoke translocation or other mechanisms of communication between two distant DNA sites during MMR in human cells. This study therefore provides significant insight into the mechanism of initiation of human MMR.

CHAPTER FOUR

MOLECULAR REGULATION OF MUTS α ATPASE AND ITS INVOLVEMENT IN MMR INITIATION

INTRODUCTION

The MutS α , which is composed of MSH2 and MSH6 subunits, exists as a heterodimer and recognizes a mismatch. In addition to mismatch recognition, MutS α possesses an intrinsic ATPase, which is critical to its cellular roles in MMR. Thus, mutations in the ATPase domain of MSH2 or MSH6 subunit of the MutS α heterodimer impair MMR (Iaccarino, Marra et al. 1998, Dufner, Marra et al. 2000). Like many other members of the ATP binding cassette (ABC) protein superfamily, both MSH2 and MSH6 have ATPase domains that contain highly conserved Walker A and Walker B motifs (Hopfner and Tainer 2003). The Walker A motif consensus amino acid sequence is GXXXXGKS/T, where X is variable as any amino acid, and S/T indicates serine (S) or threonine (T); this motif is believed to include amino acids that form the nucleotide binding pocket. The Walker B motif consensus amino acid sequence is DD/EXX, where D/E indicates either aspartic acid (D) or glutamic acid (E); this motif is assumed to require for ATP hydrolysis (Ramakrishnan, Dani et al. 2002). The Walker A motif corresponds to residues 669–676 and the Walker B motif corresponds to residues 748–751 in MSH2, while the Walker A motif corresponds to residues 1134–1141 and the Walker B motif corresponds to residues 1213–1216 in MSH6.

MSH2 and MSH6 have different affinities for nucleotide cofactors; for example, MSH6 binds ATP with higher affinity than MSH2, and stable binding of ATP to MSH6 decreases the affinity of MSH2 for ADP (Antony and Hingorani 2003, Martik, Baitinger et al. 2004). The ATPase domain of MutS α is the most highly conserved region of the protein (Warren, Pohlhaus et al. 2007), and it is also involved in MutS α dimerization (Figure 1.4). Mismatch binding by MutS α triggers downstream MMR events, including interaction with other MMR proteins, and DNA sliding (Drummond, Li et al. 1995, Alani, Sokolsky et al. 1997, Gradia, Subramanian et al. 1999). When mismatch-bound MutS α binds ATP, it undergoes a conformational change and forms a sliding clamp (Figure 1.5), which has the ability to dissociate from the mismatch due to reduced mismatch binding affinity (Gradia, Acharya et al. 1997, Gradia, Subramanian et al. 1999, Wilson, Guerrette et al. 1999, Acharya, Foster et al. 2003, Mendillo, Mazur et al. 2005). Although some biochemical functions of MutS α are relatively well known, the role of MutS α ATPase activity during the initiation step(s) of MMR is not understood in any detail. Additionally, how the Walker motifs of both MSH2 and MSH6 subunits contribute to the MutS α functions is not fully understood.

To address this issue, a series of ATPase-deficient MutS α mutants were generated through site-directed mutagenesis of the cloned MSH2 and MSH6 genes, and the mutant proteins were purified and characterized. More specifically, alanine substitution mutations were generated at K675 and G673 (K1140A and G1138A in MSH6) in the Walker A motif, and a lysine substitution mutation was introduced at E749 in the Walker B motif of MSH2 (E1140K in MSH6). Heterodimers carrying one or both mutant subunits were prepared in insect cells and extensive characterization of the mutant proteins including ATP binding, ATP hydrolysis, MMR, excision, and ATP-dependent DNA sliding was performed. In this study, it was shown that diffusion of MutS α along DNA requires ATP binding and Mg²⁺ but does not require ATP hydrolysis, which is consistent with previous findings that ATP γ S (nonhydrolyzable ATP) induced release of MutS α from the mismatch (Allen, Makhov et al. 1997, Blackwell, Martik et al. 1998, Iaccarino, Marra et al. 2000, Blackwell, Bjornson et al. 2001, Jiang, Bai et al. 2005). It is worth mentioning that the ATP binding-induced MutS α sliding is dependent on the presence of magnesium, so that the absence of magnesium leads to direct dissociation of MutS α from the mismatch (Iaccarino, Marra et al. 2000, Lebbink, Fish et al. 2010). Interestingly, we found that E-K substitutions in the Walker B motif produce a mutant MutS α that, instead of sliding off, undergoes direct dissociation from a mismatch-containing DNA molecule regardless of the presence of magnesium. This result suggests that E749 (E1140) in the Walker B motif of MSH2 (MSH6) plays a role in binding Mg²⁺ and is indispensable for MutS α conformational change to form a sliding clamp. Furthermore, we demonstrated that ATPase-defective MutS α carrying K675A in MSH2, K1140A MSH6 or both were deficient in ATP-induced sliding but promoted initiation of DNA excision at a nick. Therefore, this study supports the hypotheses 1) that DNA strand discrimination by MutS α bound to a mismatch does not require MutS α sliding away from the mismatch, and 2) that MutS α promotes communication between the mismatch and the nick in an ATP hydrolysis-independent and DNA sliding-independent manner, which implies that MutS α might be able to physically interact with the strand break. Based on these results, a model is proposed to explain how MutS α transmits signals that initiate MMR in human cells carrying DNA mismatches in newly-synthesized DNA strand.

RESULTS

Characterization of MutS α with mutations in Walker A and Walker B motifs of MSH2 and/or MSH6.

The following experiments test whether it is obligatory that MutS α slide away from the mismatch during initiation of MMR. To identify the effect of ATPase-deficient MutS α mutants on *in vitro* MMR initiation, *in vitro* MMR or excision assay was performed using ATPase-defective mutants of MutS α . The QuikChange site-directed mutagenesis method (described in Chapter 2.15) was used to generate MSH2 K675A (or MSH6 K1140A) and MSH2 E749K (or MSH6 E1214K), mutations in Walker A and B motifs of hMSH2 (or hMSH6). The position of the mutations are shown in Figure 4.1.A in which Walker A mutants were colored red while Walker B mutants were colored blue (Protocols for mutagenesis and purification of mutant proteins are described in detail in Chapter 2.). Mutations were generated in either MSH2 or MSH6 or both subunits, because previous studies suggest asymmetry in how the MutS α heterodimer binds mismatches or hydrolyzes ATP (Drotschmann, Yang et al. 2001, Antony, Khubchandani et al. 2006, Warren, Pohlhaus et al. 2007). For completeness, studies were performed with MSH2-defective heterodimer, MSH6-defective heterodimer and double-mutant heterodimer. Wild type heterodimer was used as a positive control. MutS α wild type or mutants were expressed in insect cells using the Bac-to-Bac expression system and purified through His-tag Nickel column, Mono Q column, and SuperdexTM 200 Gel Filtration (Figure 4.1.B; Chapter 2.13). To evaluate how ATPase deficiency of MutS α contributes to *in vitro* MMR, *in vitro* MMR assay (Chapter 2.8) were performed using MSH2-deficient NALM-6 (N6) nuclear extract complemented with wild type or mutant purified MutS α (Gu, Cline-Brown et al. 2002, Zhang, Yuan et al. 2005). Figure 4.1.C demonstrated that purified wild type MutS α is MMR-proficient, while the purified mutant MutS α is not, suggesting that ATPase activity of MutS α is essential for *in vitro* MMR (Note that the N6 nuclear extract is MMR-deficient in the absence of exogenous wild type MutS α .).

To address the individual contribution of MSH2 and/or MSH6 mutants to ATP processing, we examined magnesium-dependent ATP binding and hydrolysis, following previous description (Chapter 2.3 & 2.10). As previous studies have demonstrated that MSH6 subunit displays higher affinity to ATP than MSH2 subunit in the absence of magnesium (Mazur, Mendillo et al. 2006), a similar result was obtained here (Figure 4.2.A). However, all MutS α mutants except 2WT/6E1214K are cross-linked to ATP with very low efficiency (relative to wild type), suggesting that MSH2 K675 and E749 in Walker A and Walker B motif, respectively play a role in ATP binding. Alanine or lysine substitution mutations at MSH6 K1140 and E1214 (i.e., 2WT/6K1140A and 2WT/6E1214K did not appear to strongly decrease the affinity of wild type MSH2 for ATP in the presence of

magnesium, while all proteins carrying mutations of MSH2 K675A or E749K (i.e., 2KA/6WT, 2KA/6KA, 2EK/6WT, and 2EK/6EK) were completely deficient in ATP-binding. These results suggest that MSH2 plays a greater role in regulation of ATP binding by MutS α than MSH6.

The ATP hydrolysis activity of mutant MutS α proteins was examined by incubating mutant and wild type MutS α with [γ -³²P]-ATP; reaction products were analyzed by electrophoresis on a 20% denaturing polyacrylamide gel. This experiment showed a strong defect in ATPase for all MutS α mutant proteins carrying MSH2 K675A or E749K (i.e., 2KA/6WT, 2KA/6KA, 2EK/6WT, and 2EK/6EK) (Figure 4.2.B). However, a weaker but major defect in ATPase was observed in MSH6 K1140A and MSH6 E1214K (i.e., 2WT/6KA or 2WT/6EK), which was not found in MSH2 K675A and MSH2 E749K, suggesting that MSH2 plays a greater role than MSH6 during ATP binding by MutS α . Thus, as mentioned above, MSH2 and MSH6 appear to contribute asymmetrically to ATP hydrolysis by MutS α , which is consistent with the results of earlier studies. This characteristic of MutS α may partially explain the fact that mutations in MSH2 are linked to HNPCC more frequently than mutations in MSH6.

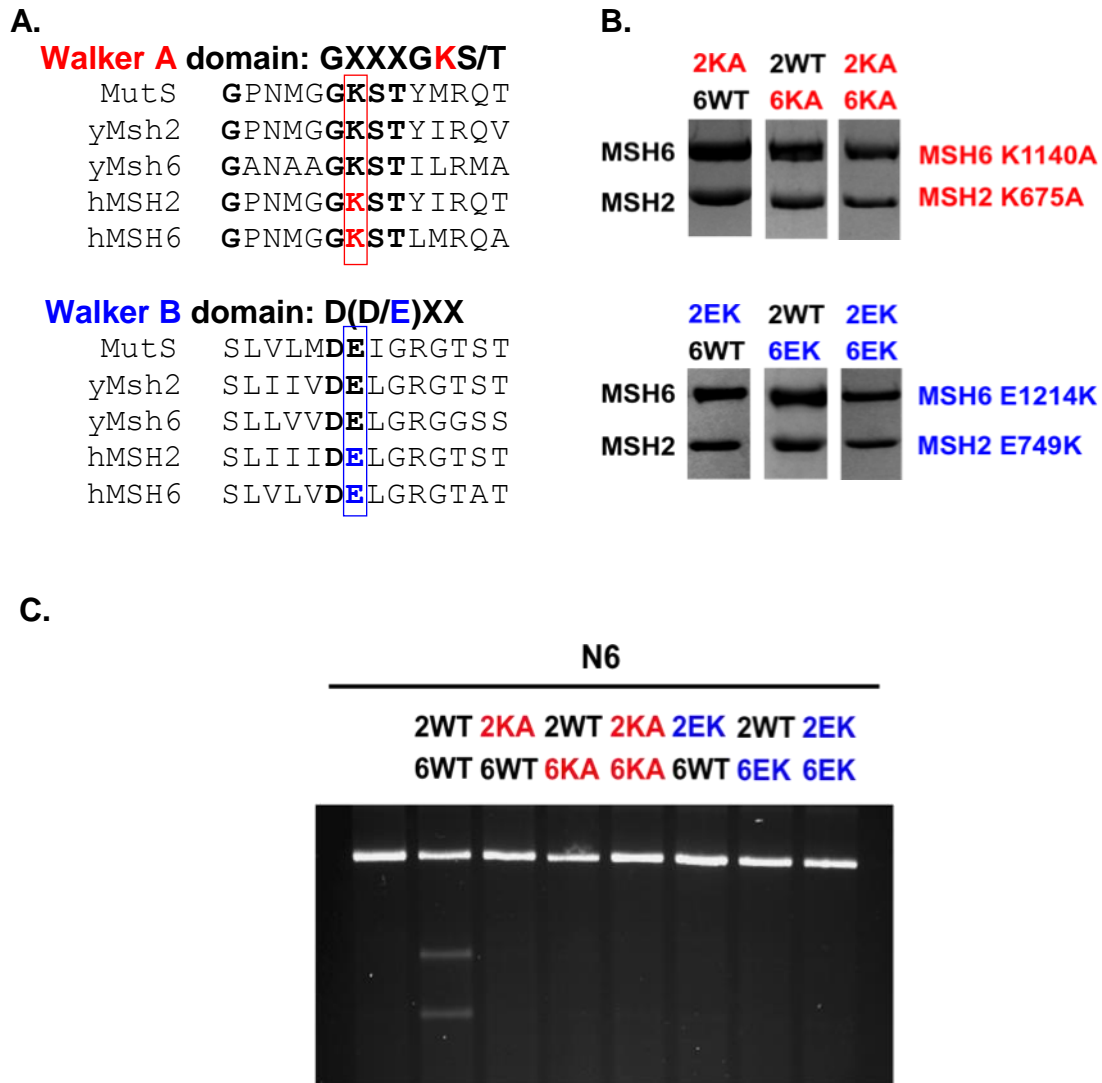
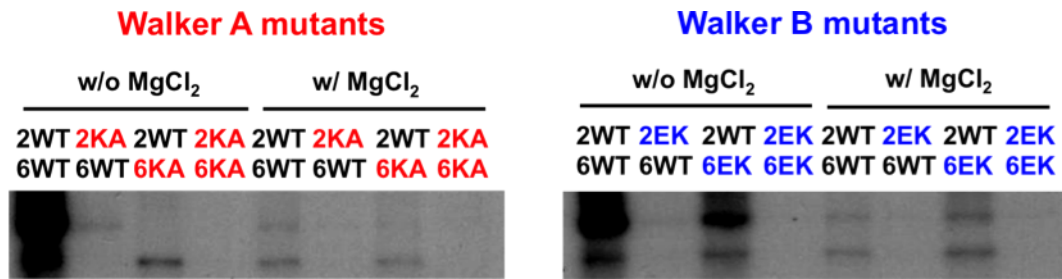


Figure 4.1 Purification and *in vitro* MMR assay of ATPase-defective MutS α mutants. (A) Conserved amino acid sequence alignment of Walker A and Walker B motifs in MutS α homologues. Position of MSH2 K675A (red) and MSH2 E749K (blue) mutations are indicated. (B) Purified wild-type (WT) and ATPase-deficient MutS α analyzed by 10% SDS-PAGE (Chapter 2.13). (C) *In vitro* MMR assays were performed using 80 μ g of MSH2-defective N6 nuclear extract and purified wild type or mutant MutS α , as indicated. None of ATPase-deficient MutS α mutants have MMR activity, suggesting that ATPase activity of MutS α is required for proficient MMR *in vitro*.

A.



B.

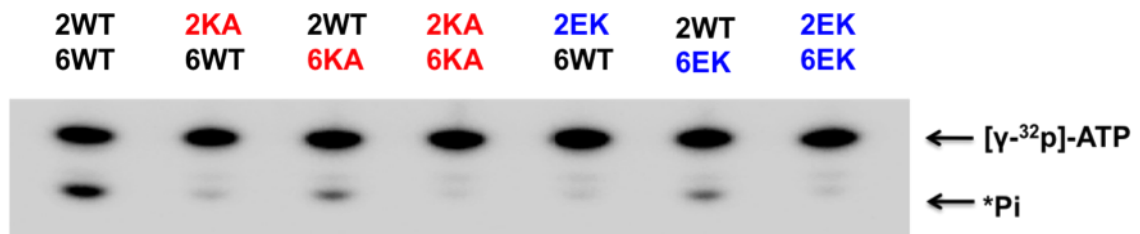


Figure 4.2 ATP binding and ATPase activities of MutS α wild type and ATPase-deficient mutants.

(A) Wild type or mutant MutS α (1 μ g) was incubated with 3000 Ci/mmol of $[\gamma\text{-}^{32}\text{P}]\text{-ATP}$ (X μ M) in the presence of G/T mismatch-containing dsDNA (100 ng) and 2 mM MgCl₂. Reactions were subjected to UV cross-linking and analyzed by SDS-PAGE (described in Chapter 2.10). Dried gels were analyzed with Typhoon PhosphorImager. (B) ATPase assay was performed under the same conditions as ATP binding (described in Chapter 2.3), except that reactions were incubated at 37°C for 20 min, and analyzed by 20% denaturing PAGE. The ³²P-labeled species were detected and quantified by using a Typhoon PhosphorImager. The bottom band indicates a phosphate derived from $[\gamma\text{-}^{32}\text{P}]\text{-ATP}$ hydrolyzed by ATPase of MutS α .

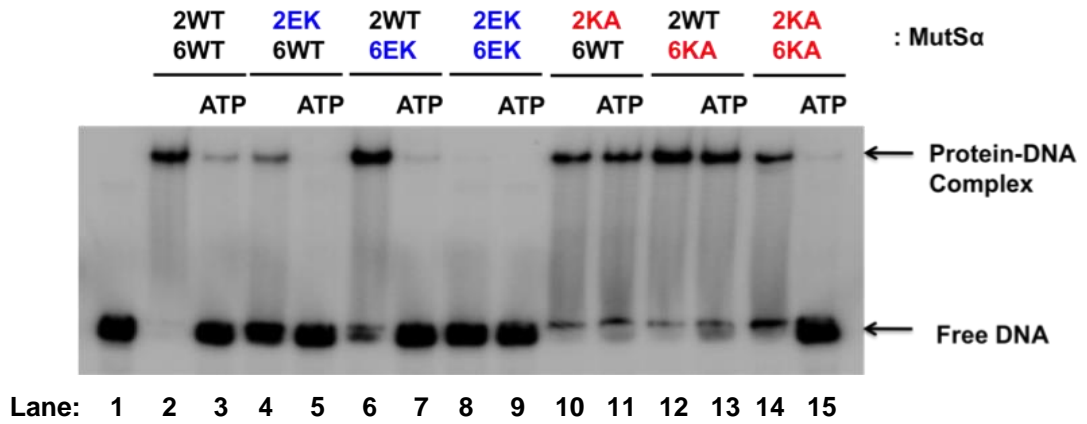
The mismatch binding activity of MutS α mutants was examined using EMSA assay, in which proteins were co-incubated with a 100 bp ³²P-labeled DNA substrate containing a G-T mismatch in the presence or absence of ATP, followed by electrophoresis under non-denaturing conditions. The results demonstrate that Walker A mutants and Walker B mutants play distinct role in mismatch binding and dissociation. All MutS α mutants, except MutS α with MSH2 K675A/MSH6 K1140A (i.e., double Walker A motif mutant) form stable complexes with the mismatch-containing substrate (Figure 4.3.A), suggesting some communication between the mismatch binding domain and the ATPase domain of MutS α even though crystal structure models show that the two domains are physically far from each other (Warren, Pohlhaus et al. 2007). However, the mechanistic basis for communication between these domains remains unanswered. Since the ATP-binding sites can be occupied by different ligands, these two distant domains exist in several different combinations, which results in that ATP-binding might alter the conformation of one or both domains (Gradia, Acharya et al. 2000, Warren, Pohlhaus et al. 2007). Thus, it has been difficult to exclusively determine ATP-binding states of MutS α in different stages of MMR events. However, distinct ATP-binding states of MutS α conformations or modes of ATP binding have not yet been correlated with different stages of MMR. Additional studies of MutS α mutants, including the Walker A motif mutant discussed above, might shed insight on these questions.

Previous studies have demonstrated that binding of ATP to MutS α is sufficient to allow MutS α to slide away from the mismatch, while the process does not require ATP-hydrolysis (Allen, Makhov et al. 1997, Blackwell, Martik et al. 1998, Iaccarino, Marra et al. 2000, Blackwell, Bjornson et al. 2001, Jiang, Bai et al. 2005). However, ATP binding fails to dissociate the Walker A mutants of MutS α from the mismatch, and a strong asymmetry in the impact of Walker A and Walker B mutants was observed (Figure 4.3.A). In particular, addition of ATP did not promote dissociation of MSH2 K675A/MSH6 WT or MSH2 WT/MSH6 K1140A (Figure 4.3.A-lane 11 & 13), while Walker B mutants and MutS α WT dissociated from the mismatch in the presence of ATP (lane 3, 5 & 7). This suggests that residues in the MutS α Walker A motif, including K675 in MSH2 (K1140 in MSH6), play an essential role in ATP-dependent MutS α sliding *per se*, and/or in release/dissociation of MutS α from a mismatch. Therefore, we conclude that the Walker A motif of MutS α , plays a role in ATP binding by MutS α , while the Walker B motif may be dispensible for ATP binding. It is worth noting that Walker A double mutant MSH2 K675A/MSH6 K1140A is deficient in both ATP binding and ATP hydrolysis (shown in Figure 4.2), but this mutant retains mismatch-specific binding as well as ATP-dependent dissociation from the

mismatch. This result suggests that mutation in both MSH2 and MSH6 subunit might induce some conformational change of MutS α , so that ATP alters the interaction of the 2KA/6KA double mutant with the mismatch even though the protein is defective in ATP binding; thus, by some unknown mechanism, ATP results in dissociation of MSH2 K675A/MSH6 K1140A from the mismatch.

Walker B mutants of MutS α (i.e., variants carrying MSH2 E749K, MSH6 E1214K or both) responded in the same manner as mismatch-bound WT MutS α to the presence of ATP; namely, ATP-induced dissociation of MutS α from the mismatch (Figure 4.3.A). The ATP binding-induced sliding also requires magnesium, while chelation of (or absence of) magnesium causes ATP-induced direct dissociation of MutS α (Iaccarino, Marra et al. 2000, Lebbink, Fish et al. 2010). To test whether E749 in MSH2 and E1214 in MSH6 (within the Walker B motif) play a role in this process, Walker B mutants of MutS α were incubated with a 300 bp GT mismatch-containing ³²P-labeled dsDNA fragment carrying Lac operator/repressor 'roadblocks' flanking the mismatch (see Chapter 3 for details about DNA substrates with Lac operator/repressor 'roadblocks'). The reaction products were analyzed by EMSA, and it appeared that E-K substitutions in the Walker B motif produce a mutant MutS α that, instead of sliding off, undergoes direct dissociation from a mismatch-containing DNA molecule regardless of the presence of magnesium (Figure 4.3.B). This suggests that the glutamate (E) residue in the Walker B motif of MSH2 or MSH6 may be required for magnesium binding. Therefore, it seems logical that the Walker B motif should also be indispensable for ATP-induced distinct conformational change of MutS α to form a sliding clamp, specifically in terms of magnesium binding during ATP binding.

A.



B.

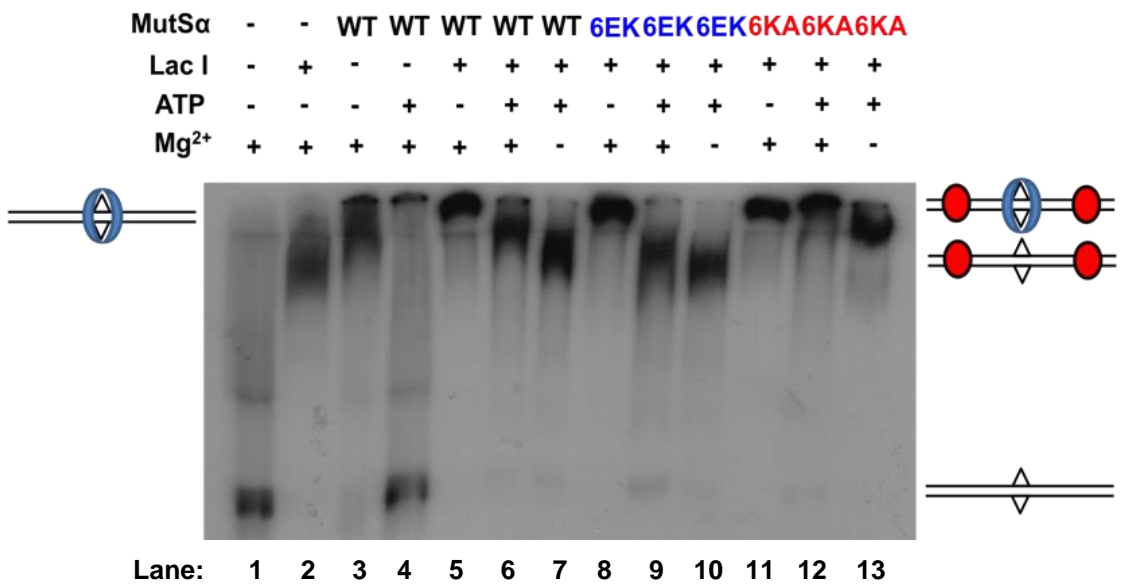


Figure 4.3 Effects of ATPase-defective MutSa mutants on mismatch binding and ATP binding-induced mismatch release.

(A) EMSA with WT and ATPase defective MutSa was carried out as previously described (Chapter 2.6) in the presence or absence of 2 mM ATP, using a 100 bp of ³²P-labeled DNA substrate (end-free) containing a G-T mismatch. (B) EMSA analysis as in (A), except 300 bp of ³²P-labeled DNA substrate carrying Lac operator/repressor "roadblocks" between the mismatch and the DNA termini, was carried out in the presence or absence of magnesium.

Initiation of Mismatch-provoked excision *in vitro* is independent of MutS α sliding, but dependent of MutS α remained bound at the mismatch.

In support of previous studies demonstrating that ATPase activity of MutS α is obviously essential for its function in MMR, all the ATPase-deficient MutS α mutants generated in this study failed to complete *in vitro* MMR (Figure 4.1.C). However, the role of MutS α -catalyzed ATP hydrolysis during the DNA excision step of MMR has not been resolved in studies reported to date. Based on the results of *in vitro* DNA excision assays described in Chapter 3, DNA excision can initiate at a nick, even when sliding of MutS α from the mismatch to the nick is blocked. To explore this further, an *in vitro* excision assay was carried out, using MutS α 2KA/6WT and 2WT/6KA proteins that are proficient in mismatch binding but deficient in ATP-dependent dissociation/sliding from the mismatch. Reaction products were analyzed by Southern blot (Figure 4.4.A). The results demonstrate normal Exo1-catalyzed DNA excision in reactions with MutS α 2KA/6WT or 2WT/6KA, confirming that DNA excision starts in the absence of MutS α sliding. Remarkably, the majority of DNA excision intermediates terminate at the mismatch, and few if any DNA excision intermediates terminate beyond the mismatch in the presence of MutS α 2KA/6WT or 2WT/6KA. In contrast, DNA excision intermediates had a strikingly different, showing nearly random length distribution in the presence of wild type MutS α . These findings suggest that excision initiated from the nick terminates when it encounters MutS α 2KA/6WT or 2WT/6KA stably bound at the mismatch due to defective ATP binding and defective ATP-dependent sliding. It is noted that the frequency of termination at the mismatch is higher in the presence of MutS α 2KA/6WT than in the presence of 2WT/6KA; this is consistent with the observation that MutS α 2KA/6WT binds ATP less efficiently than MutS α 2WT/6KA.

Previous studies demonstrated that the absence of magnesium induces direct dissociation of MutS α from the mismatch in the presence of ATP (Iaccarino, Marra et al. 2000, Lebbink, Fish et al. 2010). However, MutS α Walker B mutants exhibit direct dissociation from the mismatch, instead of sliding off, in an ATP-dependent magnesium-independent manner (Figure 4.3.B-lane 9), suggesting that the Walker B motif plays a role in magnesium binding, possibly by regulating conformational change of MutS α . To explore this further on initiation of excision, DNA excision intermediates generated in the presence of MutS α 2EK/6WT or 2WT/6EK were analyzed by Southern blot (Figure 4.4.A). Notably, MutS α 2EK/6WT and 2WT/6EK, which bind mismatches but do so in a transient or relatively unstable manner did not support initiation of Exo1-catalyzed excision, implying defective initiation of MMR in the absence of ATP binding-mediated conformational change of MutS α . One interpretation of this result is that sliding of MutS α requires a conformational change induced by binding of magnesium and ATP; hence,

Walker B mutants, which fail to undergo this conformational change because of the deficiency in ATP binding, do not support initiation of MMR. Therefore, we conclude that stable binding of MutS α to the mismatch, rather than sliding, is critical for initiation of MMR. However, once Exo1-catalyzed DNA excision initiates, MutS α must dissociate from the mismatch to allow the repair reaction to proceed beyond the mismatch. If MutS α fails to dissociate from the mismatch, Exo1-catalyzed DNA excision is blocked, the misinserted nucleotide is not removed, and the repair reaction aborts.

To confirm this above hypothesis, DNA excision reactions were terminated 3, 6 or 12 minutes after initiation in the reconstituted system using purified MutL α , RPA, and wild type or mutant MutS α . As a positive control, excision assay was performed in the presence of MMR-proficient HeLa cell nuclear extract and terminated 2, 5, 10 min after initiation. The DNA probe hybridized close to the PstI site in the DNA substrate. In the presence of HeLa nuclear extract, DNA excision intermediates were distributed nearly randomly from the nick to close to the PstI site (Figure 4.4.B). In the DNA excision reaction with wild type MutS α , excision intermediates at the mismatch site gradually disappear over time, suggesting that wild type MutS α slides away from the mismatch after (but not before) DNA excision initiates. Therefore, DNA excision correlates with but precedes initiation of MutS α sliding. Remarkably, MutS α 2KA/6WT or 2WT/6KA, which is capable of mismatch binding but incapable of ATP-induced mismatch release, terminated Exo1-catalyzed excision at the mismatch, demonstrating that DNA excision starts independently of whether MutS α slides away from the mismatch. In contrast, DNA excision was not observed at any time point in the presence of MutS α 2WT/6EK, indicating that Walker B MutS α mutants, which exhibit ATP-induced direct dissociation from the mismatch, cannot initiate excision. This result implies that stable binding of MutS α to the mismatch is essential to support initiation of excision.

Figure 4.4 Requirement for stable binding of MutS α to the mismatch during initiation of MMR.

(A) *In vitro* excision assay was performed as described in Chapter 2.8 in the presence of MutS α Walker A and Walker B mutants. 5' nick-directed G-T mismatch heteroduplex DNA was used in either HeLa nuclear extract system or reconstituted system using purified MMR proteins including MuL α , Exo1, and RPA. DNA excision products were digested with PstI and BglI and subjected to Southern blot analysis. Arrows indicate the positions of the nick and the mismatch; the yellow bar indicates the ³²P-labeled probe-annealing site. (B) Assays were carried out as in (A), except reactions were terminated at the indicated time.

MutS α -mediated signaling during initiation of MMR *in vitro*.

Data presented above demonstrated that DNA excision initiates at an upstream nick in the presence of mismatch-bound MutS α 2KA/6WT or 2WT/6KA, despite the fact that this mutants are defective in ATP binding-dependent sliding. Although this suggests that sliding of MutS α is not essential for initiation of MMR, an alternative explanation is that MutS α 2KA/6WT and MutS α 2WT/6KA may have sufficient residual ATP binding and thereby ATP-induced sliding activity to support this reaction. To rule out the latter possibility, MutS α mutants carrying MSH2 G673A and/or MSH6 G1138A were generated and characterized (Figure 4.5). Note that MutS α mutants carrying MSH2 G673A and/or MSH6 G1138A in the Walker A motif, which are proficient in mismatch binding capacity, are completely deficient in ATP hydrolysis (Figure 4.5.C), deficient in ATP binding-dependent mismatch release (Figure 4.5.D) and do not support *in vitro* MMR (Figure 4.5.E). Southern blot analysis of *in vitro* excision products showed that DNA excision initiates at the nick in the presence of MutS α 2WT/6GA and 2GA/6GA and mostly terminates at the mismatch (Figure 4.6). This result implies that MutS α 2WT/6GA or 2GA/6WT remain bound at the mismatch even after Exo1-catalyzed DNA excision initiates, suggesting that mismatch-bound MutS α probably physically interacts with the strand break to transmit an entry signal of MMR. When the DNA substrate also carried Lac repressor/operator roadblocks, the experiment result was the same. Therefore, we conclude that ATP hydrolysis and sliding of MutS α to the nick is dispensable for signal transmission of *in vitro* MMR initiation. However, interestingly 2GA/6WT exhibits like wild type of MutS α in terms of ATP binding-dependent dissociation from the mismatch (figure 4.5.D), suggesting MSH6 subunit contributes more to MutS α -induced ATP processing than MSH2 (Iaccarino, Marra et al. 1998, Antony, Khubchandani et al. 2006). In addition, Exo1-catalyzed excision was also initiated and extended by 2GA/6WT, not showing termination of excision intermediates at the mismatch (figure 4.6), which indicate that 2GA/6WT stimulated initiation and extension of excision farther beyond the mismatch. Since ATP induces

dissociation of 2GA/6WT from the mismatch, Exo1-catalyzed excision is not terminated at the mismatch. This suggestion appears linked to the fact that only MSH6, but not MSH2, has a conserved Phe-X-Glu motif that recognizes and directly binds to a mismatch (Lamers, Perrakis et al. 2000, Obmolova, Ban et al. 2000, Warren, Pohlhaus et al. 2007, Edelbrock, Kaliyaperumal et al. 2013). It is worth mentioning that although ATPase domain and mismatch binding domain of MSH6 are located far from each other, there is allostery between them (Warren, Pohlhaus et al. 2007). However, how mismatch binding domain of MSH6 coordinates with its ATPase domain for its conformational change signal is not clear. Our finding possibly is reflected in this question, demonstrating that ATP binding to MSH6 facilitates formation of appropriate sliding clamp in order to cause ATP-induced mismatch release, and leading to a reduction in mismatch binding of ATP-bound MutS α . Therefore, these studies improve our understanding of MutS α -mediated signaling during MMR and call into question the validity of the 'sliding model' for eukaryotic MMR.

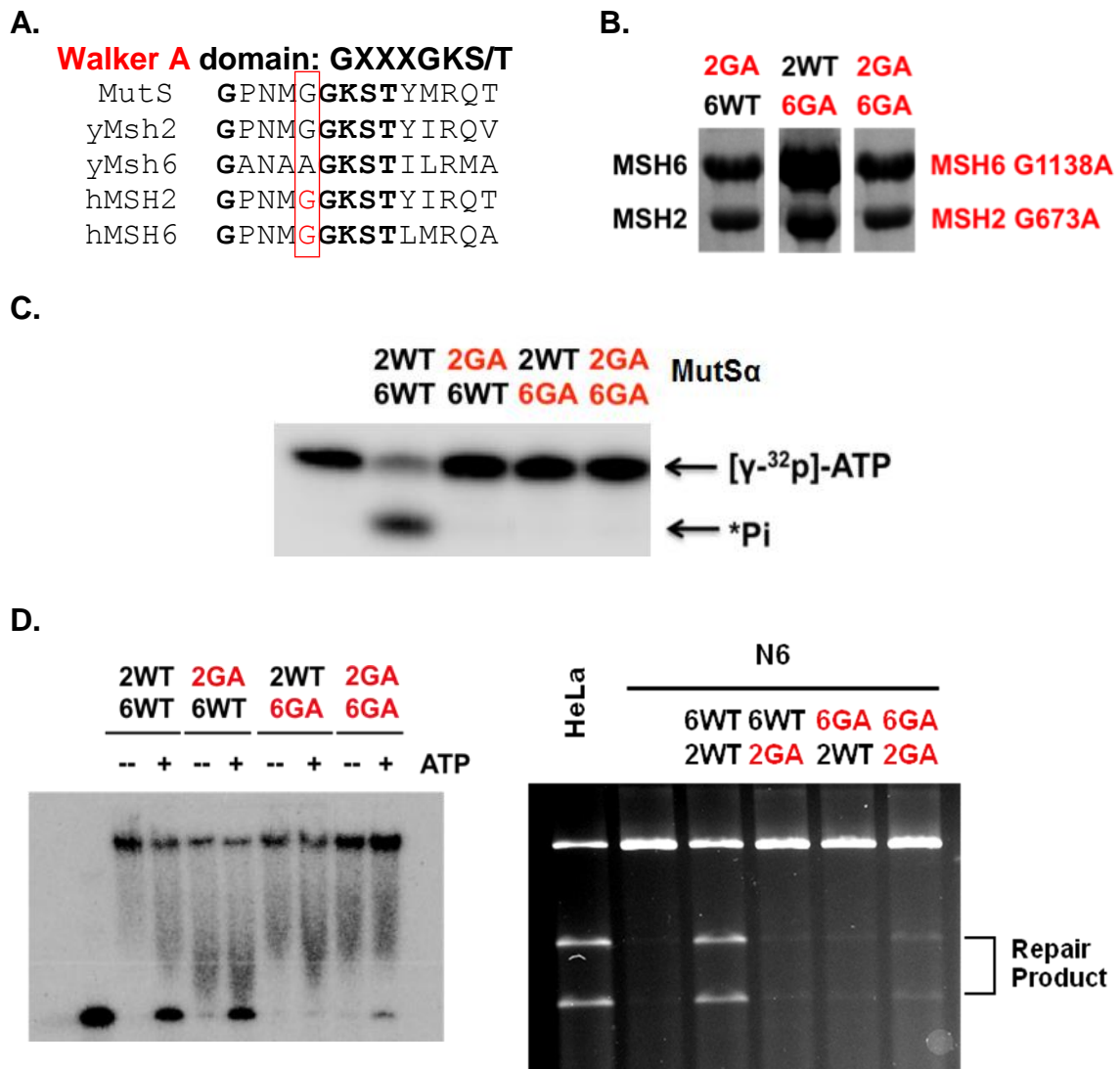


Figure 4.5 Biochemical characteristics ATPase-deficient MutSα with G-A substitution mutations in the Walker A motif.

(A) Conserved amino acid sequence of Walker A domain of MutSα homologues; MSH2 G673 and/or MSH6 G1138 (shown in red) were substituted with alanine. (B) 10% SDS-PAGE of wild type (WT) and MutSα with MSH2 G673A and/or MSH6 G1138A. (C) ATPase assay in the presence of 50 nM proteins, [γ-³²P]-ATP, 5 mM MgCl₂ in the presence or absence of 100 bp of ³²P-labeled DNA (Chapter 2.3). The ³²P-labeled species were quantified by PhosphorImager. (D) EMSA in the presence or absence of 2 mM ATP, using 100 bp ³²P-labeled DNA heteroduplex. (E) *In vitro* MMR assays were performed as described in Chapter 2.8 using 80 μg N6 nuclear extract complimented with wild type or mutant MutSα.

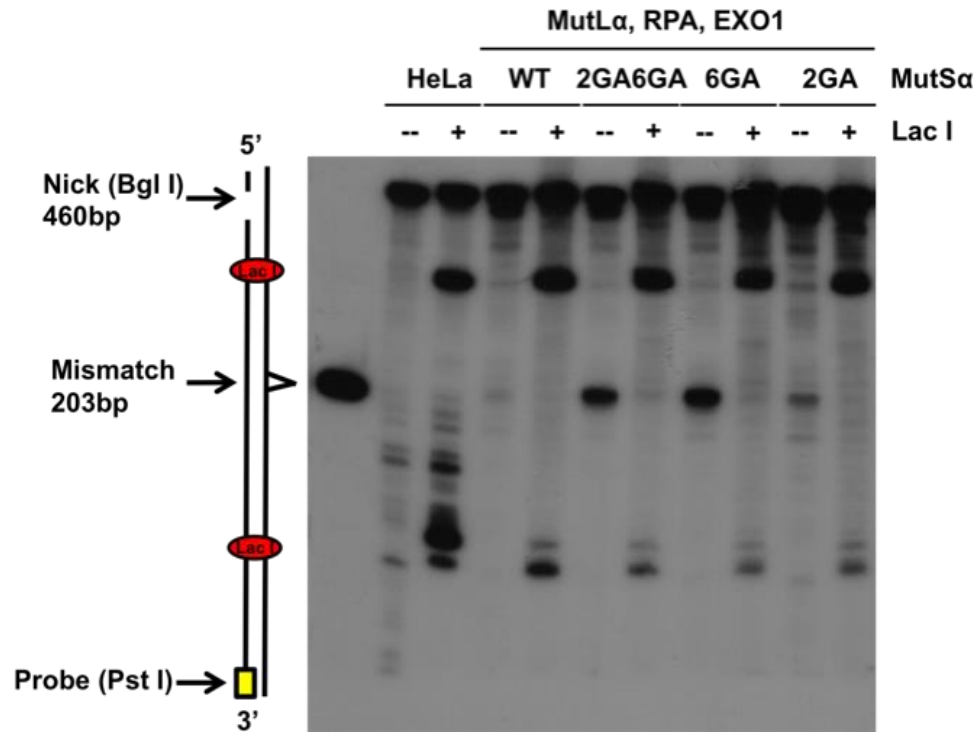


Figure 4.6 Exo1-catalyzed excision occurs efficiently from the nick independently of whether MutSa slides from the mismatch to the nick.

In vitro DNA excision assay was performed using 5' nicked heteroduplex DNA including Lac repressor/operator roadblocks in the presence of HeLa nuclear extract or reconstituted MutSa system using purified MMR proteins including MutL α , Exo1, and RPA. The excision products were analyzed by southern blotting, using 6% denaturing gel as described previously. The arrows indicate the nick and the mismatch site. Red circle and solid bar show Lac repressor binding site and 32 P-labeled probe annealing site.

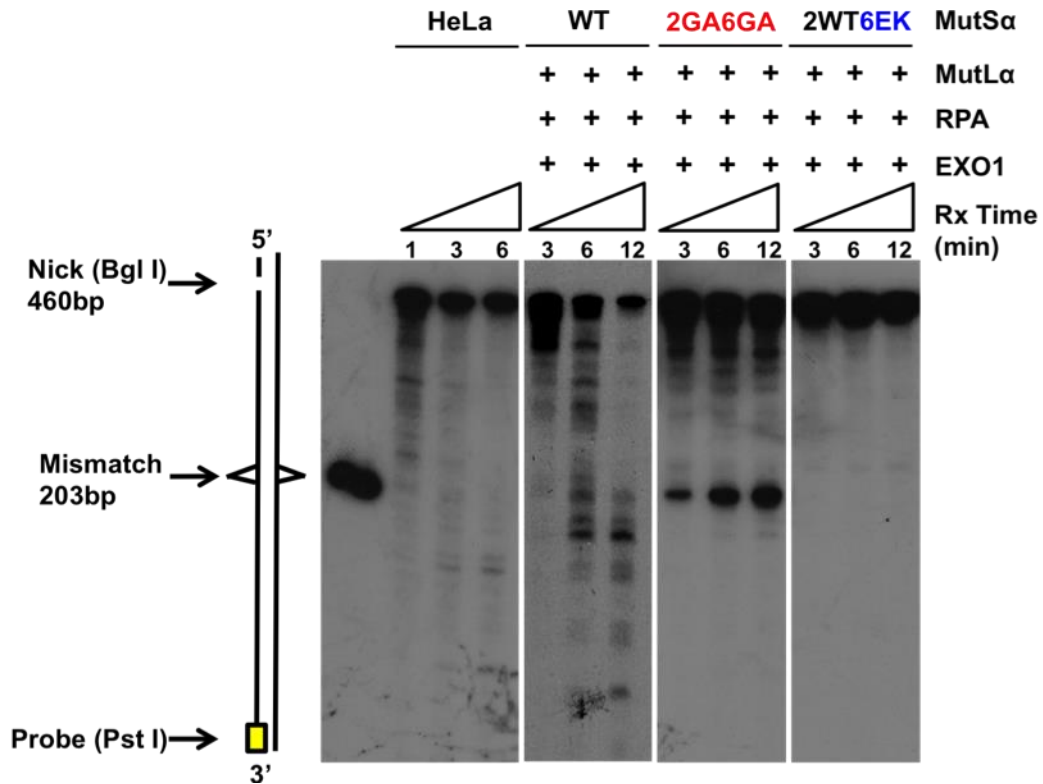


Figure 4.7 Requirement for mismatch-bound MutS α during initiation of MMR.

In vitro DNA excision assay was performed as described in Chapter 2.8, in the presence of wild type or mutant MutS α , and 5' nicked heteroduplex DNA. HeLa nuclear extract or purified MMR proteins were added, as indicated. Reactions were terminated at the indicated time. DNA excision products were analyzed as described above. Arrows indicate the positions of the nick and the mismatch; the yellow bar indicates the probe-annealing site. MutS α 2GA6GA mutant markedly promotes termination products of excision observed at the mismatch area as increasing the reaction time. It suggests that excision starts independently of whether MutS α slides from the mismatch to the strand break. The Walker B mutant MutS α , which is incapable of staying at the mismatch, did not initiate excision, indicating that MutS α remaining bound at the mismatch, rather than sliding, is essential for the initiation of excision.

DISCUSSION

Although a human homolog of MutH has not been identified (Kunkel and Erie 2005), human MMR process involves a strand specific nick, which is generated by discontinuities between Okazaki fragments on the lagging strand or the 3' terminus of replication fork on the leading strand (Lopez de Saro and O'Donnell 2001). However, in spite of extensive studies, how MutS α facilitates communication between the mismatch to the distal strand discrimination signal (the nick) to initiate MMR remains controversial. As described in the introduction, three models have been proposed to explain initiation of MMR in human cells. Major differences among these models include how MutS α translocates to the strand break and whether ATP hydrolysis of MutS α is required. In this study, we ruled out the "translocation" model (Figure 1.6 left) among these models, because MutS α slides from the mismatch to the strand break in ATP-binding dependent manner, not in ATPase dependent manner (Figure 4.3), and ATP hydrolysis is not required for the initiation of MMR. To clarify the mechanism of MMR initiation, molecular details of excision reactions containing MutS α mutants that are defective in ATP-binding dependent sliding were observed. Although all ATPase-deficient MutS α mutants did not exhibit *in vitro* MMR (Figure 4.1.C and 4.5.E), MutS α Walker A mutants, which are capable of mismatch binding but incapable of ATP-mediated sliding, appears to start Exo1-catalyzed excision (Figure 4.4 and 4.6). It suggests that MutS α sliding from the mismatch to the nick is not essential for communication between two distal sites. Moreover, majority of excision intermediates provoked by MutS α Walker A mutants was terminated at the mismatch site, indicating that they remained bound at the mismatch even after Exo1-catalyzed DNA excision initiated. This observation suggests that MutS α stayed bound at the mismatch is sufficient to transmit a MMR start signal to the strand break and then initiate MMR. In contrast, excision was not provoked by MutS α Walker B mutants (Figure 4.4), whose mismatch binding is in a transient or unstable manner, implying that stable mismatch binding of MutS α , rather than sliding, is necessary to support initiation of excision. However, once Exo1-catalyzed DNA excision initiates, MutS α must dissociate from the mismatch to allow the repair reaction to proceed beyond the mismatch. If MutS α fails to dissociate from the mismatch, Exo1-catalyzed DNA excision is blocked, the misinserted nucleotide is not removed, and the repair reaction aborts. In addition, as the reaction time increases, excision proceed efficiently from the nick beyond the mismatch by wild type of MutS α , while majority of excision reactions was terminated at the mismatch by MutS α mutants, which are defective in ATP-induced mismatch release. This result provides strong evidence to support the hypothesis that sliding of MutS α away from the mismatch is absolutely not required for translocation of MutS α to the nick to initiate MMR, suggesting that MutS α can

communicate with a distal ssDNA break by a mechanism that does not involve sliding. Mismatch-bound MutS α probably physically interact with the strand break in order to transmit an MMR start signal and then initiate MMR.

Although initiation of Exo1-provoked excision supported by MutS α mutants showed that sliding of MutS α away from the mismatch is not essential for the initiation of MMR, there is another possibility that the MutS α mutants may still have sufficient capacity of ATP-induced mismatch release to start MMR. To rule out the possibility, excision reactions including the MutS α mutants were carried out in the presence of Lac repressor roadblocks to additionally (note that mutants themselves are deficient in ATP-induced sliding from the mismatch) restrict the sliding window of ATP-bound MutS α to the DNA region intervening between two Lac repressor roadblocks. Exo1-catalyzed excision provoked by either MutS α 2WT/6GA or 2GA/6GA mutants proceeds efficiently from the strand break even in the presence of Lac repressor roadblock (Figure 3.7-lane 5 and 8), suggesting that DNA excision is indeed independent of whether MutS α can or cannot slide from the mismatch to the 5'-nick.

In contrast of the sliding model, our finding is more likely close to stationary model at the beginning of MMR events, in which sliding of MutS α is not required. However, once Exo1-catalyzed DNA excision initiates, MutS α must be released from the mismatch to allow the repair reaction to proceed beyond the mismatch. Thus, sliding of MutS α away from the mismatch is definitely essential for later process of MMR after Exo1 encounters the mismatch. In conclusion, as shown in the Figure 4.9, our proposed model is kind of mixed both stationary and sliding models. MutS α recognizes and binds a mismatch in ADP-bound state. Mismatch binding by ADP-bound MutS α triggers recruitment of MutL α to the mismatch and Exo1 to the strand break (strand discrimination signal). The ternary complex composed of MutS α and MutL α stimulates protein-protein interaction with Exo1, which brings DNA bending or looping. It is very important that MutS α should remain bound at the mismatch to communicate with the nick. In terms of protein-protein interaction, mismatch-bound MutS α transmits a signal for MMR initiation and proceeds Exo1-catalyzed excision from the nick. Once Exo1 reaches to the mismatch, ADP bound to MutS α is exchanged to ATP, leading to formation of sliding clamp. ATP-bound MutS α slides away from the mismatch and dissociate from the mismatch, which allows excision to proceed for removal of the mismatch.

In summary, we demonstrated that ATP hydrolysis of MutS α and its sliding to the strand break are not necessary to communicate between the mismatch and the nick during initiation step of MMR. However, MutS α should remain bound at the mismatch to communicate with the nick until Exo1 reaches to the mismatch from the mismatch.

Although all the finding in this study did not directly address which model is correct, they partially resolved puzzling question of how MutS α transmits a signal from the mismatch and to the distal nick to initiate MMR, providing significant support that is not reliable only on “sliding” model.

Copyright © Sanghee Lee 2014

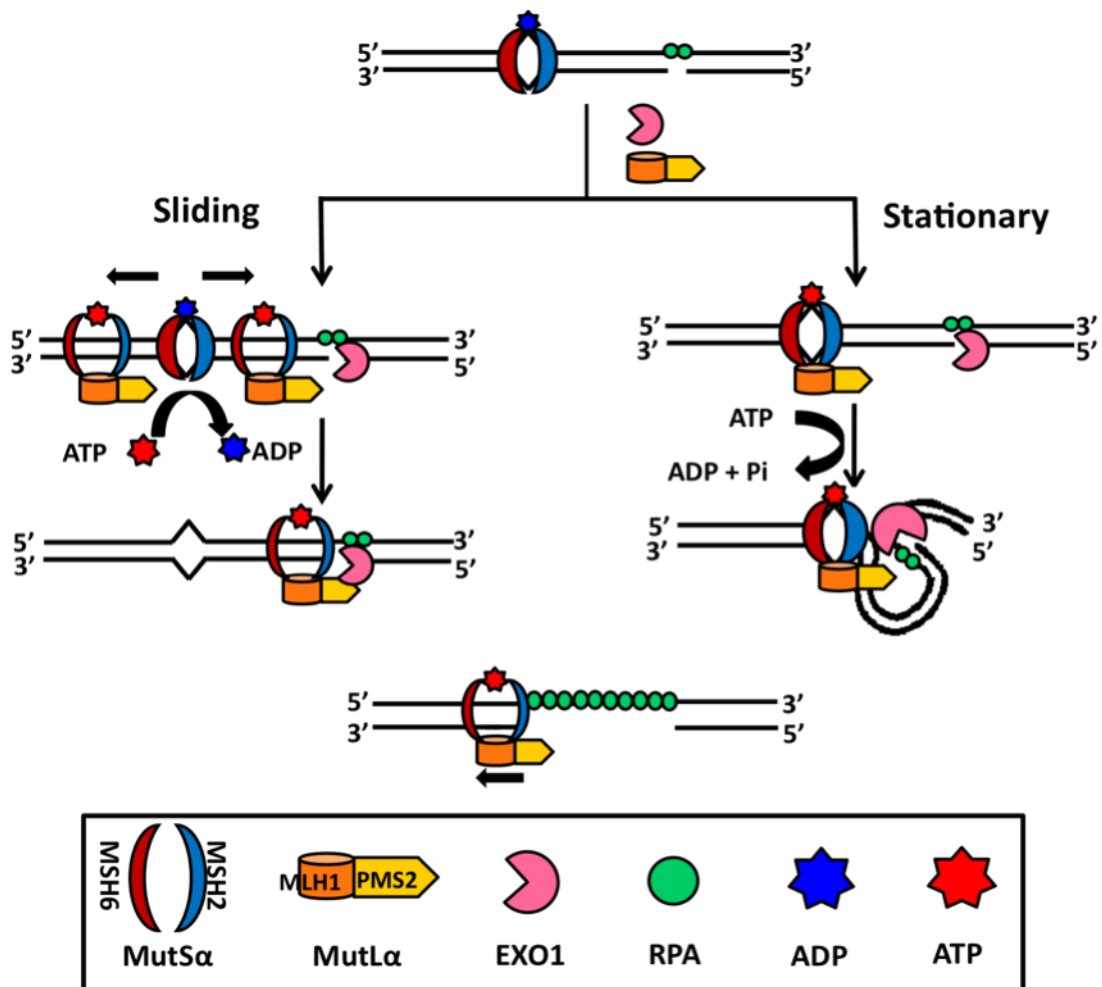


Figure 4.8 Models for signaling between the mismatch and the strand discrimination signal of MMR event.

The “sliding” model (left) proposes that ADP-bound MutS α searches for a mismatch and mismatch binding induces exchange of ADP for ATP, resulting in formation of a sliding clamp. ATP-bound MutS α then slides away from the mismatch in an ATP-hydrolysis independent manner. The “stationary” model (right) postulates that ATP-bound MutS α binds to the mismatch and remains bound to the mismatch, while interactions of MMR proteins are attributed to DNA bending or looping that brings two physical distant sites in proximity. In this model, ATP hydrolysis of MutS α is required for proofreading mismatch reinitiation and inducing MutS α interactions with other MMR proteins that trigger downstream signaling of MMR.

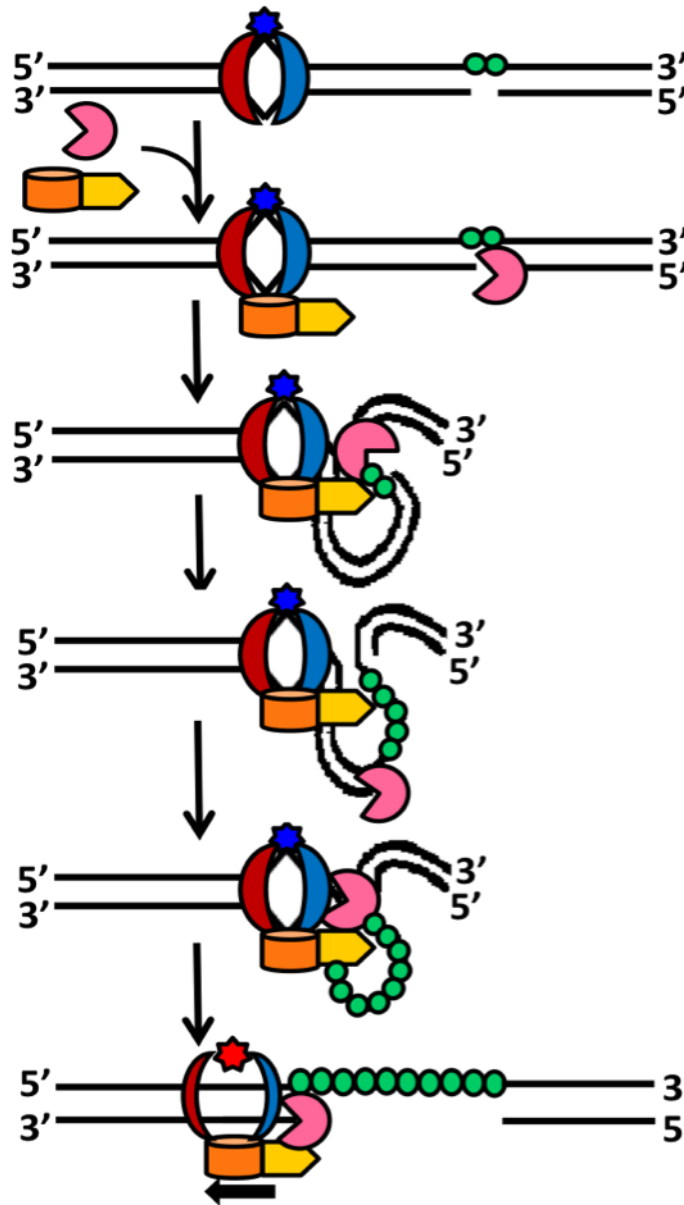


Figure 4.9 Proposed model for initiation of MMR.

ADP-bound MutS α recognizes a mismatch, and recruits MutL α to the mismatch and Exo1 to the strand break. MutS α -MutL α -DNA mismatch complex interacts with Exo1 at the 5' nick by DNA bending or looping. MutS α remains bound at the mismatch, thereby transmitting the signal for downstream MMR events. DNA excision requires mismatch-bound MutS α ExoI and a distal nick. As Exo1 reaches the mismatch, MutS α slides away from the mismatch, removing steric hindrance, which would otherwise result in termination of DNA excision.

APPENDIX

LIST OF ABBREVIATIONS

- A:** Adenine
- AML:** Acute Myeloid Leukemia
- ATP:** Adenosine triphosphate
- β-ME:** Beta Mercaptoethanol
- bp:** Base pair (s)
- BSA:** Bovine Serum Albumin
- C:** Cytosine
- C strand:** Complementary Strand
- cDNA:** complementary DNA
- CV:** Column Volume
- ddH₂O:** double distilled water
- DNA:** Deoxyribonucleic acid
- dNTPs:** deoxy Nucleotide Triphosphate
- DSB:** Double-strand Break
- dsDNA:** double strand DNA
- DTT:** Dithiothreitol
- EDTA:** ethylenediamine tetracetic acid
- EGFR:** Epidermal Growth Factor Receptor
- EMSA:** Electrophoretic Mobility Shift Assay
- EtBr:** Ethidium Bromide
- EtOH:** Ethanol
- EXO I:** Exonuclease I
- EXO V:** Exonuclease V
- FBS:** Fetal Bovine Serum
- G:** Guanine
- GST:** Glutathione-S-transferase
- HNPCC:** Hereditary Nonpolyposis Colorectal Cancer (Lynch Syndrome)
- ID:** Insertion/Deletion

IPTG: Isopropyl-1-thio- β -D-galactopyranoside
Lac I: Lac Repressor
LS: Lynch Syndrome
MMR: Mismatch Repair
MSI: Microsatellite Instability
MutL α : Complex of MLH1 and PMS2
MutL β : Complex of MLH1 and PMS1
MutL γ : Complex of MLH1 and MLH3
MutS α : Complex of MSH2 and MSH6
MutS β : Complex of MSH2 and MSH3
nm: nano meter
nt: nucleotide
NaOAc: Sodium Acetate
NFDM: Non-Fat Dry Milk
OD: Optical Density
O/N: Overnight
PAGE: Polyacrylamide Gel Electrophoresis
PCNA: Proliferating Cell Nuclear Antigen
PCR: Polymerase Chain Reaction
PBS: Phosphate-buffered saline
PMSF: Phenylmethylsulfonylfluoride
PK: Protein Kinase
RFC: Replication Factor C
RPA: Replication Protein A
RT: Room Temperature
RPM: Revolutions per Minute
SNP: Single Nucleotide Polymorphism
SSB: single-stranded binding
SSCP: Single-strand Conformation Polymorphism
ssDNA: Single-stranded DNA
SDS: Sodium Dodecyl Sulfate

T: Thymine

TBE : Tris/Borate/EDTA

TBS : Tris-buffered saline

TE : Tris-EDTA

TES : Tris-EDTA saline

UV: Ultraviolet

V Strand: Viral Strand

WB: Western Blot

X-gal: 5-bromo-4-chloro-3-indolyl- β D-galactosidase

REFERENCES

- Acharya, S., P. L. Foster, P. Brooks and R. Fishel (2003). "The coordinated functions of the *E. coli* MutS and MutL proteins in mismatch repair." *Mol Cell* **12**(1): 233-246.
- Alani, E., T. Sokolsky, B. Studamire, J. J. Miret and R. S. Lahue (1997). "Genetic and biochemical analysis of Msh2p-Msh6p: role of ATP hydrolysis and Msh2p-Msh6p subunit interactions in mismatch base pair recognition." *Mol Cell Biol* **17**(5): 2436-2447.
- Allen, D. J., A. Makhov, M. Grilley, J. Taylor, R. Thresher, P. Modrich and J. D. Griffith (1997). "MutS mediates heteroduplex loop formation by a translocation mechanism." *EMBO J* **16**(14): 4467-4476.
- Antony, E. and M. M. Hingorani (2003). "Mismatch recognition-coupled stabilization of Msh2-Msh6 in an ATP-bound state at the initiation of DNA repair." *Biochemistry* **42**(25): 7682-7693.
- Antony, E., S. Khubchandani, S. Chen and M. M. Hingorani (2006). "Contribution of Msh2 and Msh6 subunits to the asymmetric ATPase and DNA mismatch binding activities of *Saccharomyces cerevisiae* Msh2-Msh6 mismatch repair protein." *DNA Repair (Amst)* **5**(2): 153-162.
- Au, K. G., K. Welsh and P. Modrich (1992). "Initiation of methyl-directed mismatch repair." *J Biol Chem* **267**(17): 12142-12148.
- Ausubel, K. and B. Gitler (1987). "Swallow syncope in an otherwise healthy young man." *Am Heart J* **113**(3): 831-832.
- Ban, C. and W. Yang (1998). "Structural basis for MutH activation in *E. coli* mismatch repair and relationship of MutH to restriction endonucleases." *EMBO J* **17**(5): 1526-1534.
- Bellizzi, A. M. and W. L. Frankel (2009). "Colorectal cancer due to deficiency in DNA mismatch repair function: a review." *Adv Anat Pathol* **16**(6): 405-417.
- Bjornson, K. P., D. J. Allen and P. Modrich (2000). "Modulation of MutS ATP hydrolysis by DNA cofactors." *Biochemistry* **39**(11): 3176-3183.
- Blackwell, L. J., K. P. Bjornson, D. J. Allen and P. Modrich (2001). "Distinct MutS DNA-binding modes that are differentially modulated by ATP binding and hydrolysis." *J Biol Chem* **276**(36): 34339-34347.
- Blackwell, L. J., K. P. Bjornson and P. Modrich (1998). "DNA-dependent activation of the hMutSalph α ATPase." *J Biol Chem* **273**(48): 32049-32054.
- Blackwell, L. J., D. Martik, K. P. Bjornson, E. S. Bjornson and P. Modrich (1998). "Nucleotide-promoted release of hMutSalph α from heteroduplex DNA is consistent with an ATP-dependent translocation mechanism." *J Biol Chem* **273**(48): 32055-32062.
- Bocker, T., A. Barusevicius, T. Snowden, D. Rasio, S. Guerrette, D. Robbins, C. Schmidt, J. Burczak, C. M. Croce, T. Copeland, A. J. Kovatich and R. Fishel (1999). "hMSH5: a human MutS homologue that forms a novel heterodimer with hMSH4 and is expressed during spermatogenesis." *Cancer Res* **59**(4): 816-822.
- Bustin, M. (1999). "Regulation of DNA-dependent activities by the functional motifs of the high-mobility-group chromosomal proteins." *Mol Cell Biol* **19**(8): 5237-5246.
- Chen, J. and K. S. Matthews (1992). "Deletion of lactose repressor carboxyl-terminal domain affects tetramer formation." *J Biol Chem* **267**(20): 13843-13850.
- Chen, W. S., J. Y. Chen, J. M. Liu, W. C. Lin, K. L. King, J. Whang-Peng and W. K. Yang (1997). "Microsatellite instability in sporadic-colon-cancer patients with and without liver metastases." *Int J Cancer* **74**(4): 470-474.

Cho, W. K., C. Jeong, D. Kim, M. Chang, K. M. Song, J. Hanne, C. Ban, R. Fishel and J. B. Lee (2012). "ATP alters the diffusion mechanics of MutS on mismatched DNA." Structure **20**(7): 1264-1274.

Constantin, N., L. Dzantiev, F. A. Kadyrov and P. Modrich (2005). "Human mismatch repair: reconstitution of a nick-directed bidirectional reaction." J Biol Chem **280**(48): 39752-39761.

Dohet, C., R. Wagner and M. Radman (1985). "Repair of defined single base-pair mismatches in Escherichia coli." Proc Natl Acad Sci U S A **82**(2): 503-505.

Drake, J. W. (1991). "A constant rate of spontaneous mutation in DNA-based microbes." Proc Natl Acad Sci U S A **88**(16): 7160-7164.

Drake, J. W. (1999). "The distribution of rates of spontaneous mutation over viruses, prokaryotes, and eukaryotes." Ann N Y Acad Sci **870**: 100-107.

Drotschmann, K., W. Yang, F. E. Brownell, E. T. Kool and T. A. Kunkel (2001). "Asymmetric recognition of DNA local distortion. Structure-based functional studies of eukaryotic Msh2-Msh6." J Biol Chem **276**(49): 46225-46229.

Drummond, J. T., G. M. Li, M. J. Longley and P. Modrich (1995). "Isolation of an hMSH2-p160 heterodimer that restores DNA mismatch repair to tumor cells." Science **268**(5219): 1909-1912.

Dufner, P., G. Marra, M. Raschle and J. Jiricny (2000). "Mismatch recognition and DNA-dependent stimulation of the ATPase activity of hMutSalph is abolished by a single mutation in the hMSH6 subunit." J Biol Chem **275**(47): 36550-36555.

Edelbrock, M. A., S. Kaliyaperumal and K. J. Williams (2013). "Structural, molecular and cellular functions of MSH2 and MSH6 during DNA mismatch repair, damage signaling and other noncanonical activities." Mutat Res **743-744**: 53-66.

Eshleman, J. R. and S. D. Markowitz (1995). "Microsatellite instability in inherited and sporadic neoplasms." Curr Opin Oncol **7**(1): 83-89.

Falcon, C. M., L. Swint-Kruse and K. S. Matthews (1997). "Designed disulfide between N-terminal domains of lactose repressor disrupts allosteric linkage." J Biol Chem **272**(43): 26818-26821.

Fishel, R. (1998). "Mismatch repair, molecular switches, and signal transduction." Genes Dev **12**(14): 2096-2101.

Frank, S. A. and M. A. Nowak (2004). "Problems of somatic mutation and cancer." Bioessays **26**(3): 291-299.

Genschel, J., S. J. Littman, J. T. Drummond and P. Modrich (1998). "Isolation of MutSbeta from human cells and comparison of the mismatch repair specificities of MutSbeta and MutSalph." J Biol Chem **273**(31): 19895-19901.

Genschel, J. and P. Modrich (2003). "Mechanism of 5'-directed excision in human mismatch repair." Mol Cell **12**(5): 1077-1086.

Ghodgaonkar, M. M., F. Lazzaro, M. Olivera-Pimentel, M. Artola-Boran, P. Cejka, M. A. Reijns, A. P. Jackson, P. Plevani, M. Muzi-Falconi and J. Jiricny (2013). "Ribonucleotides misincorporated into DNA act as strand-discrimination signals in eukaryotic mismatch repair." Mol Cell **50**(3): 323-332.

Glascock, C. B. and M. J. Weickert (1998). "Using chromosomal lacIQ1 to control expression of genes on high-copy-number plasmids in Escherichia coli." Gene **223**(1-2): 221-231.

Gorman, J., A. Chowdhury, J. A. Surtees, J. Shimada, D. R. Reichman, E. Alani and E. C. Greene (2007). "Dynamic basis for one-dimensional DNA scanning by the mismatch repair complex Msh2-Msh6." *Mol Cell* **28**(3): 359-370.

Gradia, S., S. Acharya and R. Fishel (1997). "The human mismatch recognition complex hMSH2-hMSH6 functions as a novel molecular switch." *Cell* **91**(7): 995-1005.

Gradia, S., S. Acharya and R. Fishel (2000). "The role of mismatched nucleotides in activating the hMSH2-hMSH6 molecular switch." *J Biol Chem* **275**(6): 3922-3930.

Gradia, S., D. Subramanian, T. Wilson, S. Acharya, A. Makhov, J. Griffith and R. Fishel (1999). "hMSH2-hMSH6 forms a hydrolysis-independent sliding clamp on mismatched DNA." *Mol Cell* **3**(2): 255-261.

Grilley, M., K. M. Welsh, S. S. Su and P. Modrich (1989). "Isolation and characterization of the Escherichia coli mutL gene product." *J Biol Chem* **264**(2): 1000-1004.

Gu, L., B. Cline-Brown, F. Zhang, L. Qiu and G. M. Li (2002). "Mismatch repair deficiency in hematological malignancies with microsatellite instability." *Oncogene* **21**(37): 5758-5764.

Gu, L. and G. M. Li (2006). "Analysis of DNA mismatch repair in cellular response to DNA damage." *Methods Enzymol* **408**: 303-317.

Guarne, A., S. Ramon-Maiques, E. M. Wolff, R. Ghirlando, X. Hu, J. H. Miller and W. Yang (2004). "Structure of the MutL C-terminal domain: a model of intact MutL and its roles in mismatch repair." *EMBO J* **23**(21): 4134-4145.

Herman, J. G., A. Umar, K. Polyak, J. R. Graff, N. Ahuja, J. P. Issa, S. Markowitz, J. K. Willson, S. R. Hamilton, K. W. Kinzler, M. F. Kane, R. D. Kolodner, B. Vogelstein, T. A. Kunkel and S. B. Baylin (1998). "Incidence and functional consequences of hMLH1 promoter hypermethylation in colorectal carcinoma." *Proc Natl Acad Sci U S A* **95**(12): 6870-6875.

Holliday, R. (2007). "A mechanism for gene conversion in fungi." *Genet Res* **89**(5-6): 285-307.

Holliday, R. and J. E. Pugh (1975). "DNA modification mechanisms and gene activity during development." *Science* **187**(4173): 226-232.

Holmes, J., Jr., S. Clark and P. Modrich (1990). "Strand-specific mismatch correction in nuclear extracts of human and Drosophila melanogaster cell lines." *Proc Natl Acad Sci U S A* **87**(15): 5837-5841.

Hopfner, K. P. and J. A. Tainer (2003). "Rad50/SMC proteins and ABC transporters: unifying concepts from high-resolution structures." *Curr Opin Struct Biol* **13**(2): 249-255.

Hsieh, P. (2001). "Molecular mechanisms of DNA mismatch repair." *Mutat Res* **486**(2): 71-87.

Iaccarino, I., G. Marra, P. Dufner and J. Jiricny (2000). "Mutation in the magnesium binding site of hMSH6 disables the hMutSalpha sliding clamp from translocating along DNA." *J Biol Chem* **275**(3): 2080-2086.

Iaccarino, I., G. Marra, F. Palombo and J. Jiricny (1998). "hMSH2 and hMSH6 play distinct roles in mismatch binding and contribute differently to the ATPase activity of hMutSalpha." *EMBO J* **17**(9): 2677-2686.

Issa, J. P. (2000). "CpG-island methylation in aging and cancer." *Curr Top Microbiol Immunol* **249**: 101-118.

Iyer, R. R., A. Pluciennik, V. Burdett and P. L. Modrich (2006). "DNA mismatch repair: functions and mechanisms." *Chem Rev* **106**(2): 302-323.

Jeong, C., W. K. Cho, K. M. Song, C. Cook, T. Y. Yoon, C. Ban, R. Fishel and J. B. Lee (2011). "MutS switches between two fundamentally distinct clamps during mismatch repair." Nat Struct Mol Biol **18**(3): 379-385.

Jiang, J., L. Bai, J. A. Surtees, Z. Gemici, M. D. Wang and E. Alani (2005). "Detection of high-affinity and sliding clamp modes for MSH2-MSH6 by single-molecule unzipping force analysis." Mol Cell **20**(5): 771-781.

Johnson, P. H. and L. I. Grossman (1977). "Electrophoresis of DNA in agarose gels. Optimizing separations of conformational isomers of double- and single-stranded DNAs." Biochemistry **16**(19): 4217-4225.

Junop, M. S., G. Obmolova, K. Rausch, P. Hsieh and W. Yang (2001). "Composite active site of an ABC ATPase: MutS uses ATP to verify mismatch recognition and authorize DNA repair." Mol Cell **7**(1): 1-12.

Kadyrov, F. A., L. Dzantiev, N. Constantin and P. Modrich (2006). "Endonucleolytic function of MutLalpha in human mismatch repair." Cell **126**(2): 297-308.

Kadyrov, F. A., S. F. Holmes, M. E. Arana, O. A. Lukianova, M. O'Donnell, T. A. Kunkel and P. Modrich (2007). "Saccharomyces cerevisiae MutLalpha is a mismatch repair endonuclease." J Biol Chem **282**(51): 37181-37190.

Kane, M. F., M. Loda, G. M. Gaida, J. Lipman, R. Mishra, H. Goldman, J. M. Jessup and R. Kolodner (1997). "Methylation of the hMLH1 promoter correlates with lack of expression of hMLH1 in sporadic colon tumors and mismatch repair-defective human tumor cell lines." Cancer Res **57**(5): 808-811.

Kirsch, J. F. (1987). "Analysis of site-directed mutagenesis experiments by linear free energy relationships." Protein Eng **1**(3): 148-150.

Kirsch, R. D. and E. Joly (1998). "An improved PCR-mutagenesis strategy for two-site mutagenesis or sequence swapping between related genes." Nucleic Acids Res **26**(7): 1848-1850.

Kneitz, B., P. E. Cohen, E. Avdievich, L. Zhu, M. F. Kane, H. Hou, Jr., R. D. Kolodner, R. Kucherlapati, J. W. Pollard and W. Edelmann (2000). "MutS homolog 4 localization to meiotic chromosomes is required for chromosome pairing during meiosis in male and female mice." Genes Dev **14**(9): 1085-1097.

Kohlmann, W. and S. B. Gruber (1993). Lynch Syndrome. GeneReviews. R. A. Pagon, T. D. Bird, C. R. Dolan and K. Stephens. Seattle WA, University of Washington, Seattle.

Kolodner, R. (1996). "Biochemistry and genetics of eukaryotic mismatch repair." Genes Dev **10**(12): 1433-1442.

Kolodner, R. D. and G. T. Marsischky (1999). "Eukaryotic DNA mismatch repair." Curr Opin Genet Dev **9**(1): 89-96.

Kramer, B., W. Kramer and H. J. Fritz (1984). "Different base/base mismatches are corrected with different efficiencies by the methyl-directed DNA mismatch-repair system of E. coli." Cell **38**(3): 879-887.

Kunkel, T. A. and D. A. Erie (2005). "DNA mismatch repair." Annu Rev Biochem **74**: 681-710.

Lahue, R. S., K. G. Au and P. Modrich (1989). "DNA mismatch correction in a defined system." Science **245**(4914): 160-164.

Lamers, M. H., D. Georgijevic, J. H. Lebbink, H. H. Winterwerp, B. Agianian, N. de Wind and T. K. Sixma (2004). "ATP increases the affinity between MutS ATPase domains.

Implications for ATP hydrolysis and conformational changes." J Biol Chem **279**(42): 43879-43885.

Lamers, M. H., A. Perrakis, J. H. Enzlin, H. H. Winterwerp, N. de Wind and T. K. Sixma (2000). "The crystal structure of DNA mismatch repair protein MutS binding to a G x T mismatch." Nature **407**(6805): 711-717.

Lebbink, J. H., A. Fish, A. Reumer, G. Natrajan, H. H. Winterwerp and T. K. Sixma (2010). "Magnesium coordination controls the molecular switch function of DNA mismatch repair protein MutS." J Biol Chem **285**(17): 13131-13141.

Li, G. M. (2008). "Mechanisms and functions of DNA mismatch repair." Cell Res **18**(1): 85-98.

Li, G. M. and P. Modrich (1995). "Restoration of mismatch repair to nuclear extracts of H6 colorectal tumor cells by a heterodimer of human MutL homologs." Proc Natl Acad Sci U S A **92**(6): 1950-1954.

Lopez de Saro, F. J. and M. O'Donnell (2001). "Interaction of the beta sliding clamp with MutS, ligase, and DNA polymerase I." Proc Natl Acad Sci U S A **98**(15): 8376-8380.

Loukola, A., K. Eklin, P. Laiho, R. Salovaara, P. Kristo, H. Jarvinen, J. P. Mecklin, V. Launonen and L. A. Aaltonen (2001). "Microsatellite marker analysis in screening for hereditary nonpolyposis colorectal cancer (HNPCC)." Cancer Res **61**(11): 4545-4549.

Lynch, H. T. and A. de la Chapelle (1999). "Genetic susceptibility to non-polyposis colorectal cancer." J Med Genet **36**(11): 801-818.

Mandel, M. and A. Higa (1970). "Calcium-dependent bacteriophage DNA infection." J Mol Biol **53**(1): 159-162.

Mao, G., X. Pan and L. Gu (2008). "Evidence that a mutation in the MLH1 3'-untranslated region confers a mutator phenotype and mismatch repair deficiency in patients with relapsed leukemia." J Biol Chem **283**(6): 3211-3216.

Mao, G., F. Yuan, K. Absher, C. D. Jennings, D. S. Howard, C. T. Jordan and L. Gu (2008). "Preferential loss of mismatch repair function in refractory and relapsed acute myeloid leukemia: potential contribution to AML progression." Cell Res **18**(2): 281-289.

Martik, D., C. Baitinger and P. Modrich (2004). "Differential specificities and simultaneous occupancy of human MutSalpha nucleotide binding sites." J Biol Chem **279**(27): 28402-28410.

Matheson, E. C. and A. G. Hall (2003). "Assessment of mismatch repair function in leukaemic cell lines and blasts from children with acute lymphoblastic leukaemia." Carcinogenesis **24**(1): 31-38.

Mazur, D. J., M. L. Mendillo and R. D. Kolodner (2006). "Inhibition of Msh6 ATPase activity by mispaired DNA induces a Msh2(ATP)-Msh6(ATP) state capable of hydrolysis-independent movement along DNA." Mol Cell **22**(1): 39-49.

McCulloch, S. D., L. Gu and G. M. Li (2003). "Bi-directional processing of DNA loops by mismatch repair-dependent and -independent pathways in human cells." J Biol Chem **278**(6): 3891-3896.

Mendillo, M. L., D. J. Mazur and R. D. Kolodner (2005). "Analysis of the interaction between the *Saccharomyces cerevisiae* MSH2-MSH6 and MLH1-PMS1 complexes with DNA using a reversible DNA end-blocking system." J Biol Chem **280**(23): 22245-22257.

Modrich, P. (1989). "Methyl-directed DNA mismatch correction." J Biol Chem **264**(12): 6597-6600.

Modrich, P. (1991). "Mechanisms and biological effects of mismatch repair." Annu Rev Genet **25**: 229-253.

Modrich, P. (1997). "Strand-specific mismatch repair in mammalian cells." J Biol Chem **272**(40): 24727-24730.

Modrich, P. and R. Lahue (1996). "Mismatch repair in replication fidelity, genetic recombination, and cancer biology." Annu Rev Biochem **65**: 101-133.

Nguyen, D. X. and J. Massague (2007). "Genetic determinants of cancer metastasis." Nat Rev Genet **8**(5): 341-352.

Obmolova, G., C. Ban, P. Hsieh and W. Yang (2000). "Crystal structures of mismatch repair protein MutS and its complex with a substrate DNA." Nature **407**(6805): 703-710.

Okajima, T., T. Tanabe and T. Yasuda (1993). "Nonurea sodium dodecyl sulfate-polyacrylamide gel electrophoresis with high-molarity buffers for the separation of proteins and peptides." Anal Biochem **211**(2): 293-300.

Parker, B. O. and M. G. Marinus (1992). "Repair of DNA heteroduplexes containing small heterologous sequences in Escherichia coli." Proc Natl Acad Sci U S A **89**(5): 1730-1734.

Peltomaki, P. and H. F. Vasen (1997). "Mutations predisposing to hereditary nonpolyposis colorectal cancer: database and results of a collaborative study. The International Collaborative Group on Hereditary Nonpolyposis Colorectal Cancer." Gastroenterology **113**(4): 1146-1158.

Pluciennik, A., L. Dzantiev, R. R. Iyer, N. Constantin, F. A. Kadyrov and P. Modrich (2010). "PCNA function in the activation and strand direction of MutLalpha endonuclease in mismatch repair." Proc Natl Acad Sci U S A **107**(37): 16066-16071.

Pluciennik, A. and P. Modrich (2007). "Protein roadblocks and helix discontinuities are barriers to the initiation of mismatch repair." Proc Natl Acad Sci U S A **104**(31): 12709-12713.

Porter, G., J. Westmoreland, S. Priebe and M. A. Resnick (1996). "Homologous and homeologous intermolecular gene conversion are not differentially affected by mutations in the DNA damage or the mismatch repair genes RAD1, RAD50, RAD51, RAD52, RAD54, PMS1 and MSH2." Genetics **143**(2): 755-767.

Qiu, R., V. C. DeRocco, C. Harris, A. Sharma, M. M. Hingorani, D. A. Erie and K. R. Wenginger (2012). "Large conformational changes in MutS during DNA scanning, mismatch recognition and repair signalling." EMBO J **31**(11): 2528-2540.

Ramakrishnan, C., V. S. Dani and T. Ramasarma (2002). "A conformational analysis of Walker motif A [GXXXXGKT (S)] in nucleotide-binding and other proteins." Protein Eng **15**(10): 783-798.

Renart, J., J. Reiser and G. R. Stark (1979). "Transfer of proteins from gels to diazobenzoyloxymethyl-paper and detection with antisera: a method for studying antibody specificity and antigen structure." Proc Natl Acad Sci U S A **76**(7): 3116-3120.

Rutkauskas, D., H. Zhan, K. S. Matthews, F. S. Pavone and F. Vanzi (2009). "Tetramer opening in LacI-mediated DNA looping." Proc Natl Acad Sci U S A **106**(39): 16627-16632.

Schofield, M. J. and P. Hsieh (2003). "DNA mismatch repair: molecular mechanisms and biological function." Annu Rev Microbiol **57**: 579-608.

Selmane, T., M. J. Schofield, S. Nayak, C. Du and P. Hsieh (2003). "Formation of a DNA mismatch repair complex mediated by ATP." J Mol Biol **334**(5): 949-965.

Shell, S. S., C. D. Putnam and R. D. Kolodner (2007). "Chimeric *Saccharomyces cerevisiae* Msh6 protein with an Msh3 mispair-binding domain combines properties of both proteins." Proc Natl Acad Sci U S A **104**(26): 10956-10961.

Stojic, L., R. Brun and J. Jiricny (2004). "Mismatch repair and DNA damage signalling." DNA Repair (Amst) **3**(8-9): 1091-1101.

Su, S. S., R. S. Lahue, K. G. Au and P. Modrich (1988). "Mispair specificity of methyl-directed DNA mismatch correction in vitro." J Biol Chem **263**(14): 6829-6835.

Su, S. S. and P. Modrich (1986). "Escherichia coli mutS-encoded protein binds to mismatched DNA base pairs." Proc Natl Acad Sci U S A **83**(14): 5057-5061.

Swint-Kruse, L., C. R. Elam, J. W. Lin, D. R. Wycuff and K. Shive Matthews (2001). "Plasticity of quaternary structure: twenty-two ways to form a LacI dimer." Protein Sci **10**(2): 262-276.

Swint-Kruse, L., H. Zhan, B. M. Fairbanks, A. Maheshwari and K. S. Matthews (2003). "Perturbation from a distance: mutations that alter LacI function through long-range effects." Biochemistry **42**(47): 14004-14016.

Tautz, D. and Schlotterer (1994). "Simple sequences." Curr Opin Genet Dev **4**(6): 832-837.

Towbin, H., T. Staehelin and J. Gordon (1979). "Electrophoretic transfer of proteins from polyacrylamide gels to nitrocellulose sheets: procedure and some applications." Proc Natl Acad Sci U S A **76**(9): 4350-4354.

Umar, A. and S. Srivastava (2004). "The promise of biomarkers in colorectal cancer detection." Dis Markers **20**(2): 87-96.

Waddington, C. (1940). "The genetic control of wing development in *Drosophila*." (1): 75-113.

Wang, H. and J. B. Hays (2003). "Mismatch repair in human nuclear extracts: effects of internal DNA-hairpin structures between mismatches and excision-initiation nicks on mismatch correction and mismatch-provoked excision." J Biol Chem **278**(31): 28686-28693.

Wang, H. and J. B. Hays (2004). "Signaling from DNA mispairs to mismatch-repair excision sites despite intervening blockades." EMBO J **23**(10): 2126-2133.

Wang, T. F. and W. M. Kung (2002). "Supercomplex formation between Mlh1-Mlh3 and Sgs1-Top3 heterocomplexes in meiotic yeast cells." Biochem Biophys Res Commun **296**(4): 949-953.

Warbrick, E. (1998). "PCNA binding through a conserved motif." Bioessays **20**(3): 195-199.

Warren, J. J., T. J. Pohlhaus, A. Changela, R. R. Iyer, P. L. Modrich and L. S. Beese (2007). "Structure of the human MutS α DNA lesion recognition complex." Mol Cell **26**(4): 579-592.

Wei, K., A. B. Clark, E. Wong, M. F. Kane, D. J. Mazur, T. Parris, N. K. Kolas, R. Russell, H. Hou, Jr., B. Kneitz, G. Yang, T. A. Kunkel, R. D. Kolodner, P. E. Cohen and W. Edelmann (2003). "Inactivation of Exonuclease 1 in mice results in DNA mismatch repair defects, increased cancer susceptibility, and male and female sterility." Genes Dev **17**(5): 603-614.

Wilson, T., S. Guerrette and R. Fishel (1999). "Dissociation of mismatch recognition and ATPase activity by hMSH2-hMSH3." J Biol Chem **274**(31): 21659-21664.

Xu, H., P. Zhang, L. Liu and M. Y. Lee (2001). "A novel PCNA-binding motif identified by the panning of a random peptide display library." Biochemistry **40**(14): 4512-4520.

Yuan, F., L. Gu, S. Guo, C. Wang and G. M. Li (2004). "Evidence for involvement of HMGB1 protein in human DNA mismatch repair." J Biol Chem **279**(20): 20935-20940.

Zhang, Y., F. Yuan, S. R. Presnell, K. Tian, Y. Gao, A. E. Tomkinson, L. Gu and G. M. Li (2005). "Reconstitution of 5'-directed human mismatch repair in a purified system." Cell **122**(5): 693-705.

VITA

SANGHEE LEE

Place of Birth: Seoul, South Korea

Educations	
2010 - present	Ph.D. in Nutritional Sciences expected Graduate Center for Nutritional Sciences University of Kentucky, Lexington, KY, USA
2007 - 2010	Master's in Toxicology Graduate Center for Toxicology University of Kentucky, Lexington, KY, USA
2002 - 2007	B.S. in Biotechnology Department of Food Science and Biotechnology Kyungwon University, South Korea
Research Experiences	
2007 - Current	Research Assistant (Full time) Studying " <i>Molecular Mechanism of DNA Mismatch Repair Initiation</i> " in Dr.Guo-Min Li's Laboratory Graduate Center for Nutritional Sciences and Toxicology, University of Kentucky, Lexington, KY, USA
2004 - 2007	Research Assistant (Full time) Studying " <i>The Formation of Xylanase Inclusion Body from Bacillus pumilus expressed in Escherichia coli</i> " in Dr.Young-Seo Park's Laboratory Department of Food Science and Biotechnology, Kyungwon University, South Korea
Jul - Aug. 2004	Intern (Full-time: 40H/W) Lab. of Nuclear Medicine, Korea Institute of Radiological and Medical Sciences (KIRAMS) in Seoul, Korea Research on " <i>Animal imaging of Recombinant Single Chain anti HLA-DR antibody for Radioimmunodetection</i> "
Jul – Aug. 2004	Research on " <i>Large scale production and evaluation of single-chain Fv lym-1 antibody by pET system</i> "
Honors, Awards & Scholarship	
Apr. 2014	2014 ASBMB Best Poster Presentation Award
Apr.2014	2014 ASBMB Graduate and Postdoctoral Travel Fellowship Award
Apr. 2013	2013 ASBMB Graduate and Postdoctoral Travel Fellowship Award

Apr. 2012	2012 ASBMB Graduate and Postdoctoral Travel Fellowship Award
2007-2013	Research Assistantship for graduate students
Feb. 2007	Honor of Summa cum laude from the college (GPA 4.27 out of 4.5)
Fall. 2005	College Scholarship of academic excellence for top 3 candidates
Spring. 2005	College Scholarship of academic excellence for top 3 candidates
Fall. 2004	College Scholarship of academic excellence for top 3 candidates
Spring. 2004	College Scholarship of academic excellence for top 3 candidates University Scholarship for publicity activity as a model student
Fall. 2003	College Scholarship of academic excellence for top 3 candidates University Scholarship for publicity activity as a model student
Spring. 2003	College Scholarship of academic excellence for top 3 candidates
Fall. 2002	College Scholarship of academic excellence for top 3 candidates
Abstracts & Presentations	
Apr.20-24. 2013	<i>“Mechanism of mismatch-provoked excision in a defined mismatch repair system”</i> : Sanghee Lee, Liya Gu, Wei Yang, Guo-Min Li - Poster Presentation for 2013 Experimental Biology as a recipient of 2013 ASBMB Graduate and Postdoctoral Travel Fellowship Award
Apr.20-24. 2013	<i>“Regulation of Mismatch Repair protein MutSa Functions by its Walker A and Walker B motif”</i> : Sanghee Lee, Liya Gu, Guo-Min Li - Poster Presentation for 2013 Experimental Biology as a recipient of 2013 ASBMB Graduate and Postdoctoral Travel Fellowship Award
May. 2013	- Poster Presentation for 2013 Markey Cancer Research Day at University of Kentucky
Apr.20-24. 2012	<i>“Termination of Exonuclease 1-catalyzed Mismatch Excision Requires Physical Interaction between Exonuclease 1 and MutLa”</i> : Sanghee Lee, Zhanmin Fan, Yanbin Zhang, Lei Tian, Fenghua Yuan, Liya Gu, Guo-Min Li - Poster Presentation for 2012 Experimental Biology as a recipient of 2012 ASBMB Graduate and Postdoctoral Travel Fellowship Award
May. 2012	- Poster Presentation for 2012 Markey Cancer Research Day at University of Kentucky
May. 2011	<i>“Initiation of human DNA mismatch repair”</i> : Sanghee Lee, Lei Tian, Liya Gu, Guo-Min Li - Poster Presentation for 2011 Markey Cancer Research Day at University of Kentucky
Dec. 2010	<i>“The Mismatch Repair Protein MutLa Facilitates the Primary microRNA Processing”</i> : Guogen Mao, Sanghee Lee, Guo-Min Li, and Liya Gu - Poster Presentation for 2010 College of Medicine’s Annual Postdoctoral Poster Session at University of Kentucky.
May. 19. 2005	<i>“The effects of milk whey protein hydrolysate on blood glucose and lipid level in streptozotocin-induced diabetic rats”</i>

	<p>: Ju Hui Park, Sang Hee Lee, Jae Ho Jung, Kang Woon Lee, Hak Gil Chang, Young Seo Park</p> <p>- Presented on Spring Symposium & Conference of 2005 held by Korean Society for Food Engineering and Korea Food Industry Association & Published on p177 (2005)</p>
May. 13. 2005	<p><i>“Animal imaging of Recombinant Single Chain anti HLA-DR antibody for Radioimmunodetection”</i></p> <p>: Jae Ho Jung, Tae Hyun Choi, Kwang Sun Woo, Wee Sup Chung, Sang Hee Lee, Eun Jung Kim, Young Seo Park, Chang Woon Choi, Sang Moo Lim</p> <p>- Presented on The 13th Federation Meeting of Korean Basic Medical Scientists held by The Basic Medicine Association, Korea & Published on p399 (2005)</p>
Oct. 28-29. 2004	<p><i>“Large scale production and evaluation of single-chain Fv lym-1 antibody by pET system”</i></p> <p>: Jae Ho Jung, Tae Hyun Choi, Sang Hee Lee, Yeon I Woo and Chang Woon Choi, Sang Moo Lim</p> <p>- Presented on the Autumn Conference of 2004 held by The Korean Society of Medical Biochemistry and Molecular Biology in Seoul, Korea & Published on p114 (2004)</p>
Publications	
Sep. 2012	<p>Juana V. Martin-Lopez, Ysamar Barrios, Vicente Medina-Arana, Miguel Andujar, Sanghee Lee, Liya Gu, Guo-Min Li, Josef Ruschoff, Eduardo Salido and Richard Fishel.</p> <p><i>“The hMSH2(M688R) Lynch syndrome mutation may function as a dominant negative”</i> Carcinogenesis, 2012 Sep; 33(9): 1647-54.</p>
Jun. 2012	<p>Guogen Mao, Sanghee Lee, Janice Ortega, Liya Gu, and Guo-Min Li.</p> <p><i>“Modulation of microRNA processing by mismatch repair protein MutLa”</i> Cell Research, 2012 Jun; 22(6): 973-85</p>